DETAILED RELIABILITY MODELS OF INTEGRATED SOLAR POWER TECHNOLOGIES IN ELECTRIC

POWER SYSTEMS

A Thesis Submitted to the College of

Graduate and Postdoctoral Studies

In Partial Fulfillment of the Requirements

For the Degree of Doctor of Philosophy

In the Department of Electrical and Computer Engineering

University of Saskatchewan

Saskatoon

By

Ahmad Alferidi

PERMISSION TO USE

I agree that the Libraries of this University may make it freely available for inspection. I further agree that permission for copying of this thesis in any manner, in whole or in part, for scholarly purposes may be granted by the professor or professors who supervised my thesis work or, in their absence, by the Head of the Department or the Dean of the College in which my thesis work was done. It is understood that any copying or publication or use of this thesis or parts thereof for financial gain shall not be allowed without my written permission. It is also understood that due recognition shall be given to me and to the University of Saskatchewan in any scholarly use which may be made of any material in my thesis. Requests for permission to copy or to make other use of material in this thesis in whole or part should be addressed to:

The College of Graduate and Postdoctoral Studies

Head of the Department of Electrical and Computer Engineering

57 Campus Drive

University of Saskatchewan

Saskatoon, Saskatchewan, Canada

S7N 5A9

ABSTRACT

The contribution of solar power in electric power system has been growing rapidly due to the significant negative impact of carbon emissions generated by conventional power sources. Large scale photovoltaic (PV) and concentrated solar power (CSP) have been installed around the world. However, these technologies involve major concerns regarding the reliability of system generation. The output power generation from solar technologies acts quite differently from that of conventional generation. The PV and CSP are composed of major components that have different failure characteristics. The interactions of the different component topologies in various commercially available PV system configurations will significantly influence the reliability of a PV system. Moreover, the output power of PV and CSP are highly variable and depend on the solar irradiation resulting in discontinuous and variable electricity generation. All these factors have a direct impact on the overall generation system adequacy. It is, therefore, vital to incorporate these factors in the reliability modeling of PV and CSP systems. An analytical probabilistic technique is employed in this thesis to develop detailed reliability models of PV and CSP systems. This thesis investigates the impact of PV/CSP system components on the reliability performance of PV/CSP systems.

Different studies were conducted on test systems in this thesis considering system load variation, growth in solar capacity, geographical location, and seasonal effects. These analyses have been expanded to quantify the comparative reliability of a generation system with large scale PV and CSP. The power output of PV is also affected by dust accumulation on PV panel surfaces. The deposition of dust on PV panels will reduce the net solar irradiation absorbed by the solar panel, and lower the solar panel efficiency. This project is extended to incorporate the cumulative dust in the reliability model of the PV system. A regression model is adopted to develop a probabilistic model of PV power reduction caused by cumulative dust. This work also investigates the impact of a dust-removal strategy on the overall system adequacy. The concept and methodology discussed in this thesis can be used effectively by system planners and electric utilities to evaluate the reliability benefit of utilizing solar power in existing generation systems.

ACKNOWLEDGMENTS

Dedicated to:

In Memory of My Great Father (Helil)

To My Great Mother (Meznah) Who Gives Me All Her Love

To My Wife (Areej) Who shares Love with Me

To My Sons and Daughter (Sohib, Moayed and Lara) Who Bring Joy, Happiness and

Love

To All of Us

TABLE OF CONTENTS

LIST OF TABLES

LIST OF FIGURES

LIST OF ABBREVIATIONS

A   Availability

C   Capacitance

CC   Capacity Credit

COPT   Capacity Outage Probability Table

DIF   Diffuse Horizontal Irradiance

ELCC   Effective Load Carrying Capability

FOR   Forced Outage Rate

G_{bi} Global Solar Irradiation

GHI   Global Horizontal Irradiance

G_{std} Solar Irradiation in a Standard Environment

h/y   Hour per year

HL   Hierarchical Levels

HL-I   Hierarchical Level-I

HL-II   Hierarchical Level-II

HL-III   Hierarchical Level-III

IC	Installed Capacity
kWh	Kilowatt-hours
LLU	Loss of the Largest Unit
LOEE	Loss of Energy Expectation
LOLE	Loss of Load Expectation
LOLP	Loss of Load Probability
MTTF	Mean Time to Failure
MTTR	Mean Time to Repair
MW	Megawatt
MWh	Megawatt-hours
PL	Peak Load
P_{sn}	Equivalent Rated Capacity of PV
pu	Per Unit
PV	Photovoltaic
RBECR	Risk-based Equivalent Capacity Ratio
RBTS	Roy Billinton Test System
R_c	Certain Irradiation Point

RM	Reserve Margin
SAM	System Advisor Model
SIPS	Small Isolated Power System
Tj	Junction Temperature
U	Unavailability
λ	Failure Rate
μ	Repair Rate
πc	Contact Construction Factor
πE	Effect of Environmental Stress
πQ	Quality Factor
πS	Electric stress factor

1   Introduction

1.1   Reliability Evaluation in Power System Planning

An electric power system is a large complex network of electrical components that supplies and transfers electricity to the consumers. Its main function is to consistently fulfill the load demand at the minimum cost and an acceptable level of reliability with environmental compliance. It is, therefore, vital to plan for the future needs of electricity considering the integration of environmentally friendly energy resources, ensuring that there would be adequate reserves to meet the increasing load demand. Moreover, it is important to analyze power system reliability to limit the potential of an interruption in the electrical services. The development of reliability models of the energy source supply is key for the design and operation of reliable power systems. In general, power system reliability studies are utilized to analyze the ability of an electrical power system to provide an adequate and dependable electricity supply [1,2].

Power system reliability evaluation has a crucial role in the planning and operation of an electric power system. The evaluation of the power system reliability typically focuses on two concerns: system adequacy and system security [2] as shown in Figure 1-1. Adequacy is determined by the ability of the existing or planned system facilities to reasonably satisfy the overall system demand. System security is defined as

the ability of the power system to respond to disturbances that may occur during system operation and maintain a consistent power balance [2].

```
                        ┌─────────────────────────┐
                        │                         │
                        │    System Reliability   │
                        │                         │
                        └─────────────────────────┘
                                    │
                        ┌───────────┴───────────┐
                        ▼                       ▼
            ┌───────────────────┐   ┌───────────────────┐
            │                   │   │                   │
            │  System Adequacy  │   │  System Security  │
            │                   │   │                   │
            └───────────────────┘   └───────────────────┘
```
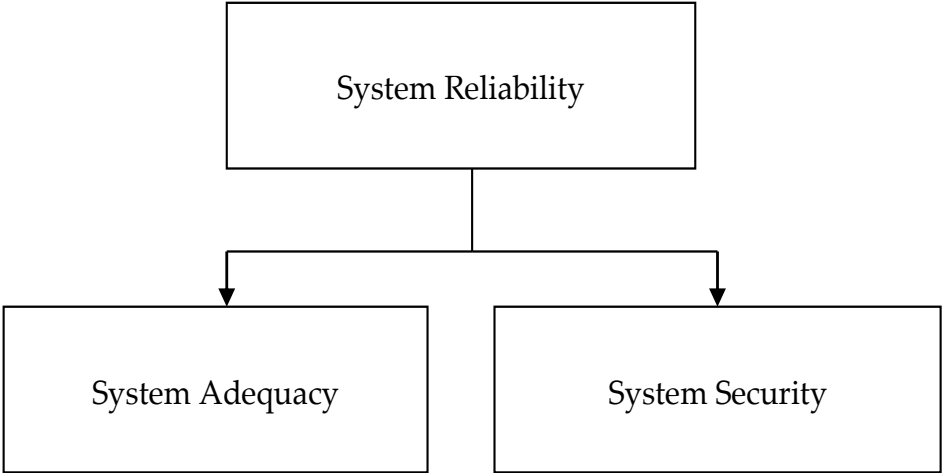
Figure 1-1: Subdivision of power system reliability

The reliability evaluation of the entire power system is inherently complex due to the size of the system, the number of components and variables and their interrelations, and different functions and objectives of the subsystems. Hence, the reliability studies on this subject are classified into three hierarchical levels (HL): HL-I, HL-II, and HL-III [3,4] as shown in Figure 1-2. The HL-I reliability assessment defines the ability of the total system generation to meet the total demand load. This evaluation can be carried out by creating a total system generation model and convolving it with the system load model. The HL-II evaluation is concerned with the function of the generation facilities and transmission equipment (lines and transformers) in meeting the load point energy demand. The HL-III analysis includes all three functional levels, i.e., generation,

transmission, and distribution, and generally only applied in past performance evaluation. Generation planning is an important task in electric power utilities, as the investment in generation facilities dominates the economics of power systems. The reliability studies carried out during this task is within the domain of HL-I adequacy. The proposed research work described in this thesis focuses on the HL-I level adequacy evaluation of generation systems including alternative solar energy technologies.
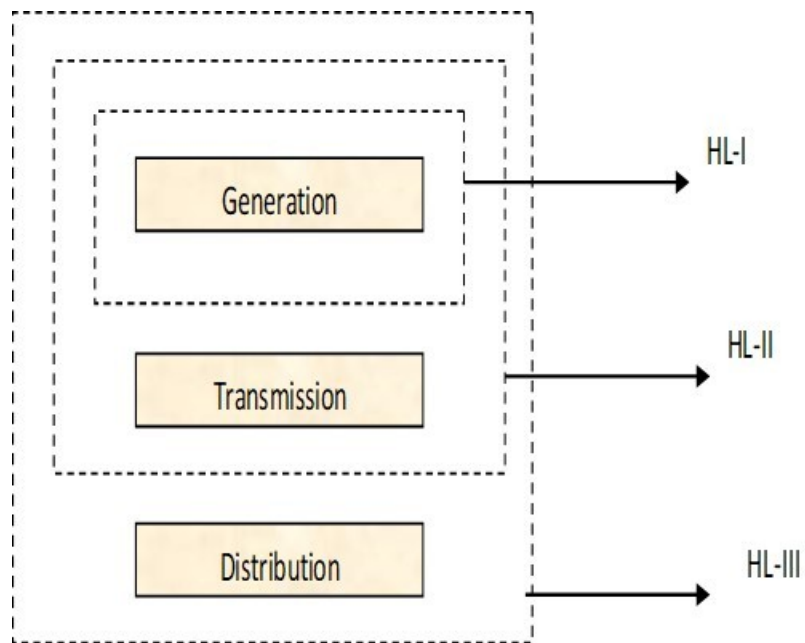
Figure 1-2: Hierarchical levels of power system reliability evaluation

Utilizing a suitable technique to evaluate the system adequacy is vital during the planning of electric power systems. Numerous research studies have presented criteria and methods used by electric utility companies in system generation planning [5,6]. The two most common types of techniques used in generation system reliability

evaluation are deterministic and probabilistic. The deterministic approach mainly employs simple rule of thumb methods, such as, specifying the Reserve Margin (RM) requirement equal to a fixed percentage of the system capacity, or a capacity reserve requirement to withstand the Loss of the Largest Unit (LLU) or (N-1). The percent RM and N-1 criteria do not respond to the stochastic nature of the system behavior, system demand, or component failures. A probabilistic technique, however, reflects inherent random system behavior [7]. Therefore, most electrical power utility companies have switched from using deterministic to probabilistic methods to provide risk-based information for generation system plans [7,8].

The probabilistic approach can be employed using either an analytical or a simulation methodology [3]. The analytical method mathematically represents the system model, and the results obtained from this method are usually long-term expected indices. This technique can provide the expected index values in relatively short computation times, even though assumptions are often needed to simplify the calculation. The simulation technique requires more computation time and resources.

This thesis focuses on the development of reliability models of two different solar energy technologies—Photovoltaic (PV) and Concentrated Solar Power (CSP) integrating these models into power system evaluation and investigate the companied benefit of these renewable energy on the overall system adequacy. The Ph.D. project is

further expanded to study the impact of the cumulative dust on the reliability modeling of the PV system.

1.2   Power Systems Including Photovoltaic System

The burning of fossil fuels has increased with growing demand for electricity. However, the world is concerned about global warming, which is believed to be caused by highly polluting emissions from conventional fossil-fueled energy sources. Reference [9] pointed out that global CO_2 emissions from fossil fuel usage were 32.2 billion tons in 2013, reaching a record high, which is almost 56.1% above the emission level in 1990 and 2.3% above 2012.   The use of alternative clean energy sources is essential to reduce the carbon emissions from electricity generation while meeting global energy demand.   Renewable energy sources are receiving considerable attention to offset energy production of electrical energy from fossil-fired energy generation. Renewable sources provide an environmentally friendly alternative as local energy resources.   CSP and PV sources are among the most promising options for environmentally friendly solar energy sources.

Solar cell technology has been developing rapidly, leading to great improvements in solar cell efficiency.   Electricity generation through PV sources is being increasingly recognized as cost-effective for both small and large electric power systems.   Reference [10] is an annual report published by Solar Power Europe and

presents the statistics of installed PV capacity in various regions of the world. The total PV capacity has increased exponentially from 100 GW in 2012 to 229.9 GW in 2015 to 306.5 GW in 2016 to 358 GW by the end of 2017 [10]. The global installed PV capacity is expected to exceed 400 GW in 2018, 500 GW in 2019, 600 GW in 2020, 700 GW in 2021 [10].

The structure of power electronic converters in commercially available PV systems can be classified into centralized inverters, string inverters, and micro-inverters. The structures of central and string PV systems have almost similar electric components; however, they are different in terms of the manner in which they connect the solar array to the inverter, as shown in Figures 1-3 and 1-4 [11]. In these two figures, for central PV system, each PV array has its own inverters, where one inverter is connected to each string. Micro-inverter topology requires the connection of one inverter per solar cell as shown in Figure 1-5 [11]. The major concern of using PV sources is that the solar irradiation is intermittent and not always available when the electricity is required. This is not a concern when energy is produced using conventional sources. PV systems exist in different topologies with multi-components connected in different configuration. The ability to incorporate probability failure of individual components is important in developing reliability models for different PV design and topologies. The development of detailed reliability models is required to incorporate PV energy sources in the overall power system reliability evaluation.
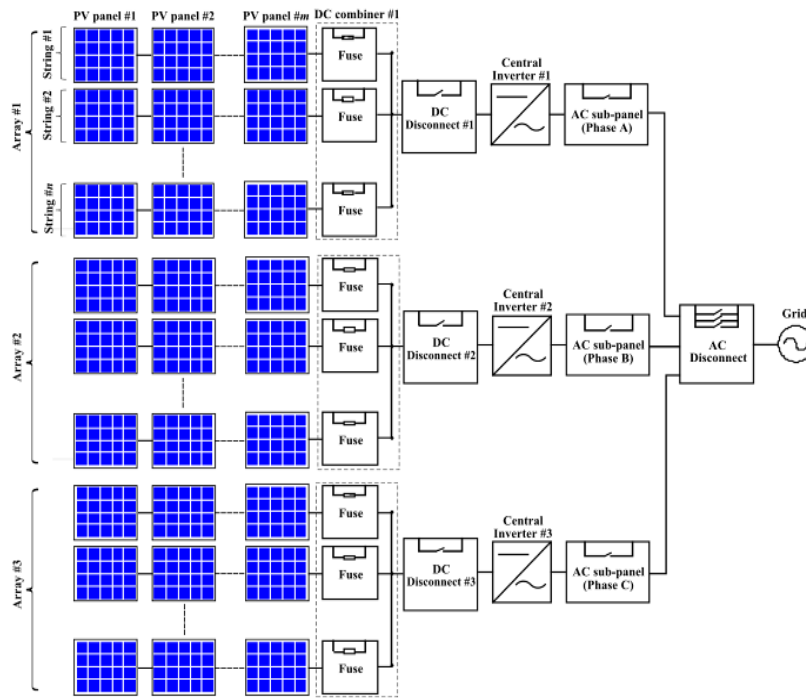
Figure 1-3 Construction of a central PV system [11]
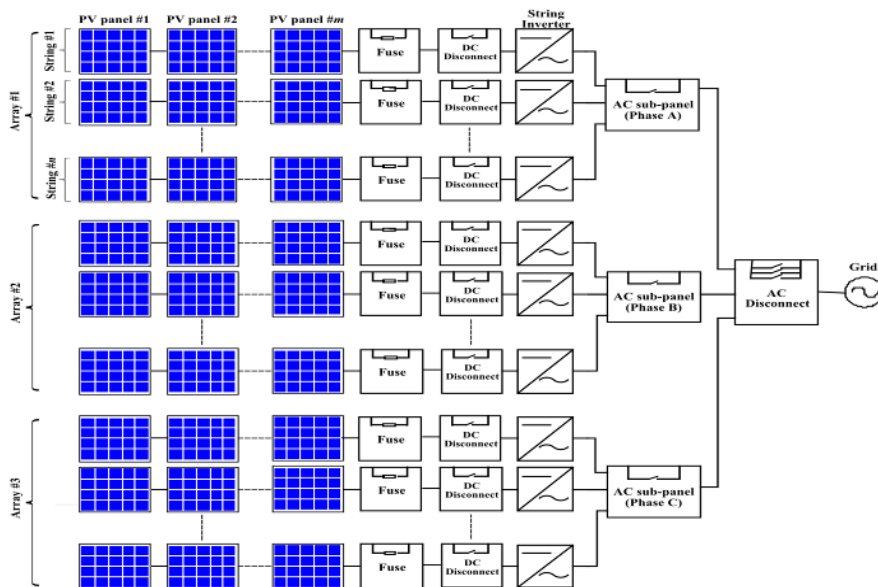
Figure 1-4: Construction of a string PV system [11]
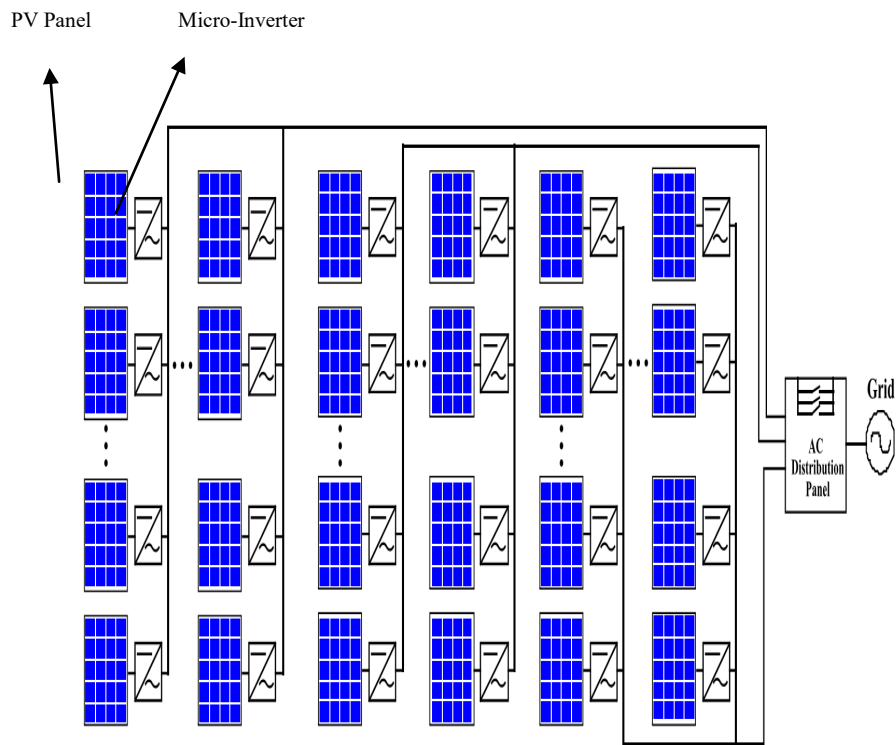
Figure 1-5: Construction of a micro-inverter system [11]

1.3   Power Systems Including Concentrated Solar Power

CSP differs from PV technology, as CSP is based on the concept of concentrating solar thermal energy to generate steam, which can then be utilized for generation of electricity using conventional power cycles. This technology uses mirrors to concentrate direct beam solar irradiance to heat a liquid or gas that is then used in a downstream process for electricity generation. CSP is a zero-carbon emission source of electricity that is best suited for areas of the world with high solar irradiation, such as Southern Europe, Northern Africa, the Middle East, South Africa, parts of India, China,

Southern USA, and Australia. Figure 1-6 [12] illustrates the potential regions to install a CSP. The first large-scale CSP plant for producing electricity was built in the 1980s in California [12].
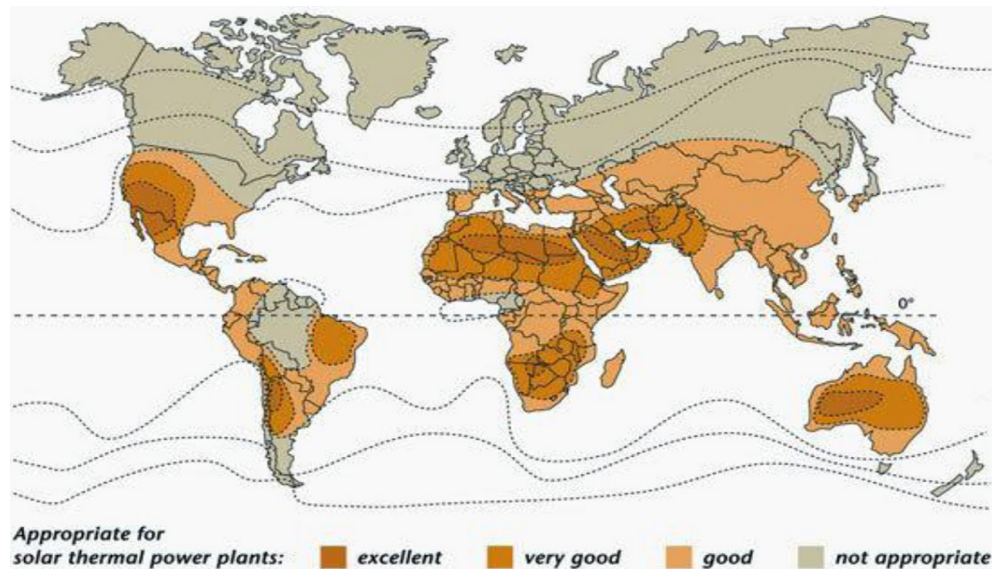
Figure 1-6: Appropriate areas for CSP [12]

CSP systems are being widely commercialized, and the CSP market has seen an addition of up to 740 MW of generation capacity in the electric system network from 2007 till the end of 2010 [13]. Spain installed 400 MW in 2010, taking the global lead with a total of 632 MW, while the US ended 2010 with 509 MW, after adding 78 MW [13]. The Middle East has also begun ramping up their plans to install CSP based projects and, as a part of these plans, Shams-I, the largest CSP project in the Middle East, has been installed in Masdar, Abu Dhabi. At the end of 2016, Spain was producing a total capacity of 2.3 GW, followed by the United States with over 1.7 GW

[14]. By the end of 2016, 4.8 GW of solar thermal electricity projects were operational worldwide and almost half of this capacity was installed in Spain, establishing it as the global market leader for CSP [14]. The power output profile of CSP is different from conventional generation sources. Increasing the penetration of CSP in an electric power system introduces major impacts on the power system reliability. An appropriate reliability model and relevant data are essential to incorporate CSP technology in generation system reliability evaluation.

Factors such as efficiency, economics, and reliability are key to the selection of the most appropriate solar technology for a power system at a specific geographic location. The system of CSP technology has a higher annual energy production rate than the PV module considering the same nominal power for both technologies [15]. Reference [16] performed a financial analysis on PV and CSP plants. This study highlighted and summarized the initial investment cost assumptions for CSP and PV power plants for the same rate of power output. The comparative analysis indicated that the initial investment costs for the CSP plant were higher than those for the PV power plant. However, CSP plants have higher economic returns than PV power plants. A reliability comparison of PV and CSP technologies has not been investigated in past work.

1.4 Research Motivation

There is a continuous need to expand the electric power generation by building new power plants, as the demand for electricity steadily increases over time. It is widely believed that average global temperatures have been rising owing to the burning of fossil fuels to generate electricity by conventional methods. Renewable energy production, which does not emit greenhouse gases, has been recognized as an alternative source of electric power. Solar power is currently receiving considerable attention as it exhibits potential for meeting the growing energy demand without adding to the air pollution and the impacts of global warming [17-19]. Many governments and organizations around the world strongly support financing the use of renewable energy, such as wind and solar power, in electric power systems.

Solar power is recognized as an environmentally friendly resource for an electric generation system owing to its zero greenhouse gas emissions and zero fossil fuel consumption. Moreover, this source is a locally available energy resource and can be operated and maintained easily. These positive factors collectively make solar power an appealing energy source. Currently, PV and CSP are the two main solar energy technologies that are receiving significant attention and becoming rapidly popular around the world.

There is an increase in the number of PV installations due to the advances in solar cell efficiency and decreasing prices. The total PV output capacity has increased exponentially, from 1400 MW in 2000, to 358 GW in 2017 [10]. Recently, the European Photovoltaic Industry Association (EPIA) studied the PV market in five European nations: Germany, France, Italy, the United Kingdom, and Spain. The study pointed out that PV will be more cost-effective in the coming years as a result of the decreasing prices of the solar cells [20]. Although there is evidence of the increasing PV penetration in electric system grids, the power output of PV systems is highly variable, due to weather and geographical climatic impacts.

CSP is another form of solar power technology that has growing potential with regard to the generation of electricity in countries or regions having strong solar resources. The International Energy Agency report [21] presents an extensive study on the potential growth of CSP. This study examined the renewable energy potential in the Middle East and the North Africa region and stated that by 2050, CSP plants could contribute about half of the region's electrical production with a total estimated capacity of 390 GW [21].

The reliability model of PV/CSP depend on design and configuration of each component. A PV system consists of an inverter, a capacitor, and a switch, which have a direct impact on the availability of the PV capacity [22]. Moreover, the structure of PV

topology can affect the PV system's adequacy. Major components of a CSP system can impact the availability of the power output of the plant. In addition, the output power of PV is highly variable, which can directly impact the overall system adequacy. A limited amount of research has been conducted for developing proper PV and CSP reliability models. The development of a quantitative framework to evaluate the reliability contribution of the entire PV or CSP system in a power system grid is, therefore, essential.

1.4.1 Previous Research on Generation System Adequacy Including Photovoltaic Systems

Many investigators have studied the different aspects of PV applications in electric power generation, from low to high-power system applications. This thesis focuses on PV applications in electric system grids. As the number of installations of PV generating units in electric power systems continues to increase globally, the influence of the random intermittency of PV sources on the overall system performance is recognized by many researchers. The power output of a PV array is uncertain and intermittent in nature, and it is, therefore, important to study the reliability contributions made by PV generation to power systems.

Although solar power provides clean energy, the power output of PV systems differs from that generated using conventional sources due to the high uncertainty of

the availability associated with PV system components [11], [23], environmental factors, and PV system configuration. Electric companies and customers are, therefore, concerned about the reliability of grid-connected PV systems. Previous studies have been carried out using both the analytical [5,6] and simulation techniques [3,4] to assess the adequacy benefit associated with installing solar energy in electric power systems. A system well-being model has also been used in past works [24,25] that combines the deterministic and probabilistic techniques to provide useful reliability indices for power systems containing renewable energy. The reliability contribution of PV and wind energy sources is evaluated in these studies. These studies, however, do not consider the detail PV system topology, component configurations and the impact of component level failure/repair characteristics on the reliability performance of the PV system. The topology of PV systems can be classified as centralized inverters, string inverters, and micro-inverters in terms of the structure of their power electronic converters. As stated earlier, the power output of PV systems is highly variable and uncertain due uncertainty in weather conditions, such as cloud cover, and random failures of system components [11], [27,28]. PV technologies are composed of vulnerable electric components that have different failure rates [11]. These vulnerable electric components, such as capacitor, inverter, and switching, should be considered when evaluating the reliability benefit for the entire PV system. Most previous works, such as [26] mainly focus on the reliability assessment of PV systems without considering the component-

level assessment of the PV system. A detailed quantitative reliability assessment is essential for the entire PV system in order to accurately determine the overall reliability contribution of solar power to electric power systems.

This thesis focuses on assessing the PV system adequacy in an electric power system to address the problems discussed earlier in this chapter. The work in this thesis was carried out to identify the key system parameters that affect the reliability contribution of PV systems, develop appropriate evaluation models, and conduct different case studies to investigate the reliability contribution of PV in an electric power system.

1.4.2 Previous Research on Generation System Adequacy Including Concentrated Solar Power

A CSP system can pose capacity planning challenges owing to the variable and uncertain nature of the power output [29]. Therefore, obtaining accurate estimates of the capacity value of such resources is vital for planning purposes. As the penetration of CSP increases in an electric power system, other considerations also become prominent, such as its impact on the overall power system reliability. Reliability evaluation is crucial for the design and operation management of a CSP plant. Very limited research has been conducted addressing the reliability model of a CSP plant, including all major CSP system components. Therefore, the quantitative assessment of

reliability for an entire CSP system is essential for determining the overall reliability contribution of a CSP plant to electric power systems.

A study reported in [29] evaluated the capacity value of CSP plant for five sites in the southwestern of United States. In this study, weather data from several years were taken, and an analytical approach was used to quantify the capacity factor for the equivalent CSP plants. Capacity factor is the ratio of the average power generated to the total installed power rating. Reference [30] provides recommendations and estimations of the effect of solar energy on power systems, and how the storage systems of CSP contribute to power system flexibility. Another study in [31] proposed a sequential Monte Carlo method, which included a series of possible trajectories of CSP production to find the capacity value of this technology.

CSP systems without thermal energy storage cannot generate power continuously due to the lack of solar energy during nighttime, adverse weather conditions during the day as well as random failures of the CSP system major components [16], [32]. These major components, such as mirrors and thermal plant components, should be taken into account when developing the reliability model of the CSP system. The contribution of a given technology or plant to system reliability is quantified by its capacity value considering the effective load-carrying capability (ELCC) of the CSP.

Reference [16] presented a technical–economic comparison between PV and CSP. It evaluated the initial costs, the maintenance costs, and the benefits derived from both the government economic incentives and sale of energy for a 40 MW PV plant and a 40 MW CSP plant. The study found that, under the same environmental conditions, the same rated power, and the same location, the economic return on CSP was significantly higher than that of a PV system [16]. The areas of land occupied by CSP plants are slightly smaller than those taken up by PV. However, the initial cost for the installation of CSP is considerably higher. Reference [33] proposed a mathematical model for the calculation of the levelized cost of electricity generated by PV and CSP.

There is a lack of research on comparative analysis of the reliability contribution and capacity value of adding CSP and PV to an electricity system. This thesis analyzes the comparative reliability of PV and CSP based on the key system variables and parameters. The developed reliability models for PV and CSP systems are utilized in this work to investigate the comparative capacity credit of the two solar technologies.

1.4.3 Previous Research on Generation System Adequacy Including Photovoltaic System Incorporating Cumulative Dust

Although significant advances have been made in PV systems in the past few decades, weather conditions are proving to be a significant factor for the PV system performance. As an example, the government of the Kingdom of Saudi Arabia (KSA)

announced their investment for installing a solar power system in KSA with a capacity

of 7.2 GW in 2019 and 200 GW by 2030 [34], but the location of KSA is associated with

relatively high levels of atmospheric dust concentrations, which causes high rates of

dust accumulation on solar PV panels. This accumulation of dust particles can block

solar light from the outer layer, causing the total solar power output to drop. The

impact of dust accumulation on the output power of the PV system depends on

seasonal dust events and the size of the dust particles.

Reference [35] studied the effect of dust on the PV module performance. This

study quantified the accumulation of dust per day on a square meter of flat surface and

the number of days in various parts of Saudi Arabia. Another study [36] analyzed the

effect of dust on the power output based on the density of the deposited dust, the

composition of the dust, and its particle distribution. Reference [37] evaluated the

humidity level, air velocity, and dust in the area where PV systems were installed.

Reference [38] studied the impact of dust on the performance of a PV system in

Bangladesh. The results of this study showed that the output power of the PV system

was reduced by 34% at the end of the month for tropical weather conditions. Another

study [39] developed analytical models of correlation between dust particle

accumulation on PV modules and the reduction in the output power of a PV system in a

dry region. This study took into consideration the grain sizes of dust. Other

researchers [11], [40] analyzed the impact of PV electronic components on the

availability of the PV power output. Reference [41] developed a probabilistic reliability model of a PV system that considered PV system electronic components and PV system configuration.

The literature review presented in this section focuses on the dust event, dust density, dust concentration in the air, dust accumulation, and the reliability model of the PV system components. The reliability contribution of the PV system has always been a major point of inquiry as the output power of this technology cannot be controlled easily. However, the reliability model of a PV system including the accumulation of dust on the PV surface modules have not been fully explored.

This work presents a PV system reliability model incorporating cumulative dust. The probabilistic model of PV power reduction caused by cumulative dust is developed first and then combined with the reliability model of the PV system. The application of dust modeling in reliability evaluation is demonstrated by using a reliability test model and is assumed to be in Riyadh and Medina, located in the KSA. The polynomial regression model was adopted from an experimental measurement of cumulative dust conducted by the College of Engineering, King Saud University [42,43]. The seasonal dust events recorded by [44] were used in this thesis to construct the linear regression model of the accumulation of dust.

1.5 Research Objectives

There is growing interest in reliability research for renewable energy technologies in electric power systems. Most of these studies focused on wind energy. Solar energy is also emerging as an important renewable resource in power grid applications. There is, however, relatively less work reported on solar energy and its contribution to grid reliability. The PV and CSP solar technologies are developing rapidly and are therefore considered in this project. The intermittency in the output power of PV and CSP can have severe impacts on the performance of overall system reliability. The PV and CSP plants are composed of major components that can affect the system adequacy. The literature review in Section 1.4 discussed a lack of reported knowledge on suitable reliability modeling of PV and CSP systems as well as a methodology to assess the overall power system reliability. The proposed research work will focus on fulfilling the following tasks:

1. Developing an appropriate PV system reliability model.

2. Developing a suitable CSP system reliability model.

3. Developing methodologies to integrate the PV/CSP models to power the system adequacy evaluation.

4. Performing case studies to assess the reliability contribution of PV/CSP energy systems to power system adequacy.

5. Comparing adequacy assessment of the large CSP and PV-integrated electric power system analysis.

6. Developing a reliability modeling of PV system incorporating cumulative dust.

1.5.1 Develop Reliability Models of Different Photovoltaic Topologies

The application of PV in large power systems is garnering considerable attention. The output power of PV systems varies depending on the availability of the PV system components and sunlight as well as the configuration of PV systems. The aim of this step is to develop a suitable analytical PV system reliability model that includes all major components for adequacy assessment. Probabilistic models will be developed for different PV topologies, such as central, string, and micro-inverter PV systems. In this step, the hierarchical Reliability Block Diagram will be developed to model the behavior of the overall PV system. Several types of system-level reliability models will be considered to come up with the most suitable model.

1.5.2 Adequacy Assessment of Different PV Topologies Integrated Electric Power System

A number of case studies will be performed with different combinations of PV topology energy sources to assess the contribution of these topologies to the overall system reliability. Sensitivity studies will also be carried out to assess the impact of different system parameters on the system adequacy. System parameters, such as site-

specific solar profile, outage probability of system components, and the system load

levels, can have a direct impact on the overall system reliability. Solar irradiation data

from different geographical locations were collected for use in the study. The data

include solar irradiation incremented at five-minute intervals from 2000 to 2005 for

different Saudi Arabian sites [45]. A reliability test system such as the Small Isolated

Power System (SIPS) will be used in this work. The incremental peak-load-carrying

capability and CC of PV different system topologies will be evaluated.

1.5.3 Probabilistic Reliability Models of Concentrated Solar Power Plants

A CSP plant includes components such as a reflector and receiver to focus direct

solar radiation onto a fluid to capture thermal energy. The captured heat can then be

converted into mechanical energy in a turbine that drives a generator to produce

electricity. The growing share of CSP plants in electric power systems creates the need

for including CSP in power system reliability studies. The availability of power from

CSP is affected by factors such as the failure and repair of the reflector, receiver, and

thermal unit in addition to the variability of solar irradiation. These factors will be

taken into account in developing a proper analytical CSP reliability model. The CSP

power plant generation also depends on Direct Normal Irradiation (DNI) and,

therefore, needs to be included in the generation model. An appropriate reliability

network model of the CSP system will be developed taking into consideration the key

system components and parameters as well as creating a probabilistic model of the power output from the CSP.

1.5.4 Adequacy Assessment of Concentrated Solar Power Integrated Electric Power System

A suitable system adequacy evaluation technique that integrates the reliability models developed in Section 1.5.3 will be developed in this step. The focus of this work is on adequacy assessment at the HL-I level and the capability of the entire generation system to incorporate different combinations of CSP capacity to satisfy continuously the total system demand. The electric generation and load models are combined to produce the risk model. A suitable test system consisting of conventional generation and CSP will be utilized to implement the overall system adequacy model developed in this work.

1.5.5 A Comparative Reliability Analysis of Electric Power Systems with A High Penetration of CSP and PV

The proposed system generation model that combines PV and CSP models to compare the system adequacy indices in a PV- or CSP-integrated power system is illustrated on a test power system. The Roy Billinton Test System (RBTS) [46] is used to perform the reliability comparison presented in this work. Several case studies have been carried out, including the impact of load growth and the growth in CSP and PV

penetration. The reliability indices obtained, with and without considering PV and CSP curtailment, are compared. The comparative analysis is categorized into the loss of load expectation (LOLE), loss of energy expectation (LOEE), effective load carrying capability (ELCC), and capacity credit (CC).

1.5.6   Incorporating the Effect of Cumulative Dust in Reliability Models of Generation System Including PV System

The main objective of this work is to incorporate cumulative dust into reliability modeling of the PV system. The application of the new analytical model in this section is demonstrated using the test power system to quantify the impact of cumulative dust on the reliability contribution of the PV system. The LOLE and LOEE indices are evaluated for both the dust-free conditions and the accumulated dust conditions in the PV system. This work is then extended to examine the impact of scheduling dust removal from the PV arrays on the generation system adequacy.

1.6   Thesis Outline

Appropriate analytical models and methods for conducting reliability assessment of the generation system encompassing different solar technologies are developed in this thesis. Several case studies are analyzed and discussed to demonstrate the applications of the proposed analytical models in a practical system.

Seven chapters are arranged and presented in this thesis to illustrate the contribution of this research project. The main content of each chapter is outlined as follows:

Chapter 1 presents a brief review of reliability evaluation concepts applicable to power system planning and the utilization of solar energy technologies in the electric system network. This chapter provides a literature review related to generation system adequacy evaluation incorporating PV and CSP. The problem statements and the main objectives are presented in this chapter.

Chapter 2 introduces a short background on the concept of generation system adequacy evaluation. The analytical generation model and system indices that are widely used in generation system reliability evaluation are presented in this chapter. The details of the two test systems and load models used in this work for the purpose of analyzing the application of the developed model is described in this chapter.

The detailed reliability model of PV system configurations is explained in Chapter 3. The Reliability Block Diagram is created for central, string, and micro PV systems with all major components taken into consideration. Chapter 3 also demonstrates the application of the developed model in a small isolated power system. The correlation of different system adequacy indices with key factors, such as system load variation, different amounts of solar energy installed, and different system PV topologies, is analyzed in this chapter.

Chapter 4 describes the reliability model of the generation system including the CSP system. The developed model considers the CSP components model and the probabilistic model of the output power of CSP. The probability distribution associated with different seasons is taken into account to build the overall COPT of a CSP. A simplified method that integrates the developed CSP model into the electric system is developed to examine the reliability contribution of CSP in a large grid-connected power system. The system reliability evaluation is quantified using different reliability indices such as LOLE, LOEE, ELCC, and CC. The impact of varying latitudes, peak-load variation, and seasonal effects on the generation system adequacy including the CSP system are examined in this chapter.

Chapter 5 provides a comprehensive analysis of the comparative reliability contribution of convolving a high penetration of CSP and PV to the electric power system. In order to compare the benefit of the two technologies studies carry out assuming the two technologies were installed at the same capacity energy level for both technologies.

Chapter 6 illustrates the impact of cumulative dust on the reliability modeling of the PV system. The polynomial regression model is created based on an experimental test provided by a group of researchers in KSA [42,43]. The impact of the accumulated dust on the PV surface on the reliability contribution of the PV system is studied.

Thereafter, scheduling dust removal is applied to quantify the impact of scheduled maintenance on the system adequacy of PV.

Chapter 7 summarizes the main contributions of this research work.

1.7   Summary

An extensive survey has been presented in this chapter to determine the state of art research done on the reliability modeling of solar technologies.   This review highlighted the required parameters to develop a new appropriate reliability modeling generation system incorporating PV and CSP systems. These parameters include major components and system topologies. Moreover, the literature survey underlined the lack of research of incorporating the cumulative dust on the reliability modeling of PV system. The methodology and application of the developed PV/CSP model have been addressed.   The importance of developing proper PV/CSP models and creating methodology to integrate them in the overall system model are discussed in this chapter.

2   Review Generation System Adequacy Assessment

2.1   Introduction

System adequacy evaluation is an important task in the planning, design, maintenance, and upgrade of an electric power system.   The generation system connected to an electric power system network should be able to produce adequate power to meet the load demand at all times.   Therefore, system planners should periodically assess the availability of the generation system to make sure that a specified adequacy criterion is continually met.   Figure 2.1 shows the conceptual reliability model at the HL-I level in which the entire system generation is represented by a generation model and is connected to the overall system load model.
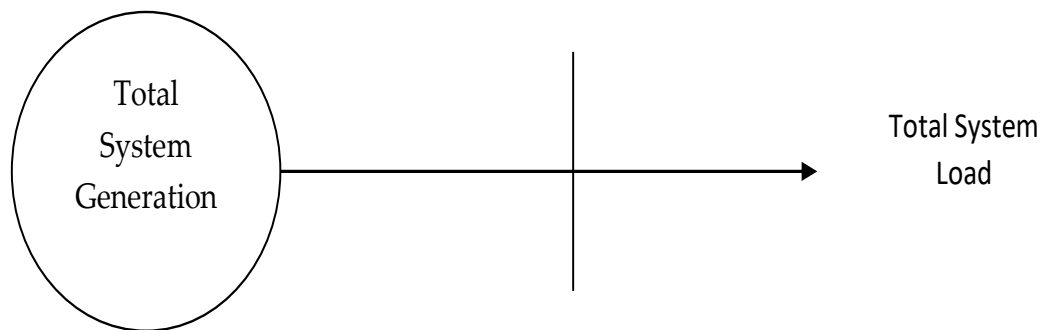
Figure 2-1: Generation adequacy evaluation model

The transmission system is not considered in the generation system reliability evaluation at the HL-I level. The basic concepts involved in the development of the generation system model, load model, and reliability assessment methods are introduced in this chapter. The common reliability indices used to quantify system adequacy are also discussed in this chapter.

Deterministic methods were conventionally used to estimate the required generation capacity reserve in a power system to maintain acceptable system adequacy. These methods are easy to apply and are still used in different areas of power systems to ensure acceptable reliability. The following section describes the various deterministic approaches used in generation system adequacy.

2.2 Deterministic Techniques for Generation System Adequacy

Deterministic methods have been adopted in power system planning for many years [47], [48]. These methods have been used to determine the system RM or the required capacity in a generation system to satisfactorily meet the system demand. The most commonly used deterministic criteria in capacity planning are:

1. Capacity Reserve Margin

RM is defined as the amount of generation capacity beyond the system peak load (PL) and is required to account for generating-unit random failures and uncertainty in customer demand. RM is expressed as a percentage of the system PL or the total

installed capacity (IC), as shown in (2.1). A fixed percentage of RM is used as a criterion

for evaluating the capacity requirement in this method.

$$RM = \frac{IC - PL}{IC} \times 100\% \qquad (2\text{-}1)$$

2. Loss of the Largest Unit (LLU) or (N-1)

The LLU or N-1 criterion [3] requires the RM of the generation system to be at

least equal to the largest generating unit in the system. This criterion ensures that the

system load is satisfied even when the largest generating unit is out of service. In other

words, the load will not be curtailed if any single generating unit in the system fails.

3. Loss of the Largest Unit and Capacity RM

The LLU and capacity RM is a combination of the previous two criteria, in which

the capacity RM should be equal to or greater than the sum of the largest unit and a

fixed percentage of the PL or IC system.

The deterministic method can be used easily to evaluate the total capacity

required in the overall power system. However, it is not capable of accounting for the

random nature of power system behavior [2]. The three aforementioned criteria do not

define the true risk in the power system. Most electric power companies have the

propensity to use probabilistic techniques for capacity planning with the increase in

uncertainty in power generation due to rapid growth of renewable and intermittent generation sources. Table 2-1 illustrates the results of a survey conducted in 1964–1977 regarding the criteria used in capacity reserve planning [7]. Table 2-1 shows that electric power companies have gradually adopted probabilistic criteria. In 1987, most utilities turned to probabilistic techniques, with only one utility using a deterministic criterion along with supplementary checks for the probabilistic index.

Table 2-1: Criteria used in generation capacity planning

Criterion	Survey Date					
	1964	1969	1974	1977	1979	1987
Percent RM	1	4	2	2	3	1*
LLU	4	1	1	1	-	-
Combination of 1 and 2	3	6	6	6	2	-
Probabilistic Method	1	5	4	4	6	6
Other Methods	2	1	-	-	-	-

*With supplementary checks for probabilistic index LOLE

2.3 Probabilistic Techniques for Generation System Adequacy

Probabilistic methods are capable of responding to the stochastic nature of power systems and can provide quantitative risk assessment in generation system adequacy evaluation. The need for the application of probabilistic methods for evaluating the risk indices [1,2] to respond to the random nature of system behavior has been widely recognized. Probabilistic techniques have been implemented by the majority of Canadian electric utilities for system adequacy evaluation at the HL-I level [7].

The HL-I reliability indices quantify the ability of a particular generation configuration to continuously satisfy the load demand. These indices are influenced by a range of factors, such as the number and capacity of generating units, unit failures, load levels, and load variation patterns. The unavailability (U) of a generating unit [1], [3] is defined as the probability of the unit undergoing a random failure and not being available to serve the load. This is conventionally known as the forced outage rate (FOR). This is an essential input parameter of each generating unit that is required to create the generation model for HL-I evaluation [1], [3]. The availability (A) is the complement of the unavailability, or A = 1 – U. Because of the various operating conditions as shown in Figure 2.2 [49], a generating unit may be available or unavailable at any point in time.
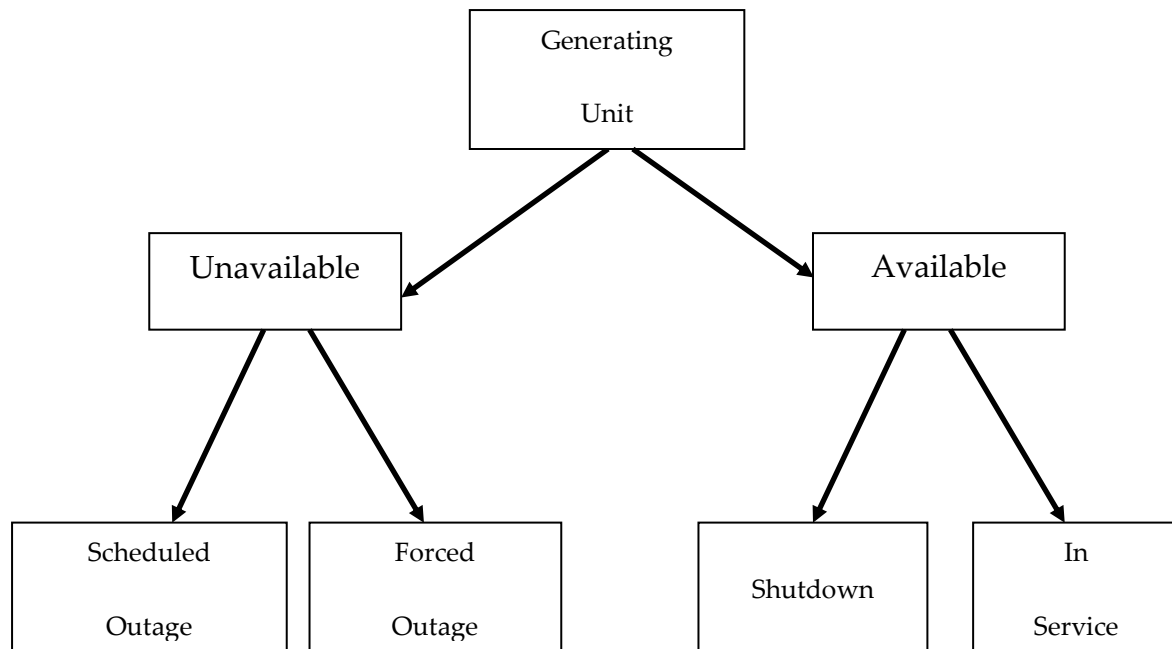
Figure 2-2: Generating-unit states

Probabilistic approaches can be broadly classified into the following two techniques: 1) the analytical technique and 2) the simulation technique [3], [4]. The adequacy evaluation results from the application of these two probabilistic approaches are outlined in the following sections:

2.4   Analytical Techniques

Analytical techniques represent the system using numerical models and evaluate the system indices from these models using mathematical solutions. These approaches estimate the system risk using a mathematical mode. These techniques can provide accurate system indices through a simple method in a short time. The broad range of analytical techniques utilized in HL-I and HL-II studies is demonstrated in [5], [50-52].

The basic approach in HL-I adequacy evaluation is to develop a generation model and a load model for the complete power system and then convolve the two models to formulate the system risk model as shown in Figure 2-3.
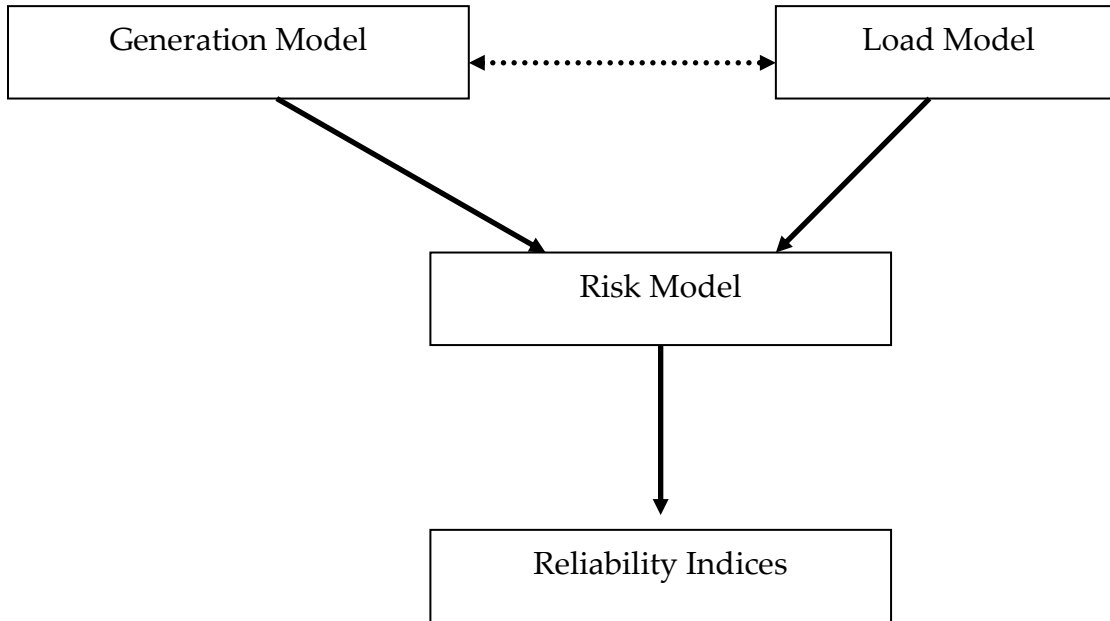
Figure 2-3: Elements of generation reliability evaluation

2.4.1   Generation and Load Models

The FOR or the unavailability of each generating unit is required to construct the system generation model [3]. The base-load generating units that operate continuously are represented by a two-state Markov model, in which the generating unit can be represented as being either in the operating or "Up" state, or failed or "Down" state, as shown in Figure 2-4. The A and U can be defined using Equations (2-2) and (2-3), respectively [3], where λ and μ are the failure rate and repair rate of the generating unit.

The reciprocals of λ and μ are the mean time to failure (MTTF) and the mean time to repair (MTTR) respectively. The generating system model used for generation capacity adequacy evaluation is a discrete probability distribution of available or unavailable capacities, that can be tabulated in the form of a capacity outage probability table (COPT). Table 2-2 depicts the layout of a COPT where the first and second columns represent the capacity on outage and the corresponding probability.

```
┌──────────────────┐        ┌──────────────────┐
│       Up         │───────▶│      Down        │
│                  │◀───────│                  │
└──────────────────┘        └──────────────────┘
```
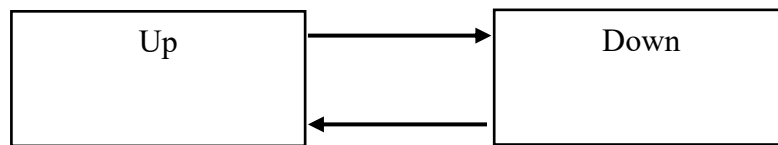
Figure 2-4: Two state generation model

$$A = \frac{\mu}{\mu+\lambda} = \frac{m}{m+r} = \frac{\Sigma\,\text{Up time}}{\Sigma(\text{Up time}+\text{Down time})} \qquad (2\text{-}2)$$

$$U = \frac{\lambda}{\mu+\lambda} = \frac{r}{m+r} = \frac{\Sigma\,\text{Down time}}{\Sigma(\text{Up time}+\text{Down time})} \qquad (2\text{-}3)$$

where:

$$m = \text{Mean time to failure} = \text{MTTF} = \frac{1}{\lambda} \qquad (2\text{-}4)$$

$$r = \text{Mean time to repair} = \text{MTTR} = \frac{1}{\mu} \qquad (2\text{-}5)$$

Table 2-2: Typical capacity outage probability table (COPT)

Capacity Out	Associated Probability
List all combinations of possible capacity outage states	List all corresponding probabilities of each capacity state

A test SIPS and the RBTS [46] were employed in this thesis to illustrate the reliability analysis. The contrasts between these systems are the size and the configuration. A SIPS is usually located in a remote area or in island communities with a typically low load demand. This system, in fact, may or may not have transmission lines, and it is not connected with any other electric power system. The test system adopted in this thesis has one 70-kW and two 40-kW generating units with a total system capacity of 150 kW. Each generating unit has a FOR of 5%. The peak load is of 80 kW. This system is designated as SIPS and meets the deterministic LLU or N-1 criterion [3]. A 1995 survey of SIPS in Canadian utilities is shown in Table 2-3 [53].

Table 2-3: SIPS in Canadian utilities

Utility	Number of SIPS	Total Installed Capacity (kW)	Largest System (kW)	Smallest System (kW)
Newfoundland Hydro	30	46,775	18,750	90
Hydro Quebec	21	56,000	11,200	550
Ontario Hydro	23	20,226	2,350	170
Manitoba Hydro	12	18,445	4,085	350
Saskatchewan Power	1	132	132	132
Alberta Power Ltd.	27	35,295	16,880	40
BC Hydro	9	35,550	9,420	1,850
NWT Power Corp.	47	188,000	52,560	70
Yukon Electrical	7	8,855	5,050	245

The RBTS has been employed for over 20 years by researchers conducting reliability assessments and other probabilistic applications in electric power systems. This system was developed at the University of Saskatchewan for learning and research

purposes. It is larger than SIPS and includes 11 generating units, six buses, and nine transmission lines, as illustrated in Figure 2-5. The generating-unit data for RBTS are shown in Table 2-4. The total installed generation capacity is 240 MW, and the system peak load is 185 MW. The annual chronological hourly load profile of the IEEE-RTS [54] is shown in Figure 2-6 and is utilized in both test systems. Both test systems utilize the annual chronological hourly load profile of the IEEE-RTS [54].
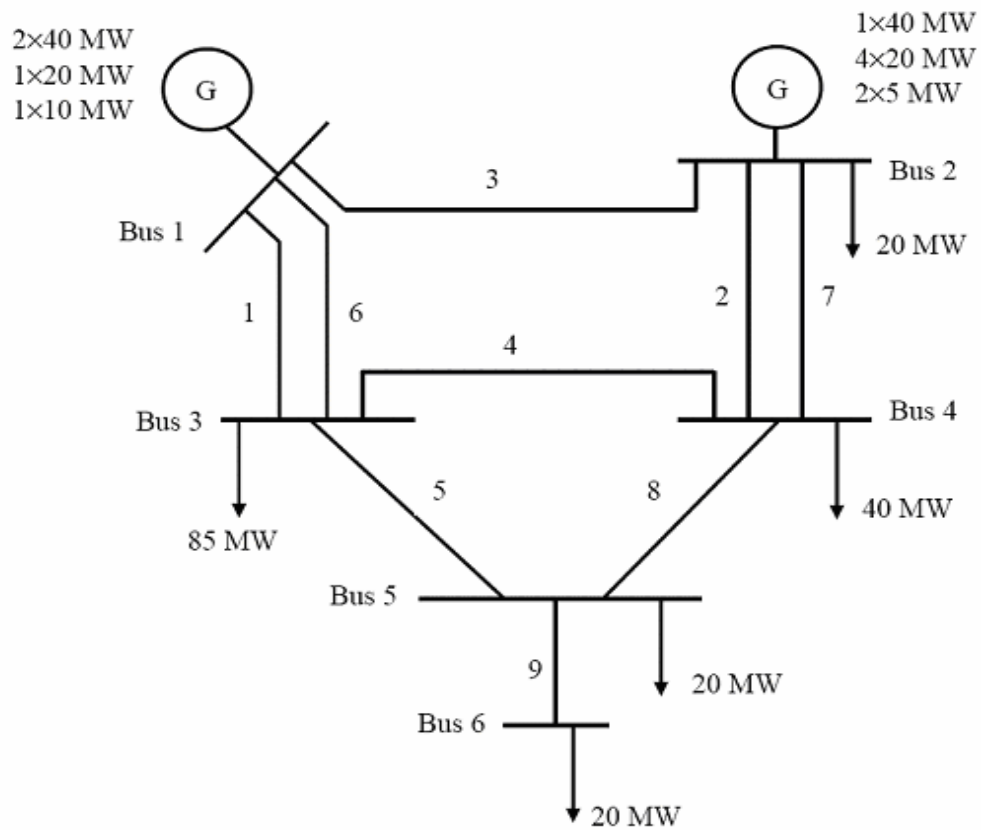
Figure 2-5: Roy Billinton test system [46]

Table 2-4: RBTS data

Unit Type	No. of Units	Rated Power (MW)	MTTF (hr)	MTTR (hr)	FOR
Hydro	1	40	2920	60	0.02
Thermal	1	10	2190	45	0.02
Thermal	1	20	1752	45	0.025
Hydro	2	5	4380	45	0.01
Thermal	2	40	1460	45	0.02
Hydro	4	20	3650	55	0.015
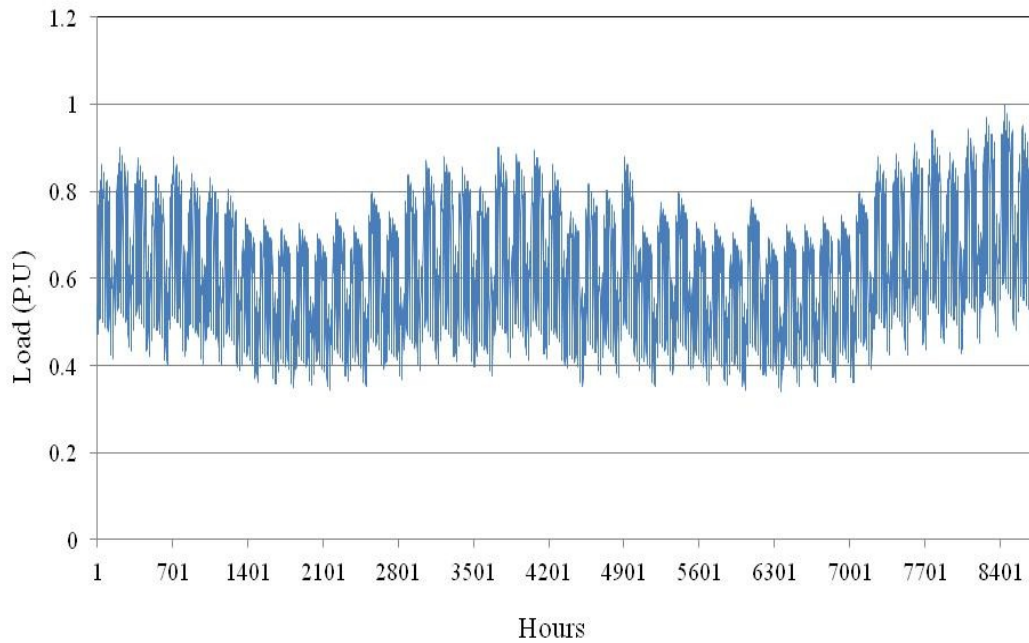
Figure 2-6: Hourly load model

2.4.2 System Risk Indices

The system generation model in the form of a COPT [4] is convolved with the system load model to obtain the system risk indices. The loss of load expectation (LOLE) and the loss of energy expectation (LOEE) are the most widely used adequacy indices at the HL-I level [3]. The LOLE is the expected number of days (or hours) in a year that the system generation cannot meet the system load demand. The LOEE is an energy-based index defined as the expected energy not supplied in a year due to inadequate capacity, and it provides information about the magnitude of the forced

outage.   The LOLE and LOEE are determined using Equations (2-6) and (2-7),

respectively, as shown in Figure 2-7.

$$\text{LOLE} = \sum_{k=1}^{n} p_k \times t_k = \sum_{k=1}^{n} P_k \times (t_k - t_{k-1}), \qquad (2\text{-}6)$$

$$\text{LOEE} = \sum_{k=1}^{n} P_k \times E_k, \qquad (2\text{-}7)$$

where,

n = the number of capacity outage states,

p_k = probability of the capacity outage O_k ,

t_k = the time for which load loss will occur due to O_k ,

P_k = cumulative outage probability for capacity state O_k ,

E_k = energy not supplied.
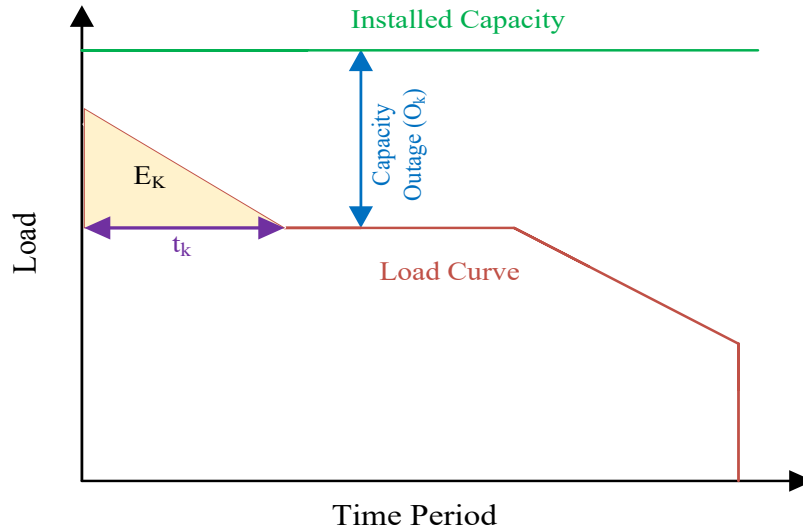
Figure 2-7: Evaluation of loss of load expectation (LOLE) and loss of energy expectation

(LOEE) using an hourly load curve.

The capacity contribution of an installed generation unit in maintaining the reliability of the overall system is a function of many factors. These include the rated capacity, type, and FOR of the generation unit, the system load profile, and the acceptable system risk level. The expected load carrying capability (ELCC) and capacity credit (CC) are used in this work to evaluate the capacity value contribution of the solar generation systems. The capacity credit of a conventional generating unit is close to its rated value. The capacity credit of intermittent generation sources, such as PV and CSP are much lower than their rated values. The methodology for calculating the ELCC is described in [55,56]. Figure 2-8 shows the mathematical method for the estimation of the ELCC.

Figure 2-8 illustrated that the ELCC is the additional load that can be carried with the addition of new generation while maintaining the LOLE at a constant value. When ELCC is expressed as a percentage of the rated capacity C_A of the generating unit, as expressed in Equation (2-8), it is known as its CC This is another important index in capacity value evaluation. The overall system reliability evaluation process is shown in Figure 2-9.

$$CC = \frac{ELCC}{C_A} \times 100 \qquad (2-8)$$
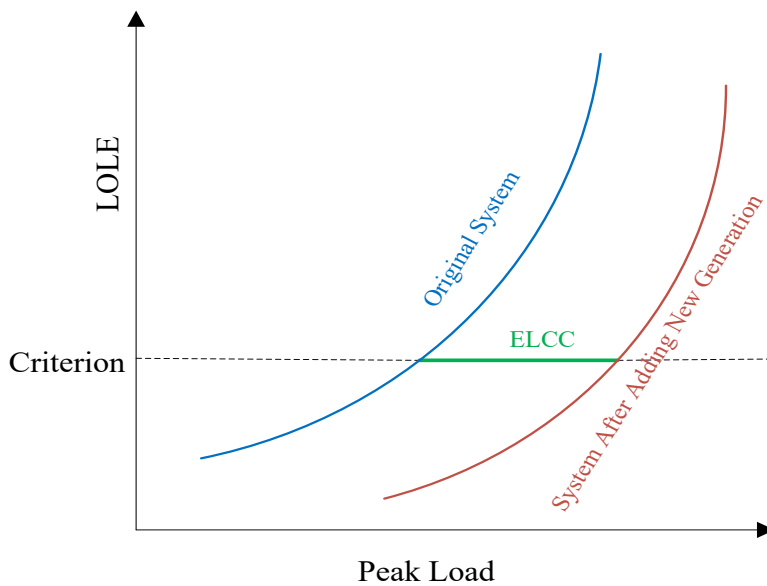
Figure 2-8: Evaluation of effective load-carrying capability (ELCC).

Identify the System	• Define all major system components. • Compute the force outage rate of these components. • Construct the COPT of the overall system generation
Identify the system load model	• Construct system load model using hourly load data, daily data, or seasonal data.
Identify the system criteria	• Define an acceptable system risk level.
Developing the system model	• Convolve all system generation models and combine this with the load model
Evaluate the basic reliability indices	• Calculate the loss of load probability, LOLE, LOEE.
Sensitivity studies	• Using different impact factors such as peak load variation, different system generation capacity, seasonal study, geographical location, weather, etc.

Figure 2-9: Generation system adequacy model construction process

2.5   Base Case Studies for SIPS and RBTS

A generation capacity adequacy evaluation of the test SIPS and the RBTS were performed using the analytical method. The first study was carried out on the SIPS. The total installed generation capacity of SIPS is 150 kW, and the system peak load is 80 kW. The LOLE and LOEE results are shown in Table 2-5. A similar study was also conducted on the RBTS. The total installed generation capacity of the RBTS is 240 MW, and the system peak load is 185 MW. The LOLE and LOEE of RBTS are given in Table 2-5. The base case LOLE and LOEE results shown in Table 2-5 provide a base reference framework for system development and sensitivity analysis presented in subsequent chapters.

Table 2-5: The annual system indices for using SIPS and RBTS

SIPS		RBTS	
LOLE (h/y)	LOEE (kWh/y)	LOLE (h/y)	LOEE (MWh/y)
32.26	483.46	1.09	9.86

2.6   Summary

System adequacy evaluation is an important aspect in electric generation system expansion planning. This assessment is periodically done to ensure that the generation capacity is sufficient to deliver the adequate electricity when

required. A wide range of methods have been developed and used to evaluate the generation system adequacy. This chapter discussed the deterministic methods and the probabilistic methods used in HL-I evaluation. The analytical method signifies the system model mathematically and computes the system reliability indices using a numerical solution. The process involved in the analytical method in terms of generation, load, and risk models are illustrated. This chapter discussed the reliability indices LOLE, LOEE, ELCC, and CC that are important in HL-I adequacy measurement. Two test systems, designated as the RBTS and the SIPS, are described and utilized to illustrate the analytical method. The LOLE and LOEE results obtained in the base case study presented in this chapter will provide a e reference for further studies that are reported in the following chapters of the thesis.

3   Reliability Models of Generation Systems Including Different Photovoltaic Topologies

3.1   Introduction

PV systems contain solar cell panels, power electronic converters, high-power switching, and often, transformers. These components collectively play an important role in determining the reliability of PV systems. Moreover, the power output of PV systems is variable, so it cannot be controlled as easily as conventional generation owing to the erratic nature of the weather conditions. Therefore, solar power has a different influence on generation system reliability as compared with conventional power sources. Recently, different PV system designs have been constructed to maximize the output power of PV systems. These different designs are commonly adopted based on the scale of a PV system. Large-scale grid-connected PV systems are generally connected in a centralized or a string structure. Central and string PV schemes are different in terms of the nature of the connection of the inverter to PV arrays. Another PV topology is the micro-inverter system. It is, therefore, important to evaluate the reliability contribution of the PV systems under these topologies.

This chapter provides a comprehensive overview of the reliability models of PV systems and presents the reliability quantification process of central, string, and micro-inverter PV systems. The developed models are embedded in the reliability evaluation

47

methodology to obtain a discrete probability distribution in the form of COPT [3]. This is done using individual component failure and repair rates assuming the exponential distribution of times to failure and repair

The LOLE [3] and LOEE [3] indices are used in this work to quantify the reliability of the PV-integrated systems. The CC and ELCC are calculated to estimate the capacity values of the different PV system topologies. The application of system reliability risk indices provides valuable quantitative risk measures and is illustrated using a small isolated power system. The main contribution of this work is the development of a detailed analytical reliability model of a PV system that accounts for PV system components and topologies. The benefits of adding the different PV system topologies are quantified using the indices, LOLE, LOEE, ELCC, and CC.

3.2 Modeling of PV Systems

This section presents a probabilistic framework for developing an overall reliability model of the PV system. There are three types of system-level reliability models: part-count, combination, and state-space models. Part-count is utilized in this project because this model can provide adequate reliability estimation. Three assumptions are made in order to apply this model.

A. The overall system will fail if any component or subsystem fails.

B. The failure rate of each component remains constant during its useful lifetime.

C. The overall system is modeled as a series reliability block network as shown in Figure 3-1.

The probability of an up (P_{up}) and down (P_{down}) state system model can be evaluated using Equations (3-1) and (3-2), respectively. This section is divided into four subsections.

$$P_{up} = \frac{\mu_1}{\mu_1 + \lambda_1} \times \frac{\mu_2}{\mu_2 + \lambda_2} \times \frac{\mu_3}{\mu_3 + \lambda_3} \times \cdots \cdots \times \frac{\mu_n}{\mu_n + \lambda_n} \tag{3-1}$$

$$P_{Down} = 1 - P_{up} \tag{3-2}$$
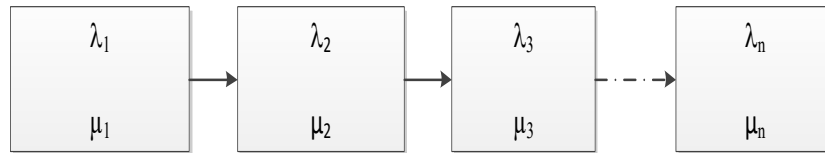
Figure 3-1: Series reliability block network with n subsystems

3.2.1 Modeling the Output Power of a Solar Cell

The analytical model used in evaluating the power output of solar cells depends on the following two main factors: solar cell efficiency and solar irradiation. The efficiency of a solar cell varies with the amount of solar irradiation, and it can be evaluated applying (3-3) and (3-4) [57]. The power output from a solar cell can be calculated using (3-5) and (3-6) as shown in Figure 3-2 [57].
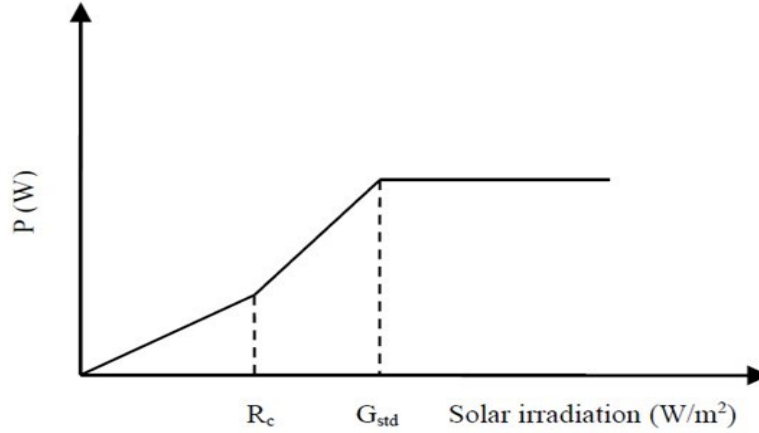
Figure 3-2: The power output of a solar cell

$$\text{Eff} = \frac{\eta_c}{R_c} \times G_{bi} \qquad\qquad 0 \leq G_{bi} < R_{c'} \qquad\qquad\qquad (3\text{-}3)$$

$$Eff = \eta_c \qquad\qquad R_c \leq G_{bi'} \qquad\qquad\qquad (3\text{-}4)$$

$$P = P_{sn} \times \frac{G_{bi}^2}{G_{std} \times R_c} \qquad\qquad 0 \leq G_{bi} < R_{c'} \qquad\qquad\qquad (3\text{-}5)$$

$$P = P_{sn} \times \frac{G_{bi}}{G_{std}} \qquad\qquad R_c \leq G_{bi} < G_{std'} \qquad\qquad\qquad (3\text{-}6)$$

where P is the power output of the solar cell in W; G_{bi} is global solar irradiation in W/m²; G_{std} is solar irradiation in a standard environment set as 1000 W/m²; R_c is a certain irradiation point set as 150 W/m²; and P_{sn} is the equivalent rated capacity of PV in W. The solar irradiation data is grouped into a number of intervals. A step size of 50 W/m² was used to create these intervals. The output power associated with each interval is represented by the mid value of the interval. The probability of the power output can

be obtained from Equation (3-7), where N_i is the number of data occurrences in the interval i.

$$\text{Probability}_i = \frac{N_i}{\text{Total Number of Samples}} \qquad (3\text{-}7)$$

The power output and its probability are calculated for each interval, and a discrete probability distribution of available power from the PV system created to form the PV capacity model. This approach was used to create the capacity model for PV system considering historical solar irradiation data of Medina located in Saudi Arabia [45]. The data include solar irradiation at five-minute intervals during 2000–2005 for different sites [45]. The total collected data of solar irradiation at five-minute intervals for five years are 525,600 samples. The power output of the solar cell device depicted in Table 3-1 is in per unit (pu) and was created using Equations (3-3)– (3-7).

Table 3-1: Capacity model of PV considering 100% reliable PV system components

State	Capacity (pu)	Probability	State	Capacity (pu)	Probability
1	0	0.4774	12	0.525	0.023
2	0.004	0.0763	13	0.575	0.0223
3	0.037	0.0313	14	0.625	0.0255
4	0.104	0.0217	15	0.675	0.0300
5	0.175	0.0195	16	0.725	0.0274
6	0.225	0.0252	17	0.775	0.0239
7	0.275	0.0212	18	0.825	0.0223
8	0.325	0.0201	19	0.875	0.0244
9	0.375	0.0172	20	0.925	0.0193
10	0.425	0.0219	21	0.975	0.0182
11	0.475	0.0235	22	1	0.0081

Since PV systems can produce power during daytime only, a daytime capacity model is developed to model the contribution of these intermittent power sources. Different seasons have different durations of daylight time depending on the geographical location. The same process using (3-3)– (3-7) as described earlier is

applied for different seasons considering respective daytime data. Tables 3-2, 3-3, 3-4, and 3-5 show the daytime capacity model of a PV at the Medina location.

Table 3-2: Winter daytime capacity model of PV considering 100% reliable PV system

State	Capacity (pu)	Probability	State	Capacity (pu)	Probability
1	0.004	0.1426	12	0.575	0.0627
2	0.037	0.0798	13	0.625	0.0789
3	0.104	0.0466	14	0.675	0.0798
4	0.175	0.0219	15	0.725	0.0627
5	0.225	0.0561	16	0.775	0.0342
6	0.275	0.0523	17	0.825	0.0314
7	0.325	0.0513	18	0.875	0.0181
8	0.375	0.0257	19	0.925	0.0000
9	0.425	0.0494	20	0.975	0.0000
10	0.475	0.0542	21	1	0.0000
11	0.525	0.0523			

Table 3-3: Spring daytime capacity model of PV considering 100% reliable PV system

State	Capacity (pu)	Probability	State	Capacity (pu)	Probability
1	0.004	0.1439	12	0.575	0.0406
2	0.037	0.0403	13	0.625	0.0401
3	0.104	0.0492	14	0.675	0.0401
4	0.175	0.0472	15	0.725	0.0398
5	0.225	0.0454	16	0.775	0.0474
6	0.275	0.0296	17	0.825	0.0517
7	0.325	0.0388	18	0.875	0.0606
8	0.375	0.0354	19	0.925	0.0574
9	0.425	0.0430	20	0.975	0.0522
10	0.475	0.0391	21	1	0.0241
11	0.525	0.0341			

Table 3-4: Summer daytime capacity model of PV considering 100% reliable PV system

State	Capacity (pu)	Probability	State	Capacity (pu)	Probability
1	0.004	0.1339	12	0.575	0.0322
2	0.037	0.0819	13	0.625	0.0279
3	0.104	0.0362	14	0.675	0.0447
4	0.175	0.0162	15	0.725	0.0531
5	0.225	0.0396	16	0.775	0.0356
6	0.275	0.0482	17	0.825	0.0478
7	0.325	0.0400	18	0.875	0.0672
8	0.375	0.0191	19	0.925	0.0591
9	0.425	0.0287	20	0.975	0.0719
10	0.475	0.0452	21	1	0.0262
11	0.525	0.0453			

Table 3-5: Fall daytime capacity model of PV considering 100% reliable PV system

State	Capacity (pu)	Probability	State	Capacity (pu)	Probability
1	0.004	0.1620	12	0.575	0.0396
2	0.037	0.0312	13	0.625	0.0592
3	0.104	0.0469	14	0.675	0.0643
4	0.175	0.0526	15	0.725	0.0592
5	0.225	0.0497	16	0.775	0.0620
6	0.275	0.0308	17	0.825	0.0488
7	0.325	0.0369	18	0.875	0.0438
8	0.375	0.0460	19	0.925	0.0212
9	0.425	0.0431	20	0.975	0.0043
10	0.475	0.0421	21	1	0.0078
11	0.525	0.0485			

3.2.2 Modeling Central PV System

Each component of the PV system is represented by 2-state Markov model in which the component is either in the operation state or the failed with certain probabilities. The multi-state PV capacity model described in Section 3.2.1 is combined with a two-state model of central PV system components described in this section. The main components of a typical central PV system are illustrated in Figure 3-3. This

56

central PV system consists of a solar array, bulk DC-link capacitor, inverter, line filter, AC switch, AC circuit breaker, and transformer. The functional block diagram of this PV system is shown in Figure 3-4.

Past reliability research of power electronic components has focused on the failure rate models of conductors, capacitors, and magnetic devices [58,59]. However, field experience has demonstrated that electrolytic capacitors and switch devices are the most vulnerable components [60]. The MIL-HDBK-271F second edition military handbook [61] provides an extensive reliability database for power electronic components. This database was used in this work to evaluate the failure rate of power electronic components.
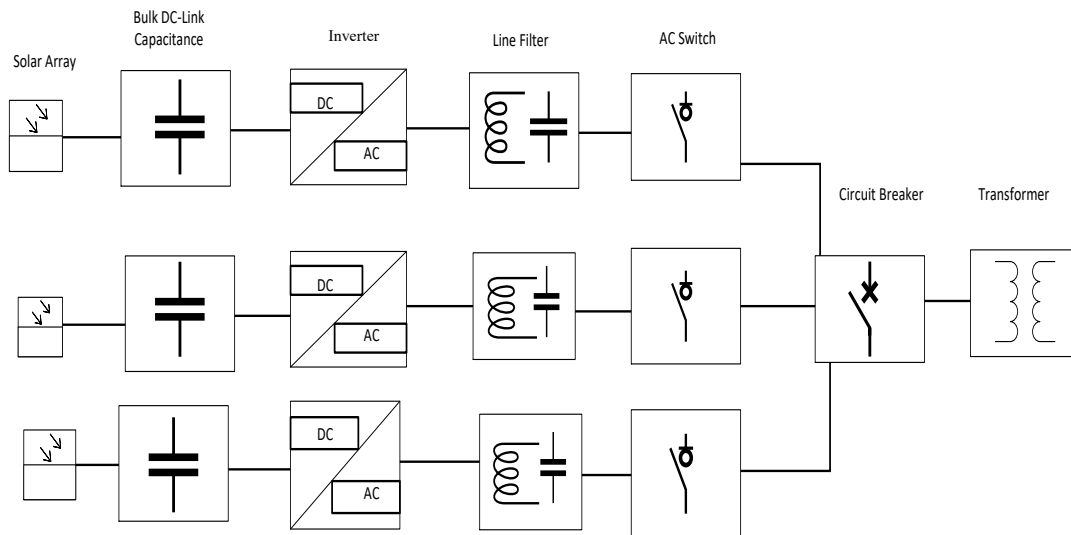
Figure 3-3: Schematic of a typical central PV system

```
                    ┌─────────────────────────┐
                    │       Solar Array       │
                    └─────────────────────────┘
                                 │
                                 ▼
                    ┌─────────────────────────┐
                    │    DC-Link Capacitance   │
                    └─────────────────────────┘
                                 │
                                 ▼
                    ┌─────────────────────────┐
                    │      DC/AC Inverter      │
                    └─────────────────────────┘
                                 │
                                 ▼
                    ┌─────────────────────────┐
                    │    AC Circuit Breaker    │
                    └─────────────────────────┘
                                 │
                                 ▼
                    ┌─────────────────────────┐
                    │        Transformer       │
                    └─────────────────────────┘
```
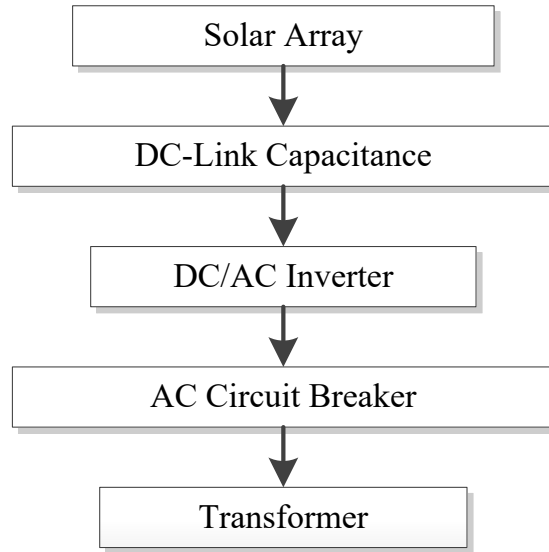
Figure 3-4: A functional block diagram of a central PV system

➢ Solar panel

Solar panels consist of solar cells. The solar cells have a very low failure rate. Most manufacturers offer a warranty of 20–25 years on their solar module [62] and have demonstrated very high reliability in the field with a mean time between failure (MTBF) of 522 and 6666 years for residential and utility systems, respectively [63]. The effect of PV panel architecture on the overall system reliability is therefore not considered in this work.

➢ DC-link Capacitor

The failure rate of capacitors is considered as one of the major factors that lead to the failure of PV systems. Capacitors can be made from different materials, such as an

electrolytic capacitor, paper, plastic film, tantalum, and ceramic [64]. The failure rate

[64] depends on the material. The electrolytic capacitor is considered in this work. The

failure of inductors is not considered because it has a low failure rate [65]. Equations (3-

8)–(3-10) are used to evaluate the failure rate of capacitors (λ_{cap}) [66-68], where n is the

total number of components in the system; λ_{base} is the base failure rate of capacitors and

equal to 0.0314 occur/year; π_E is the effect of environmental stress and is equal to 1; π_Q is

the quality factor and is equal to 1; C is the capacitance value in microfarad (μF); and T_j

is the junction temperature, which is 50 °C. The total failure rate of the DC-link

capacitor is 0.4449 occur/year.

$$\lambda_{cap} = n \times \lambda_{base} \times \pi_{cv} \times \pi_Q \times \pi_E \times \pi_T \tag{3-8}$$

$$\pi_{cv} = 0.34 \times C^{0.18} \tag{3-9}$$

$$\pi_T = \exp^{-4061.74 \times (\frac{1}{T_j+273} - \frac{1}{198})} \tag{3-10}$$

➢ Inverter

The MTBF of a PV inverter is between 1 and 16 years [63]. The inverter is

considered as another major factor in the failure of PV systems. A three-phase two-

level voltage-source inverter is considered in this work. This inverter has six switches

and diodes. This work does not treat the inverter as one black box. Each component

inside the inverter is considered a major factor in failure. A Reliability Block Diagram

[69,70] is developed in this project based on reliability network modeling concepts. This technique involves the use of switches and diodes connected in series, and this is known as a series Reliability Block Diagram as shown in Figure 3-1. The failure rate of the inverter (λ_{inv}) can be evaluated using Equation (3-11). Equations (3-12)– (3-15) are used to evaluate the failure rates of diodes (λ_{diode}) [66-68].

$$\lambda_{inverter} = 6 \times \lambda_{diode} + 6 \times \lambda_{switch}, \tag{3-11}$$

$$\lambda_{diode} = n \times \lambda_{base} \times \pi_s \times \pi_Q \times \pi_E \times \pi_T \times \pi_c, \tag{3-12}$$

$$\pi_T = \exp^{-3091 \times (\frac{1}{T_j+273} - \frac{1}{198})}, \tag{3-13}$$

$$\pi_s = \begin{pmatrix} 0.054 & V_s \leq 0.3 \\ V_s^{2.48} & 0.3 \leq V_s \leq 1 \end{pmatrix}, \tag{3-14}$$

$$V_s = \frac{Operated\ Volatge}{Rated\ Volatge}, \tag{3-15}$$

where n is the total number of components in the system; λ_{base} is the base failure rate of diodes and is equal to 0.025 occur/year; π_E is equal to 6; π_S is the electric stress factor; the operating voltage and rated voltages are 607 V and 690 V respectively; π_Q is equal to 5.5; π_j is the temperature stress factor; T_j is equal to 50 °C; and π_c is the contact construction factor. Equations (3-16) and (3-17) are used to evaluate the failure rates of the switches (λ_{switch}) [66-68].

$$\lambda_{switch} = n \times \lambda_{base} \times \pi_Q \times \pi_E \times \pi_T, \qquad (3\text{-}16)$$

$$\pi_T = \exp^{-1925 \times (\frac{1}{T_j + 273} - \frac{1}{198})}, \qquad (3\text{-}17)$$

where λ_{base} is the base failure rate of the switches, which is 0.012 occur/year; π_E is equal to 1; π_Q is equal to 5.5; and T_j is equal to 50 °C. The total failure rate of the inverter is 0.095 occur/year.

➢   AC Circuit Breaker and Transformer

The reliability database provided by [71] is used to calculate the probability of failure of these components. The reliability data of common PV system components are presented in Table 3-6. The probability of up and down states of a central PV system is shown in Table 3-7. Table 3-7 is then combined with Tables 3-2 to 3-5 to build the overall central PV system model. This model represents the multi-states model of the power output of a central PV system including the component failure factors as shown in Figure 3-5.

Table 3-6: Failure and repair data

Component	Failure Rate (occur/year)	Repair Time (hour)
Capacitor	0.0314	100
Diode	0.025	96
IGBT	0.012	513
Circuit Breaker	0.003	54
Transformer	0.006	168

Table 3-7: The two-state model of a central PV system

State	Probability
Up	0.98
Down	0.02
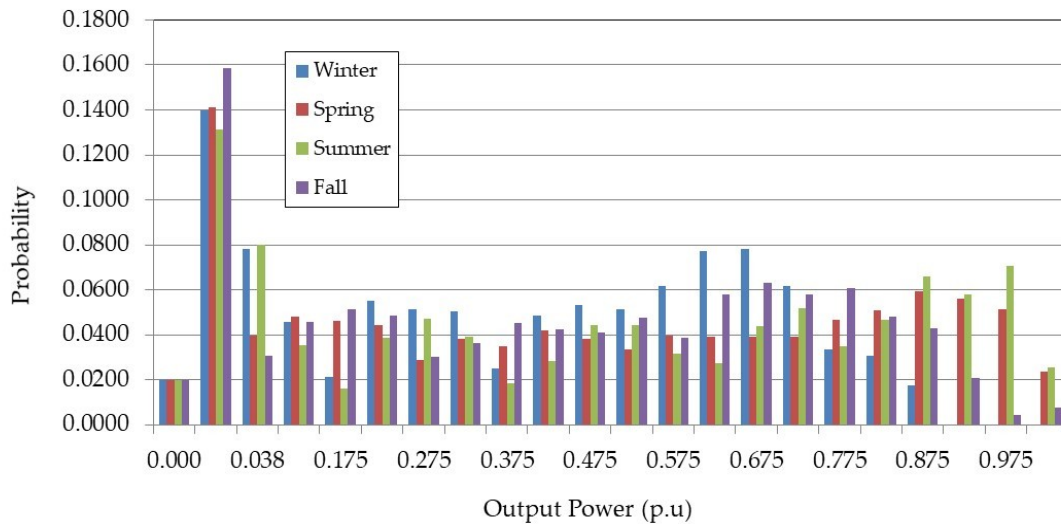
Figure 3-5: Seasonal daytime capacity models of a central PV system

3.2.3   Modeling a String Inverter PV System

As noted earlier, the schematic construction of a PV inverter plays an important role in the availability of power from a PV system. A typical PV inverter system, as illustrated in Figure 3-6, is utilized in this work. In this design, each string inverter is rated at 10 kW, and hence, five string inverters are required to produce 30% of the total installed capacity. The functional block diagram of this PV system is illustrated in Figure 3-7.

Bulk DC-Link
Capacitance

Solar Array

DC
DC

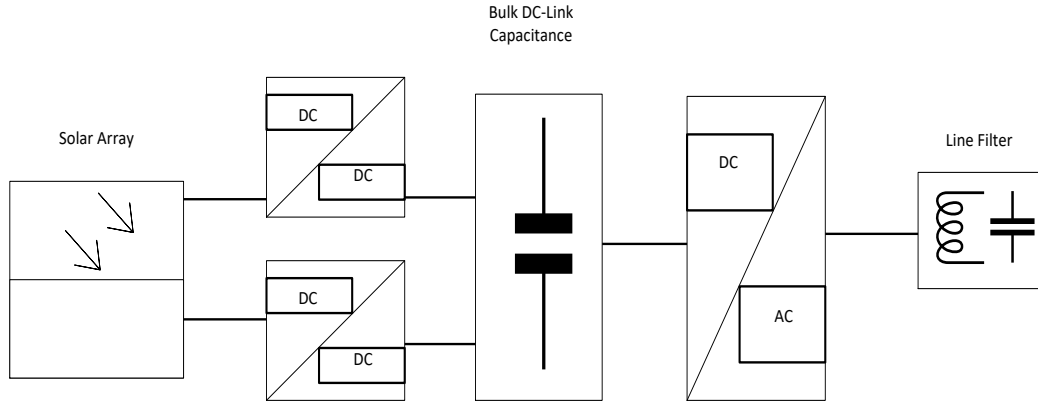DC
DC

DC

AC

Line Filter

Figure 3-6: Schematic of one string PV system inverter

Solar Array

DC/DC   DC/DC

DC-Link Capacitance

DC/AC
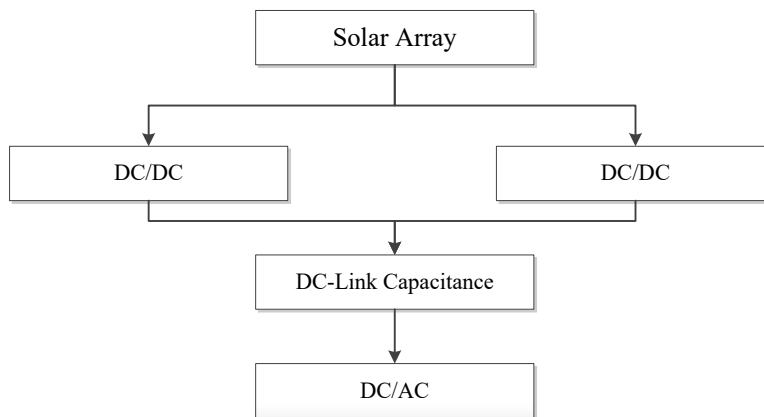
Figure 3-7: A functional block diagram of a string PV inverter

➢ DC/DC Converter

The boost converter used in this work has one switch, two diodes, and one capacitor. The two DC/DC converters are considered in redundancy. Each component inside the converter is considered as a major factor for failure in this work. The failure rate of the converter ($\lambda_{DC/DC}$) can be defined using Equation (3-18). The methodology used to evaluate the failure rate of each component can be found in MIL-HDBK-217F second

edition [61]. Equations (3-12)–(3-17) are used to evaluate the failure rates λ_{diode} and λ_{switch} [66-68], where T_j is 60 °C.

$$\lambda_{DC/DC} = \lambda_{diode} + \lambda_{switch} \qquad (3\text{-}18)$$

➢ DC-Link Capacitor

As mentioned earlier, the capacitor is recognized as a major contributor to the failure of PV systems. Equations (3-8)– (3-10) are utilized to estimate the failure rate of capacitors (λ_{cap}) [66]-[68]. The probability of up states and down states in a string PV inverter system is shown in Table 3-8. This table is then combined with Tables 3-2 to 3-5 to build the multi-state capacity model of a string PV system including the component failure factors as shown in Figure 3-8. A multiple string PV system is used in this work; therefore, the multi-state models obtained are aggregated to obtain the overall capacity model for the multi-string PV system.

Table 3-8: The two-state model of a string PV system

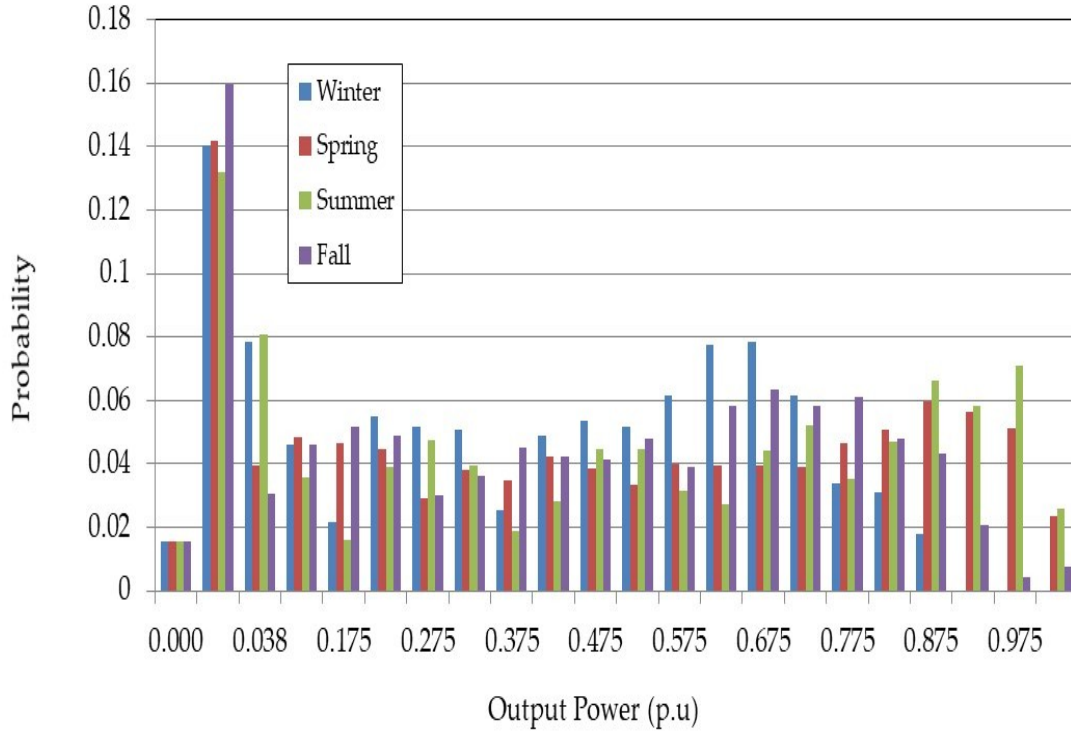| States	Probability
Up	0.9880
Down	0.0119

Figure 3-8: Seasonal daytime capacity models of a string PV system

3.2.4 Modeling a Micro-Inverter PV System

The main components of a micro-inverter PV system are illustrated in Figure 3-9. The functional block diagram of this PV system is shown in Figure 3-10. The steps described in Sections 3.2.2 and 3.2.3 are utilized in this section to build the capacity model of a micro-inverter PV system. The probabilities of up and down states of micro-inverter PV system components are presented in Table 3-9. Thereafter, this model is combined with the overall PV system model shown in Tables 3-2 to 3-5. The result of this combination is the multi-state capacity model of a micro-inverter PV system as shown in Figure 3-11. A multiple micro-inverter PV system is used in this work;

therefore, the multi-state capacity models obtained for each string are aggregated to obtain the overall capacity model.
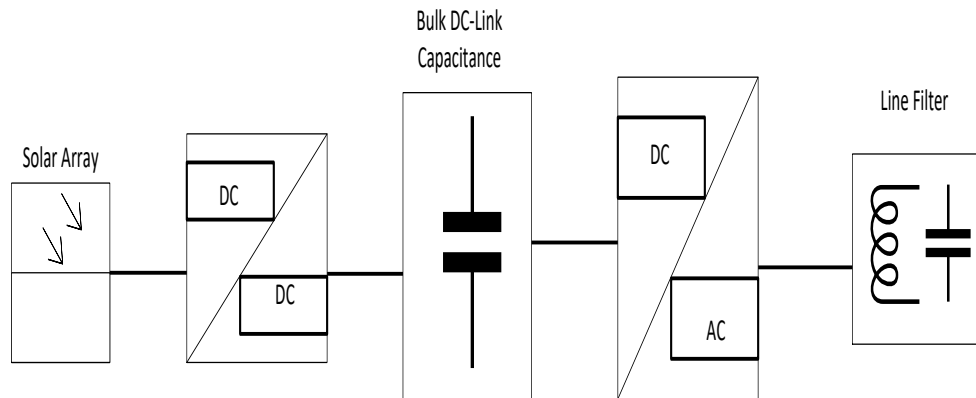
Figure 3-9: Schematic of a micro-inverter PV System
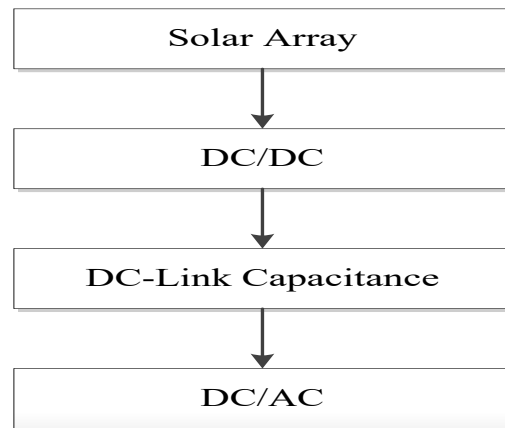
Figure 3-10: A functional block diagram of a micro-inverter PV System

Table 3-9: The two-state model of micro-inverter PV system components

States	Probability
Up	0.9869

Down	0.0131
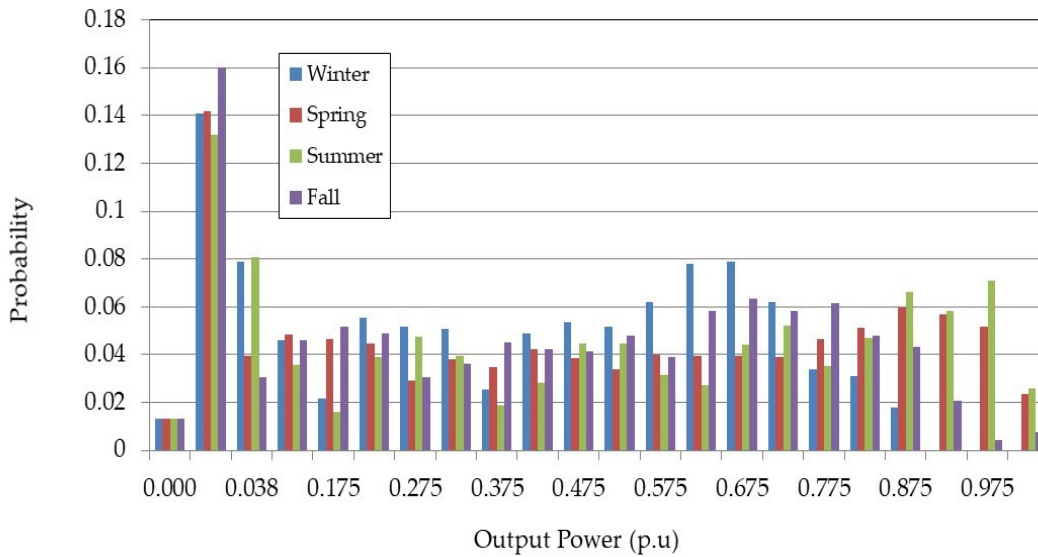
Figure 3-11: Seasonal daytime capacity models of a micro-inverter PV system

3.3 Generation System Reliability Model Including PV Generation

The conceptual generation system adequacy model for an electrical power system including PV system is shown in Figure 3-12. The output power of a PV unit is represented by a multi-state probabilistic capacity model described previously.

Figure 3-12: Basic reliability evaluation model of a PV-integrated power system

3.4   Sensitivity Case Studies

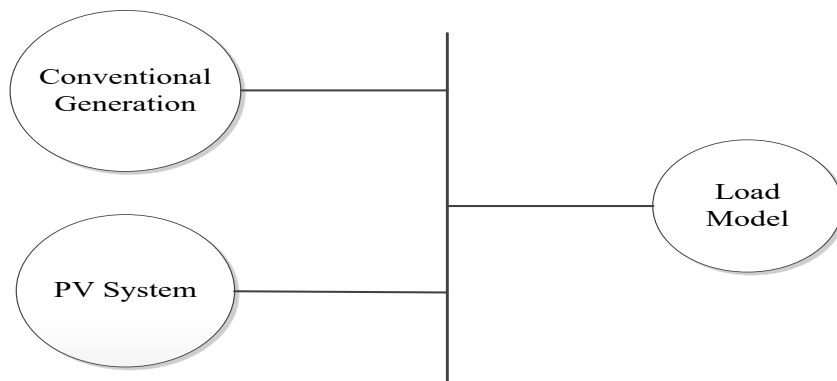The reliability impact of the different PV technologies is illustrated on the test SIPS described in Section 2.4.1. Many SIPSs use the deterministic N-1 criterion, also known as the "LLU" criterion, to determine the capacity reserve required in their systems. This criterion ensures that the peak load can be satisfied in the event of the failure of the largest generating unit. The test SIPS with 150 kW of installed capacity and a peak load of 80 kW just meets the N-1 criterion. The LOLE and LOEE of the test system are 32.26 h/year and 483.46 kWh/year respectively. This LOLE value is, therefore, chosen as the probabilistic risk criterion in the following studies.

Two case studies were carried out to investigate the reliability impacts of the different PV technologies. The first study examines the reliability contribution of adding PV generation to the SIPS. The second study analyzes the capacity value of the installed PV system. The three different PV topologies are taken into consideration in both studies. Table 3-10 shows all studies investigated in this work. Installed PV capacity levels of 15, 30, and 45 kW, corresponding to approximately 10%, 20%, and 30% of the SIPS capacity respectively, are considered.

Table 3-10: Case studies

Study	Evaluation	Factors Considered
1	System Adequacy (LOLE, LOEE)	• Using different PV Topologies. • Increasing load demand for the test system by approximately 10% every year ranging from 80 to 118 kW.
2	Capacity Value (ELCC, CC)	• Using LOLE of 32.26 h/year as the reliability criterion. • Using different system PV capacity ranging from 10% to 30% capacity value (ELCC, CC). • Using different PV Topologies

3.4.1   Impact of System Load Level and PV Technology on System Adequacy

This study examines the reliability contribution of the three different PV technologies as a function of the system peak load.   Figures 3-13 and 3-14 show the

LOLE and LOEE of the SIPS respectively when 30% of PV is added to the system. The historical solar irradiation data of Medina in Saudi Arabia located at 24.91° N, 46.41° E, are used to evaluate the power generation of the PV system [45]. It can be observed in these two figures that the LOLE and LOEE increase as the peak load increases in all PV topologies. These two figures additionally show that using the micro-inverter topology can provide more incremental reliability benefits compared with the other PV topologies. However, this increment decreases at certain percentages of the installed PV system where no more benefit can be obtained by further increasing the installed PV capacity, as discussed in the next section.
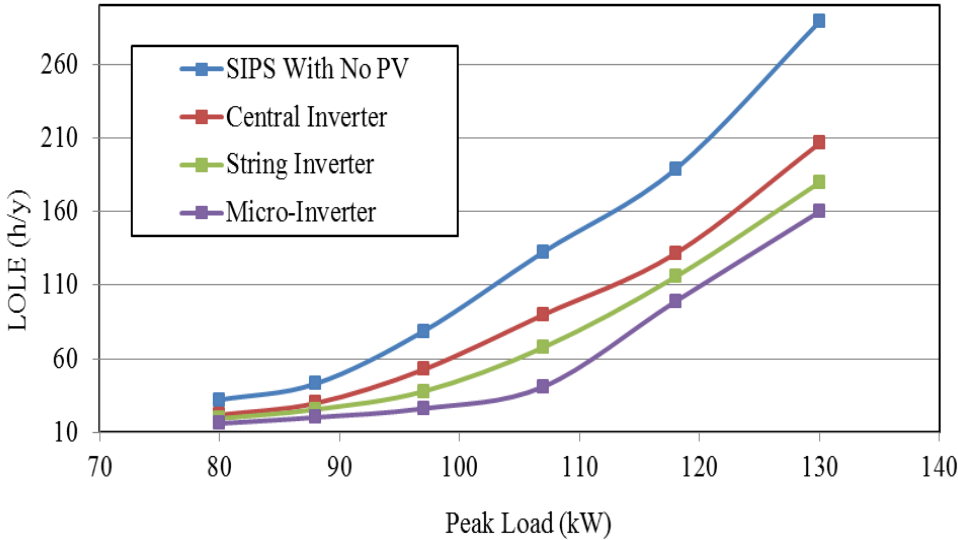
Figure 3-13: Variation in risk level (LOLE) with system demand load for different PV topologies.
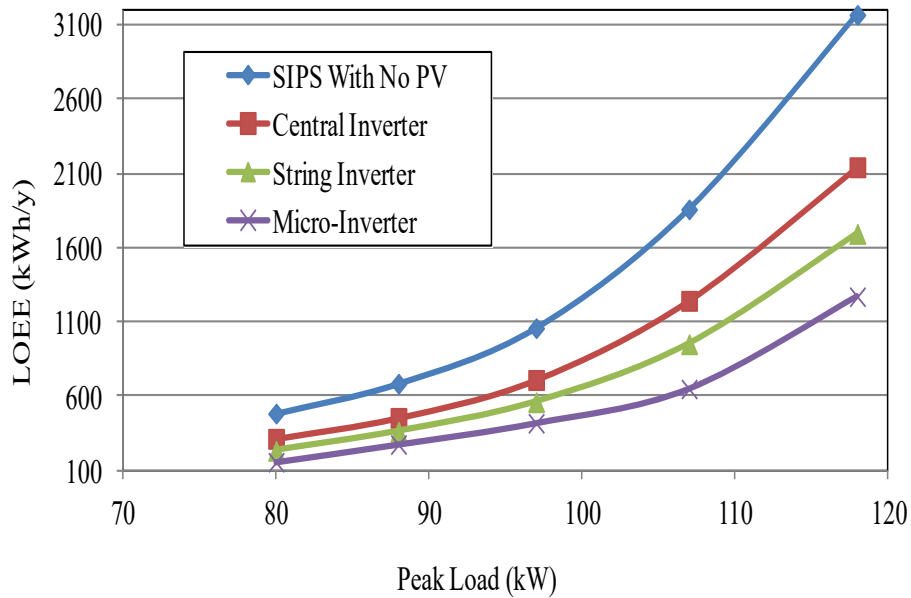
Figure 3-14: Variation in risk level (LOEE) with system demand load for

different PV topologies.

3.4.2 Impact of Different PV Topologies on ELCC

The ELCC of a PV system for different PV topologies are investigated in this work. The LOLE was used in this study to evaluate the ELCC for each PV topology. The maximum allowable peak load at adequacy risk of system generation of 32.26 h/year is used. The amount of load that can be carried by a PV system is estimated by calculating the difference between the two risk indices of LOLE before and after adding PV systems. Figure 3-15 shows the ELCC associated with the addition of 10–30% of PV systems to SIPS at the three different PV topologies.
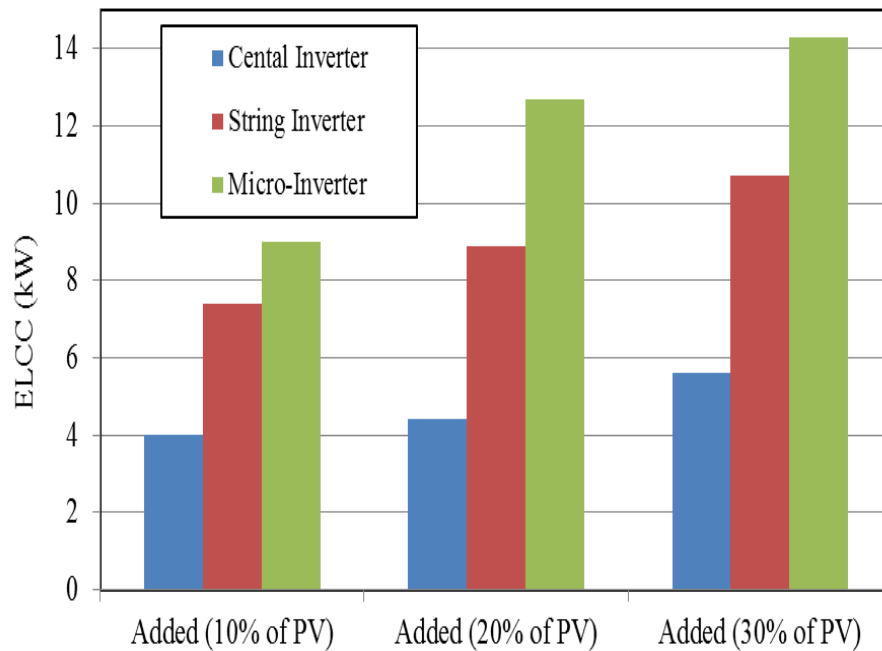
Figure 3-15: Effective load-carrying capability for different PV topologies.

3.4.3 Replacing a Conventional Generating Unit with a PV System

This work evaluates PV capacity required to replace conventional generation capacity while maintaining the same level of system reliability. This study compares replacing diesel generation with a PV system considering the different PV topologies. The 40 kW diesel generating unit is first removed from the test SIPS. The LOLE is increased to 340.34 h/y when the 40-kW conventional unit is removed from the system. Table 3-11 represents the required capacity of the PV technology to maintain the LOLE criterion of 32.26 h/year. When the central PV capacity is used, the LOLE is restored to 32.26 h/year if 270 kW of PV is added. This indicates that 270 kW of PV capacity using a

73

central PV system is capable of replacing a 40-kW conventional generating unit. However, a 180 kW and 98 kW string and micro-inverter PV capacity is required to maintain the system risk level at the original level of LOLE = 32.26 h/year.

The equivalence between the replaced conventional generating unit and replacing PV system can be expressed by the ratio of PV capacity to conventional generating unit, and this ratio is known as the risk-based equivalent capacity ratio (RBECR) [72]. Equation (3-19) is used to determine the RBECR. The results indicate that one unit of conventional capacity is approximately equivalent to 7, 5, and 3 units of central, string, and micro-inverter PV capacity respectively, as shown in Table 3-11.

$$RBECR = \frac{Total\ amount\ of\ installed\ PV\ capacity}{Total\ amount\ of\ replaced\ conventional\ generation\ capacity} \qquad (3\text{-}19)$$

Table 3-11: Replacing a conventional generating unit by a PV System

PV Topology	PV Capacity Required (kW)	RBECR
Central	270	6.75
String	180	4.50
Micro-inverter	98	2.45

3.4.4   Impact of Increasing PV Penetration on its Capacity Credit

Equation (2-8) is utilized in this case to evaluate the capacity value of PV systems for different PV topologies. Figure 3-16 demonstrates the PV CC for the three different topologies. Several important observations can be obtained from this analysis.

There is evidence of improvement in the overall system adequacy when more PV systems are installed. However, the relative reliability benefits estimated by capacity value decrease with the addition of PV capacity. Previous studies have also found that the capacity value of PV declines when installing more PV in the electric power system [73,74]. The PV topology plays an important role in the contribution of PV capacity value as shown in Fig. 3-16. The result clarifies that the micro-inverter PV system provides the largest PV capacity contribution. The CC of the PV system increases from 19% to almost 31.68% when the central PV inverter topology is replaced with a micro-inverter at a 30% installed level of PV.
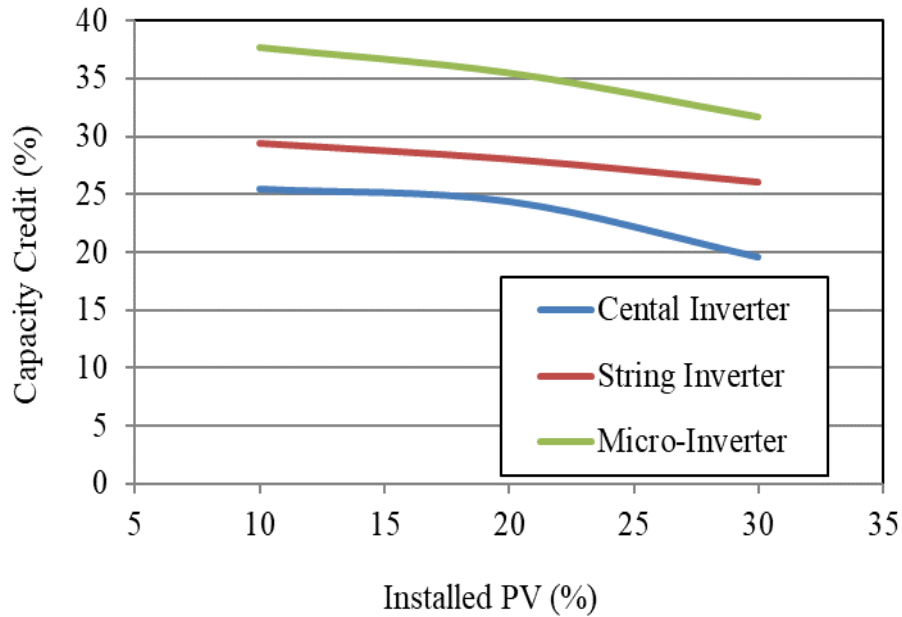
Figure 3-16: Capacity credit for three different topologies.

3.5 Summary

PV systems are composed of components that are vulnerable to failures with different probabilities. The structure of power electronic converters in PV systems can be broadly classified into centralized inverters, string inverters, and micro-inverters. The structures of central and string PV systems often have similar electric components but are differently configured in terms of the manner of connecting the solar array to the inverter. A central PV system topology is composed of multi-string topologies that are connected to only one inverter. However, one inverter is connected to each string in a string PV system topology. Micro-inverter topology, on the other hand, requires one inverter per solar panel. Previously published works did not consider all the

aforementioned topologies. The quantitative assessment of reliability for an entire PV system is essential for determining the overall reliability contribution of adding solar power to electric power systems. This has not been sufficiently addressed in the existing pool of literature.

This chapter introduces a detailed reliability model of a PV system. All major electrical components of PV systems are involved in the model. This model is then applied to a test system to quantify the reliability contribution of adding PV generation considering all three PV topologies. Different factors, such as the effect of system peak load and the installed PV capacity for different PV topologies, are discussed in this work.

The reliability contribution of PV is expressed in terms of LOLE, LOEE, ELCC, and CC. The results indicate that the inverter can have a significant impact on the reliability contribution as compared with other electric and electronic devices in a PV system. The analysis also indicates that the reliability contribution of the PV capacity is highly dependent on the PV system configuration. The result demonstrates that using a micro-inverter PV system provided the largest reliability contribution from the installed PV generation. The system adequacy indices utilized in this work provide a practical approach to evaluate the reliability of the generation system.

4   Probabilistic Reliability Models of Generation Systems Including CSP

4.1   Introduction

CSP is an emerging technology in the field of renewable energy and is a promising addition to electric power systems. Generating electric power using solar thermal technology is a good substitute for reducing the negative environmental impacts of conventional energy sources. The output power of CSP is highly variable owing to the intermittent nature of solar energy resources and the availability of CSP components. Limited research has been conducted with regard to the development of CSP reliability models. Therefore, the development of a quantitative framework to evaluate the reliability contribution of CSP systems in a power system grid is essential. Moreover, obtaining accurate estimates of CSP's CC is important for capacity planning purposes.

A probabilistic model of CSP has been developed for determining the effects of variation in direct solar irradiation and air temperature on generation system adequacy. The developed model is applied to the RBTS to investigate the impact of various factors on the reliability indices, such as the LOLE, LOEE, CC, and ELCC, of a CSP-integrated power system. The impact of factors, such as the system peak load, installed CSP capacity, and different sites, are taken into consideration in this work.

4.2 Modeling of CSP Systems

The evaluation of a CSP plant performance requires the application of multiple disciplines, such as concentrator optics, heat transfer, and thermodynamics. Preliminary analysis is often performed using thermodynamic models or commercially available tools such as NREL's System Advisor Model (SAM) [29]. SAM is provided by the National Renewable Energy Laboratory (NREL), which is operated by the Midwest Research Institute (MRI) for the Department of Energy (DOE).

SAM utilizes detailed weather data, including solar radiation and ambient temperature as the input data to model the dynamics of the solar field. The software determines how much solar thermal energy is collected by the solar field of the CSP plant every hour. It also accounts for the effects of temperature on the efficiency of the solar field with regard to collecting solar thermal energy. SAM produces a range of outputs related to the cost and performance of systems, including system power output, peak and annual system efficiency, levelized cost of electricity (LCOE), and hourly system production. SAM and other available programs simulating CSP plant [75] can provide relatively high accuracy; however, they require extensive input data which demands more computational time. For example, in an individual CSP system based on Parabolic Troughs, the Solar Tower requires a large input of data parameters.

There exist a variety of CSP simulation programs and models; yet, most of them are computationally complex. The models used in commercially available programs is not fully known and they cannot incorporate new models or variations in applied methodology. This work addresses the gap created by simplified models, particularly for models that predict the energy output of solar thermal systems. This study accomplishes this by focusing only on the major parameters. The adequacy results obtained from the reduced models is compared with the predictions made by the SAM.

There are several types of CSPs in the commercial space today: such as the Parabolic Trough (PT), Central Tower (CT), Linear Fresnel (LF), and Solar Dish (SD). In this work, a PT is used because it is considered to be the most mature technology available. In general, a CSP consists of three important components, as shown in the reliability block diagram in Figure 4-1. They are Direct Normal Irradiation (DNI), a solar field (SF) that includes a solar collector and receiver, and a power block (PB) that uses a heat engine to convert thermal energy into electricity. The aim of this study is to develop a simple probabilistic reliability model.
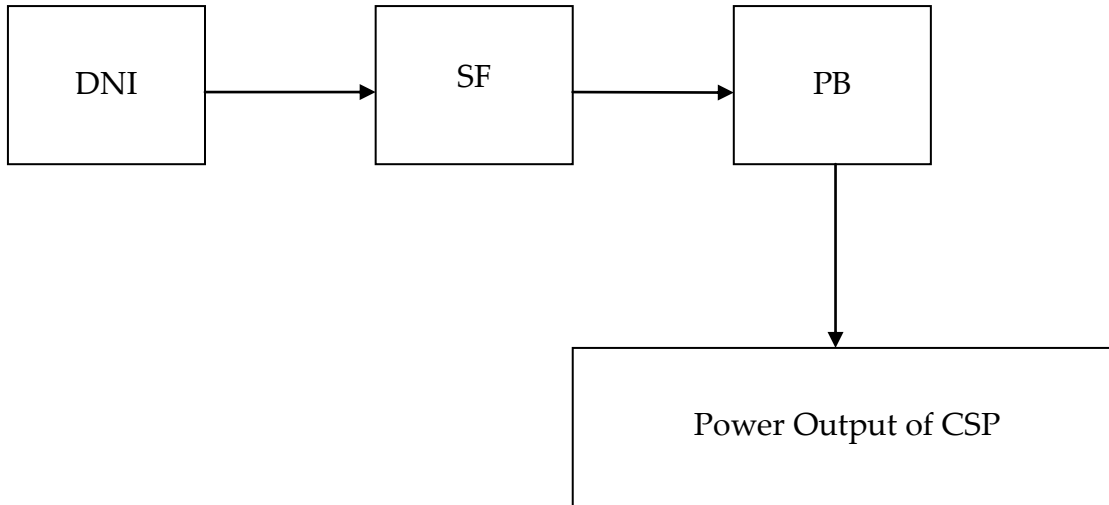
Figure 4-1: Equivalent Functional Block Diagram of CSP

4.2.1 Component Reliability Modeling of CSP

The CSP components consist of two important features; a SF with a collector and a PB with a heat exchanger, pump, condenser, turbine, and generator. The collector has demonstrated high reliability in the field; therefore, the FOR is neglected for these components. The FOR of a conventional thermal unit is considered for the PB of CSP. The MTTF and MTTR of the PB are taken as 2941 h and 58.24 h, respectively, in the study. Table 4-1 shows the two-state model of CSP components using (4-1) and (4-2).

$$\text{FOR or } P(\text{Down}) = \frac{MTTR}{MTTR + MTTF} \qquad (4\text{-}1)$$

$$P(\text{Up}) = \frac{MTTF}{MTTR + MTTF} \qquad (4\text{-}2)$$

Table 4-1: Two-state model of CSP

State	Probability
Up	0.98
Down	0.02

4.2.2 Modeling the Output Power of CSP

The CSP is operated like a large Rankine steam power plant, apart from the fact that it acquires its thermal energy from a large solar collector. This technology produces electric power when the sun shines, and shuts down or runs on a backup source, such as fossil or biomass fuel, when solar energy is not available. In this study, it is assumed that there is no auxiliary backup to supply the thermal plant when there is no sun or when the DNI is not sufficient to heat the thermal fluid to produce electric power. Therefore, the CSP starts up and shuts down daily. In other words, the solar field is operated whenever sufficient DNI is available to generate power. The energy required to warm up the fluid heat transfer in the solar field is based on the amount of DNI. In the adopted model, the lower limit of DNI is assumed to be in the plane to heat up the collector, which is approximately 300 W/m^2 [76]. The SF produces electric power when the warm up is completed using (4-3) [77].

$$P_{CSP(t)} = G_{b(t)} \times A \times \eta_{SF} \times \eta_{PB(t)} \times \eta_{par} \times \eta th, \tag{4-3}$$

Where:

$P_{CSP(t)}$: The output power of CSP at time t

$G_{b(t)}$: Hourly Direct Normal irradiation (W/m²)

A   : Net aperture area

η_{SF} : Efficiency of collector and receiver

η_{par} : Parasite efficiency, depends on the solar multiple (96.1 – 1.4 × SM) % [78](in this work, SM = 1 is used)

η_{th} : Thermodynamic efficiency or Carnot efficiency equal to Z × (1 – T_{amb}/T_A), where Z = 0.6 [78]

The power block efficiency (η_{PB}) is defined as the ratio of the electrical power produced to the thermal power collected in the solar field, and it depends on the hourly DNI and ambient temperature. Equation (4-4) shows the mathematical model to estimate this ratio [77].

$$\eta_{PB(t)} = \left[\eta_{opt} - \left(\frac{\tau \times F_g}{\eta \times G_{b(t)}} \times \left(U \times (T_A - T_{amb(t)}) + \varepsilon \times \sigma \times \left(T_A^2 - T_{amb(t)}^2\right)^2\right)\right)\right] \qquad (4\text{-}4)$$

η_{PB} : Power block efficiency (some study assumed this between 35 and 48%)

λ : Conversion factor, 3.6 × 10⁶ J/kWh [79]

U   : Convective losses coefficient equal 2 $W/m^2/K$ [79]

T_A : Absorber temperature equal 653 K [79]

T_{amb} : Ambient temperature, (in this work, hourly ambient temperature is used)

ε   : Emissivity ($0.04795 + 0.0002331 \times$ TA) [79]

η_{opt} : Optical efficiency equal 75% [79]

Fg   : Geometric factor ($\frac{\pi}{C}$) [79]

C   : Concentrating Factor equal 80 [79]

σ   : Constant (5.67×10^{-8} $W/m^2/K^4$) [77]

The approach described in Figure 4-2 is used to create the multi-state model of the solar thermal power generation capacity. The multi-state model is obtained by dividing the DNI into segments. The states associated with zero solar irradiation are categorized into an individual state. Equation (4-5) is used to calculate the probability of a given state, where N_i is the number of occurrences of state i. The multi-state model obtained in this step is combined with the two-state models, shown in Table 4-1, in order to obtain the overall CSP system reliability model.

$$\text{Probability}_i = \frac{N_i}{\text{Total Number of Samples}}$$
(4-5)

The probabilistic model is applied to an example system, taking solar irradiation data from Seville (located in Spain) into consideration. Figure 4-3 shows the annual CSP model using the probabilistic model described in this section and the SAM model. The probability of zero output power of CSP is 0.7 and 0.73 for the probabilistic and SAM models, respectively.
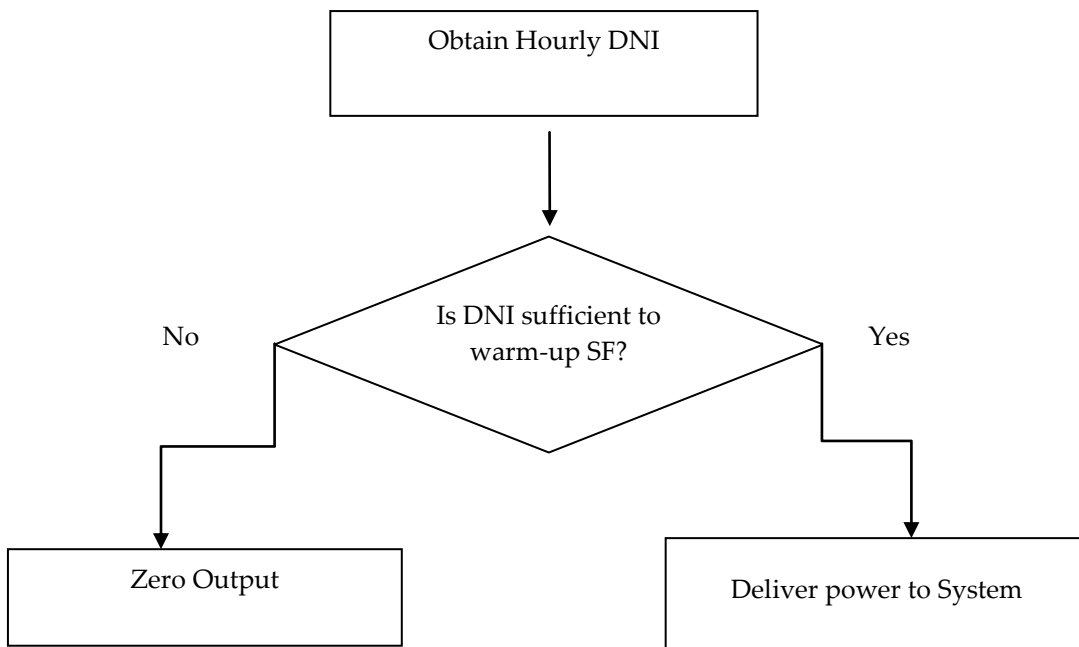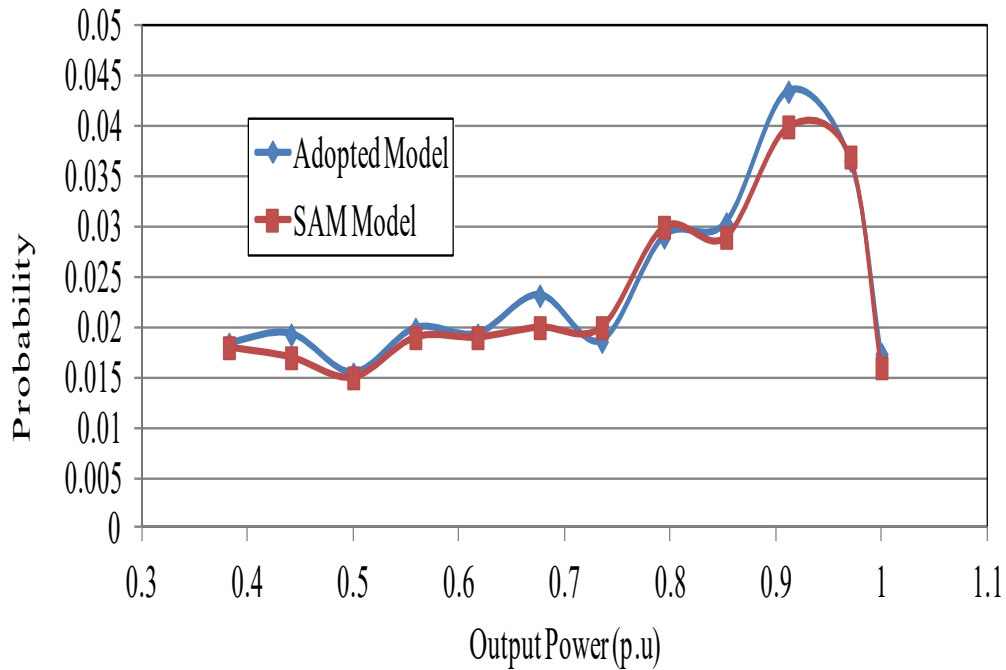

Figure 4-2: Dispatch Strategy of CSP

Figure 4-3: The annual CSP generation model in pu at Seville

The main observations and summary from this study are as follows:

• The performance of the developed probabilistic analytical reliability model of CSP is validated using SAM simulations as the baseline reference.

• The total number of required parameters to predict CSP plant production using the adopted model is less than the parameters required for SAM.

• The probabilistic analytical model is sufficient to provide a realistic pattern of the plant production throughout the year as well as to provide the typical values of the

yearly energy output. Therefore, this model is used in all the following studies to obtain the CSP output power states owing to its simplicity compared with SAM.

4.3 Reliability Evaluation Model for a CSP-integrated Generation System

The CSP produces more power during summer and less during winter. The annual indices of LOLE and LOEE are therefore divided into season classes and the hourly load profile of each day is divided into day and night loads. The nighttime load is supplied with conventional generation and the daytime load is supplied with both conventional and CSP generation. The total annual LOLE and LOEE can be evaluated using (4-6) and (4-7).

$$\text{LOLE (Annual)} = \sum_{\text{Seasons}} \left(\sum_{\text{Night}} \text{LOLE} + \sum_{\text{Day}} \text{LOLE} \right) \tag{4-6}$$

$$\text{LOEE (Annual)} = \sum_{\text{Seasons}} \left(\sum_{\text{Night}} \text{LOEE} + \sum_{\text{Day}} \text{LOEE} \right) \tag{4-7}$$

To conduct this study, first, the probabilistic reliability model of CSP is developed and then combined with the RBTS model. The physical system generation model utilized for this study is shown in Figure 4-4. The CSP and RBTS generation models are combined with the load models for the designated periods to obtain the system reliability indices. A range of studies were conducted in this work to investigate the reliability impact of load growth, growth in CSP penetration, and the geographical

locations of the CSP installations when CSP is integrated with the test system. The

reliability impacts are quantified using the system indices LOLE, LOEE, and ELCC.
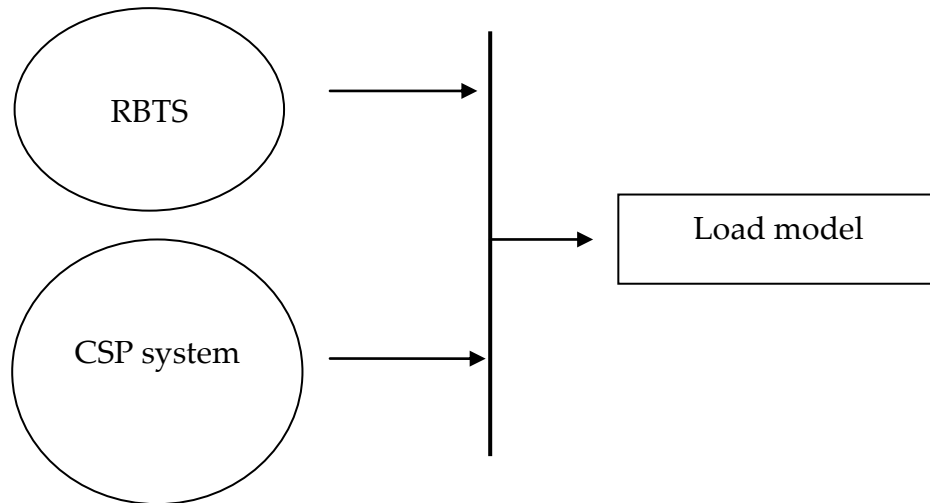

Figure 4-4: System reliability evaluation model incorporating CSP generation

Figures 4-5, 4-6, 4-7, and 4-8 represent the COPT of CSP for different seasons in

Medina. As noted earlier, the RBTS LOLE before installing CSP was 1.09 h/y. A study

was carried out considering the additional CSP plant using solar data from different
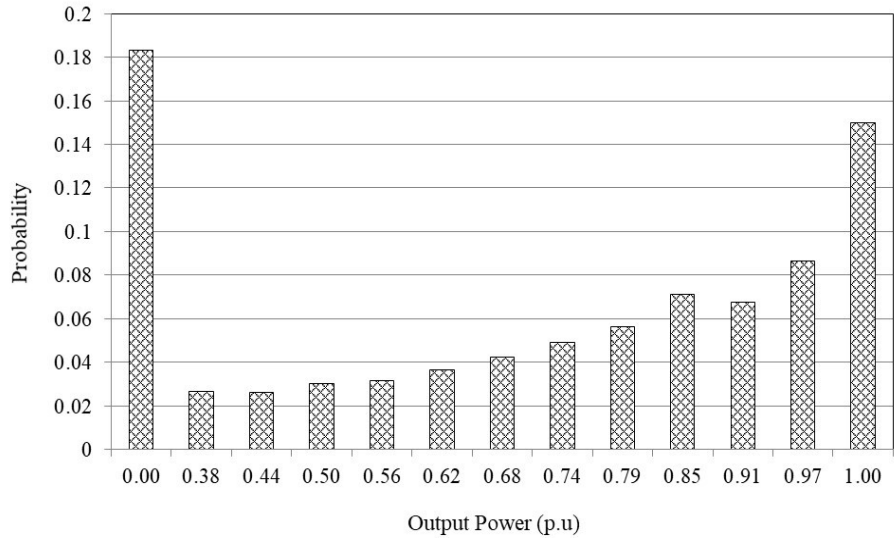
locations.

Figure 4-5: The probability distribution of available capacity of a CSP system during the winter
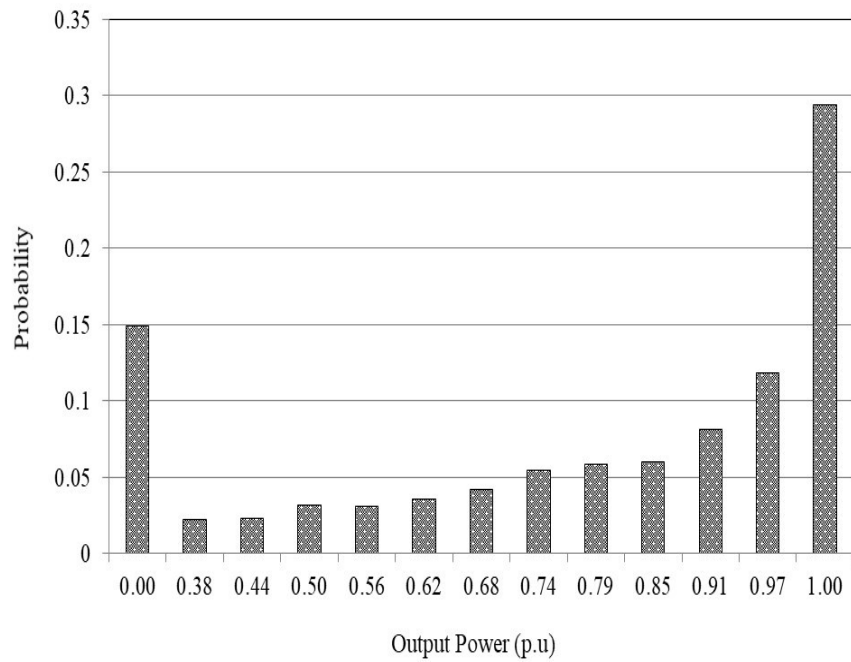
season

Figure 4-6: The probability distribution of available capacity of a CSP system during the spring
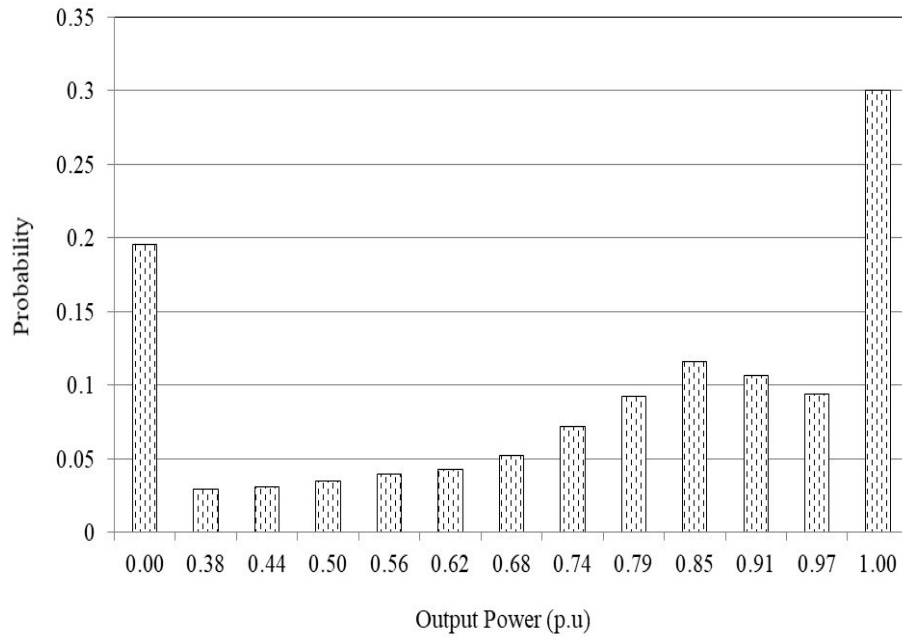
season

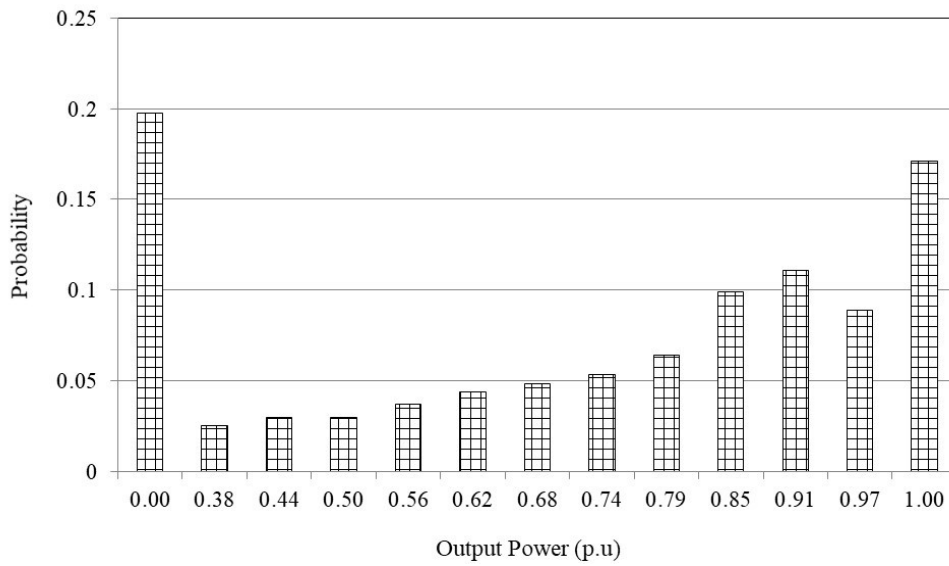Figure 4-7: The capacity available probability of a CSP system for summer

Figure 4-8: The capacity available probability of a CSP system for fall

4.4   Sensitivity Case Studies

4.4.1   The Impact of Load Variation

The developed generation system model demonstrated in Section 4.3 was convolved with the appropriate load model considering different system load variations to investigate the impact of load variation on the system adequacy of CSP. This study was repeated using solar data from different sites: Daggett (located in the USA), Seville (located in Spain), and Medina (located in Saudi Arabia).   Figure 4-9 to 4-12 represent the discrete probability distribution of the output power of CSP at Seville and Daggett for the four seasons.
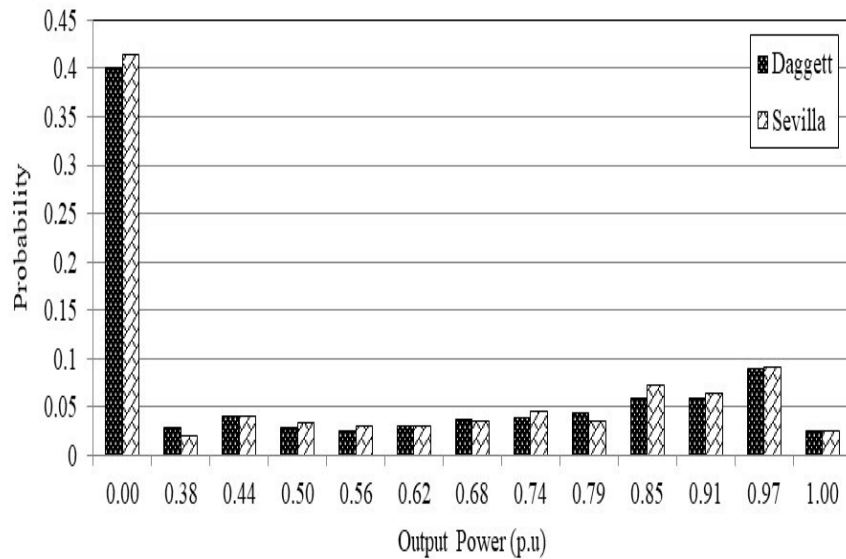

Figure 4-9: The capacity available probability of a CSP system for winter
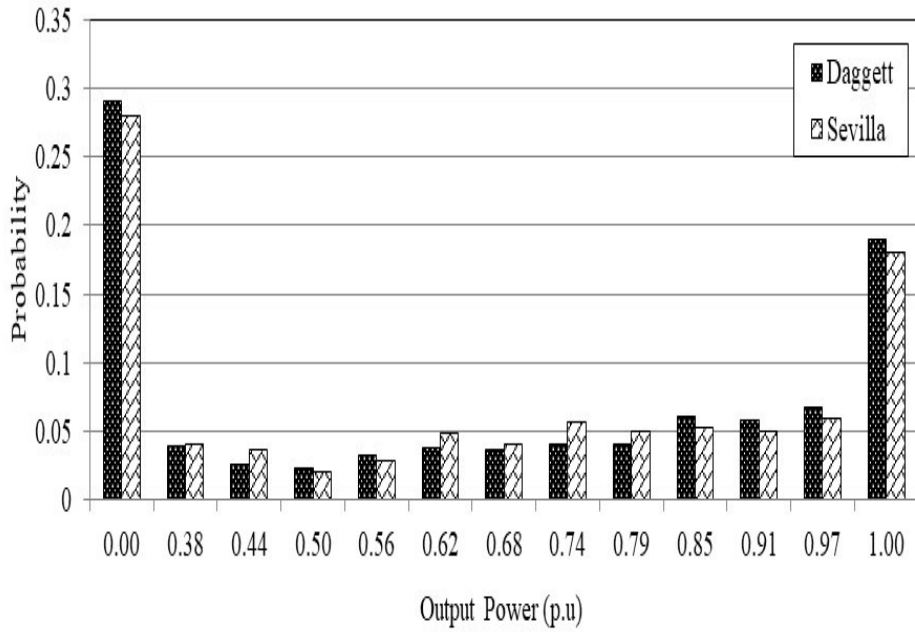
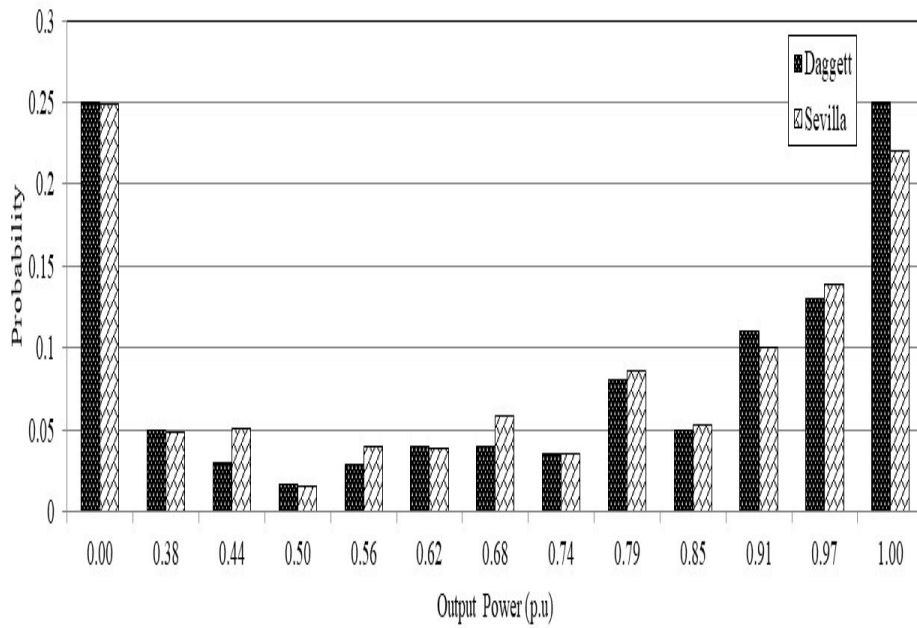Figure 4-10: The capacity available probability of a CSP system for spring

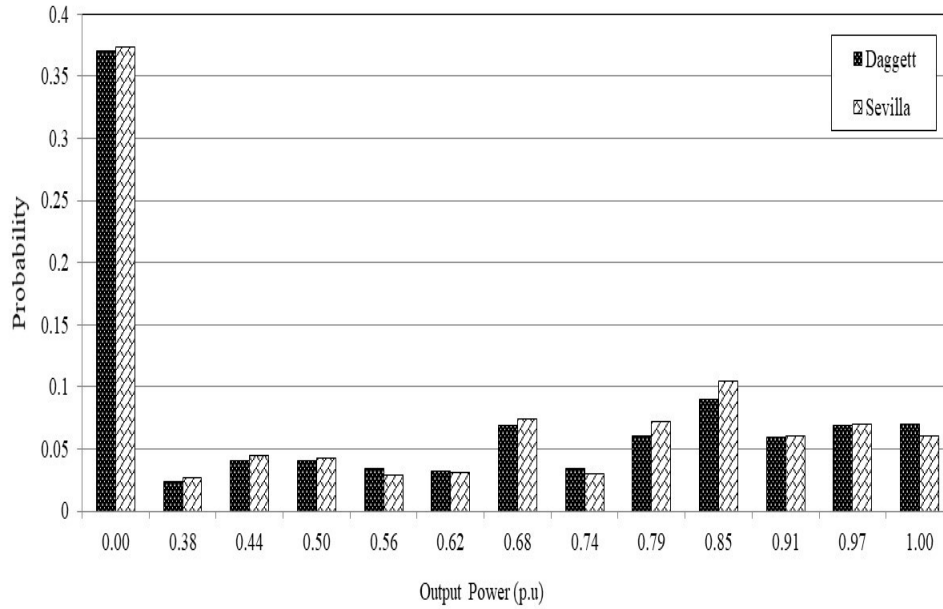Figure 4-11: The capacity available probability of a CSP system for summer

Figure 4-12: The capacity available probability of a CSP system for fall

A study was carried out considering the addition of a 24-MW CSP plant to the RBTS. The ratio of the CSP capacity to the overall system generation capacity, or the CSP penetration, is 10%. Solar data from three different locations, Daggett, Seville, and Medina, were used in the study. Figures 4-13 and 4-14 show the results obtained upon using Equations (4-6) and (4-7) for calculating the annual system risk of LOLE and LOEE of the RBTS integrated with the CSP system. The results are shown for the peak loads of 166.5, 185, and 203.5 MW. At the peak load of 203.5 MW, the system LOLE is almost 4.75 h/y and the LOLE becomes approximately 2.1, 2.81, and 2.76 h/y upon adding 24 MW of CSP at Medina, Seville, and Daggett, respectively. It can also be seen that the LOLE and LOEE indices increase significantly with load growth, and therefore, justify capacity additions to maintain an acceptable level of reliability as the load grows over

93

time. The figures also show that the LOLE and LOEE decrease as the CSP is added to the test system for all locations but not to the same degree. Figure 4-15 quantifies the LOEE impacts of CSP addition at different locations for the peak load of 185 MW. It clearly shows that the reliability contribution of CSP greatly depends on the solar irradiation data available at the installation site.
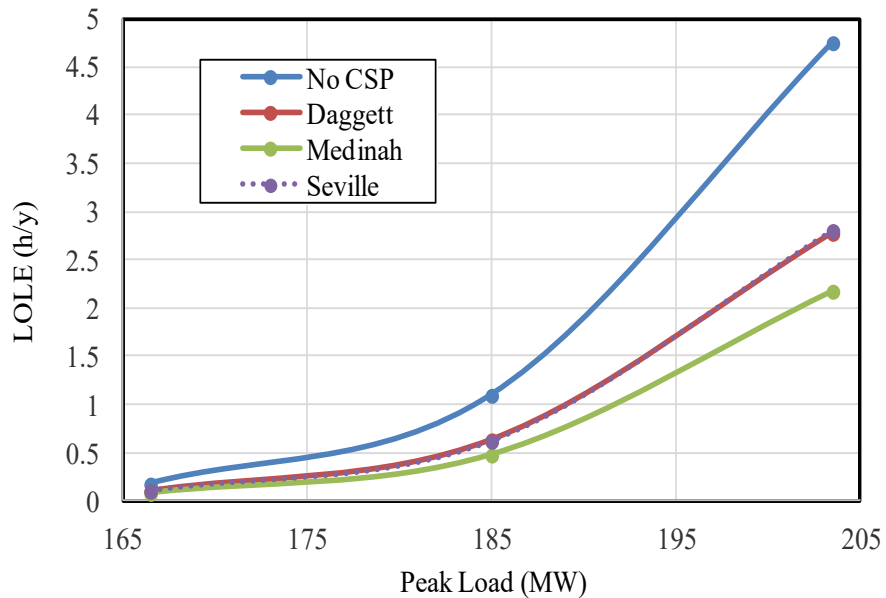

Figure 4-13: Variation in LOLE with load growth considering CSP at different locations
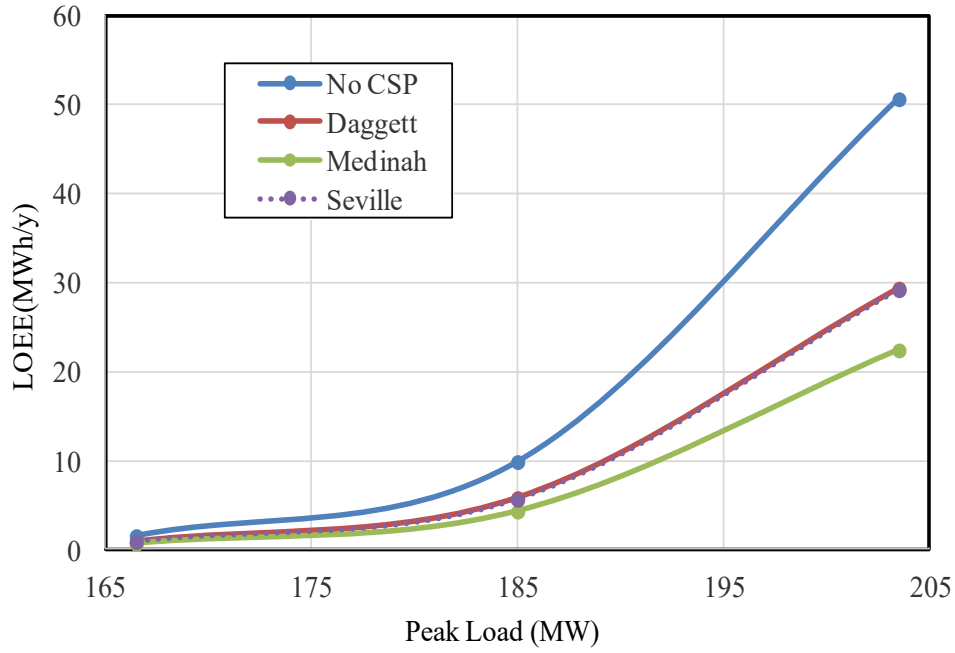
Figure 4-14: The variation in LOEE with load growth for considering a CSP at different

locations
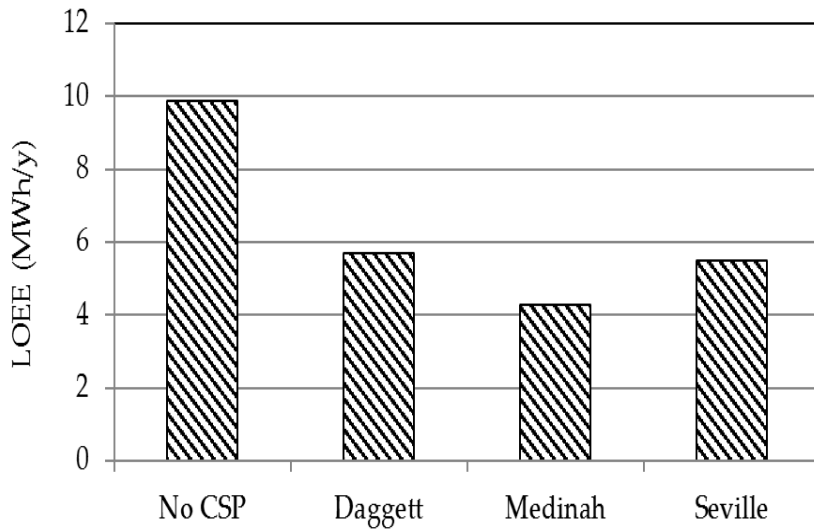
Figure 4-15: System LOEE comparison CSP installation at different locations

4.4.2 The Impact of Adding Different Amounts of CSP

The planning of capacity expansion is required over time to supply the annual incremental system load. A study was carried out to assess the reliability impact of growth in CSP penetration in a power system using Daggett's solar data. The CSP capacity was increased from 24 MW to 48 MW to 72 MW in accordance with the 10%, 20%, and 30% addition to RBTS, respectively. Figure 4-16 shows the system LOLE of the CSP-integrated RBTS considering a peak load of 185 MW. The results indicated a decrease in the incremental reliability contribution benefits of adding CSP capacity to the power system.
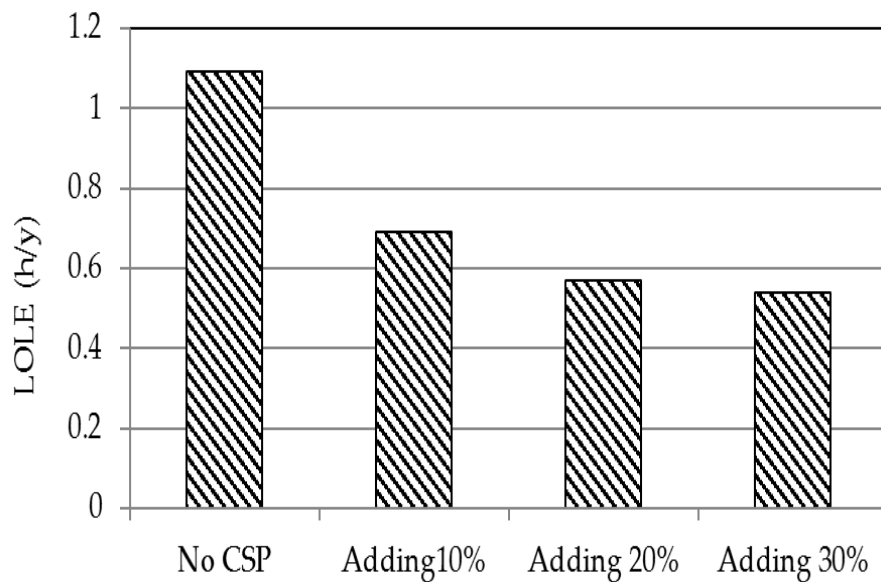
Figure 4-16: System LOLE comparison of the CSP installation at Daggett

4.4.3 CSP Capacity Value at Different Geographical Locations

The capacity value of a CSP system installed at different locations is evaluated in this work. A study was done with 24 MW of CSP added to the RBTS considering solar data from Daggett, Medina, and Seville. Figure 4-17 shows the LOLE for a range of peak loads with the solar data from the three locations. The amount of load that can be carried by the added CSP at the same reliability level was evaluated by measuring the difference in the LOLE profile before and after the CSP was added, as shown in Figure 4-17. The results obtained in this step indicated that installing 24 MW of CSP at Daggett and Seville can carry almost a similar amount of load of 4 MW. However, the ELCC associated with adding similar CSP capacity at Medina is 7 MW.
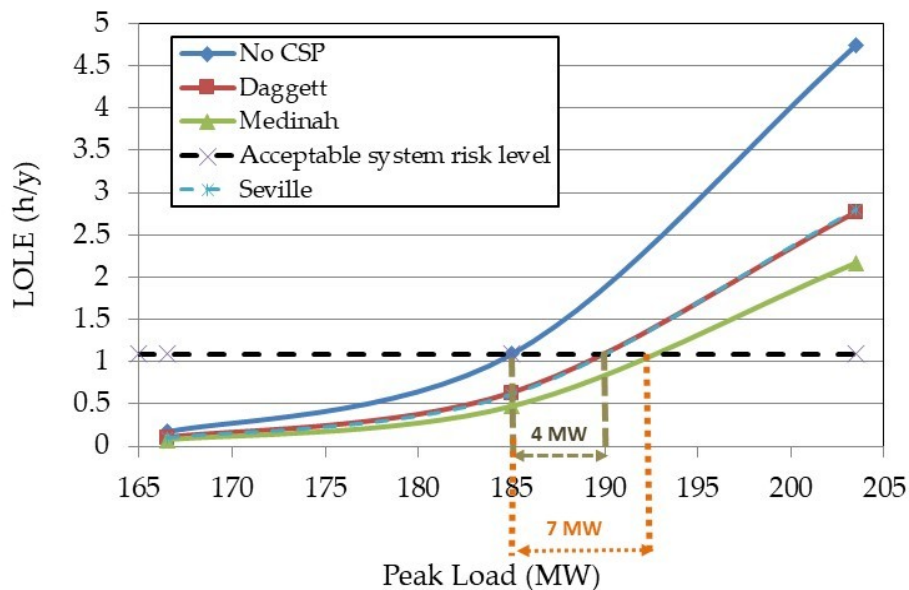
Figure 4-17: Variation in the RBTS LOLE upon installing 10% of CSP at different locations with the annual peak load

Figure 4-18 shows the ELCC of the RBTS after increasing the CSP penetration from 10% to 30% at the three different locations. The results obtained in this study highlight the fact that the CSP at different locations provide different contributions to system reliability and environmental benefits.
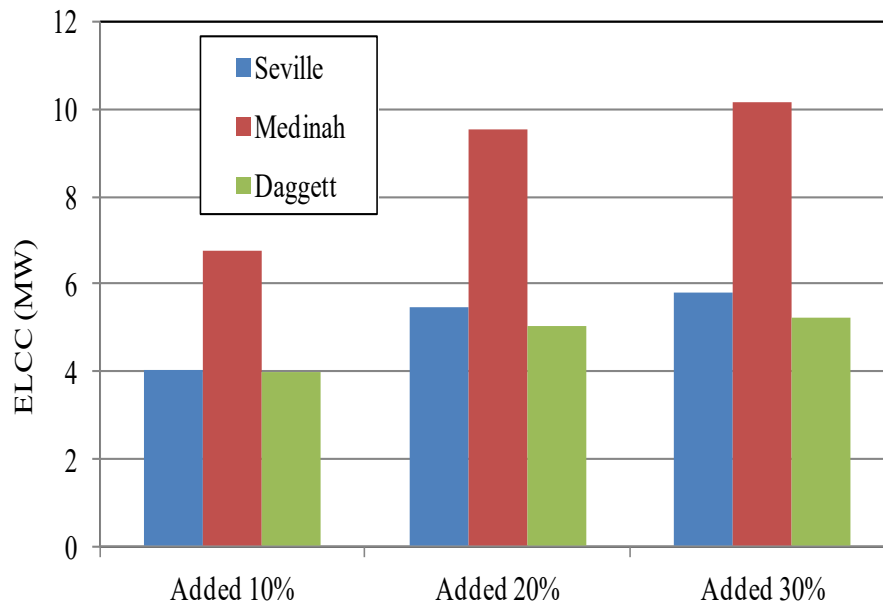
Figure 4-18: Effective load-carrying capabilities for different locations

This work was expanded to evaluate the CC of CSP for different penetration levels and at different locations. The CC, characterized by (2-8), can be used to represent the capacity value of CSP and applied during system capacity planning. It can be seen from Figure 4-19 that the CC of the CSP plant expressed as a percentage of its capacity decreases as CSP penetration is increased in the system. The CC values greatly depend on the locations of the CSP plant.
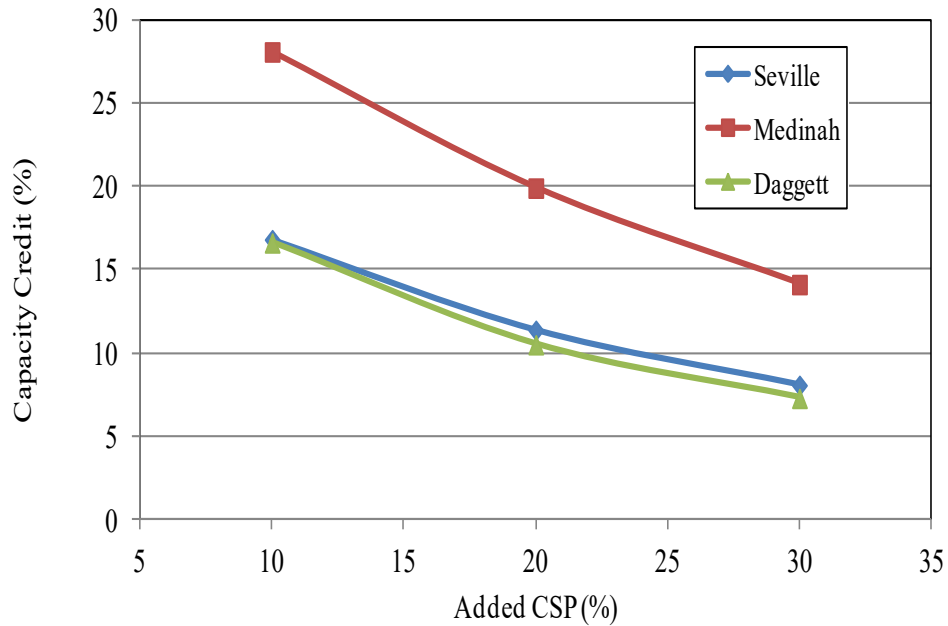
Figure 4-19: Capacity credit for three different locations

4.5   Summary

This chapter proposes a practical method to evaluate the reliability contribution of adding CSP to a power system. A reliability model of the integrated system is developed and presented, and the results are validated using the SAM program. The adequacy of a CSP-integrated power system has been evaluated considering several different system parameters, mainly the load growth, increase in CSP penetration, and geographic location of the CSP installations. The results indicate that the system adequacy performance improves upon increasing the CSP capacity. However, the improvement in reliability due to CSP addition is relatively small compared with the

addition of conventional power generation. There is a decaying benefit in the reliability

contribution of CSP with the increase in penetration of CSP.

5   Comparative Reliability Analysis of Electric Power Systems with High Penetration

of CSP and PV

5.1   Introduction

The demand for electric energy increases with time, and the rate of growth depends on various factors. For example, the annual electricity demand is increasing at the rate of 8% [80] in the Kingdome of S. A. The two major consumptions driving this high rate are water desalination for human requirements and high air conditioning load for the hot summer months from May to the end of September. Although KSA currently meets its electric energy requirements using fossil fuels, including coal and natural gas, it has implemented policies to gradually remove oil subsidies to support the use of alternative energy sources. The government of KSA plans to integrate alternative solar energy sources into the electric power system. Both PV and CSP have been investigated to determine the proper solar technology for investment. Large-scale CSP and PV generation systems are also being installed in other regions.

The methodologies presented in Chapters 3 and 4 are be applied to conduct a comparative reliability assessment of a power system including large-scale integration of CSP and PV. Historical data on solar irradiation, including DNI, diffuse horizontal irradiance (DIF), and global horizontal irradiance (GHI), were obtained at five-minute intervals in the period between 2000 and 2005 from different sites [45] in west KSA. The

solar irradiation data collected at five-minute intervals over the period of five years from Medina, located in Saudi Arabia [45], are considered in this chapter for analyzing the impact of the two solar technologies on generation system adequacy.

5.2   Solar Irradiation and Power Output of CSP and PV Systems

The reliability contributions of solar power sources in solar integrated power generation systems largely depend on the amount of DNI and GHI incident on the CSP and PV collectors/panels. The GHI is the net amount of irradiation received by the surface, including both direct and diffused irradiation. The DNI is the amount of solar irradiation that comes straight from the sun. Figures 5-1 and 5-2 show the amount of DNI and GHI evidenced in Medina on a sunny and a cloudy day. Although the power output of a PV system is influenced by the total solar irradiance, the output of a CSP system is mainly dictated by the DNI. It can be observed that on a typical sunny day, a CSP can collect more DNI and generate more power than a PV of an equal rating. However, the PV system can absorb more total irradiation on cloudy days in Medina and generate more power than a CSP because the amount of GHI is higher than DNI. This work, therefore, is intended to provide a comprehensive comparative adequacy analysis of a system generation incorporating CSP and PV systems.
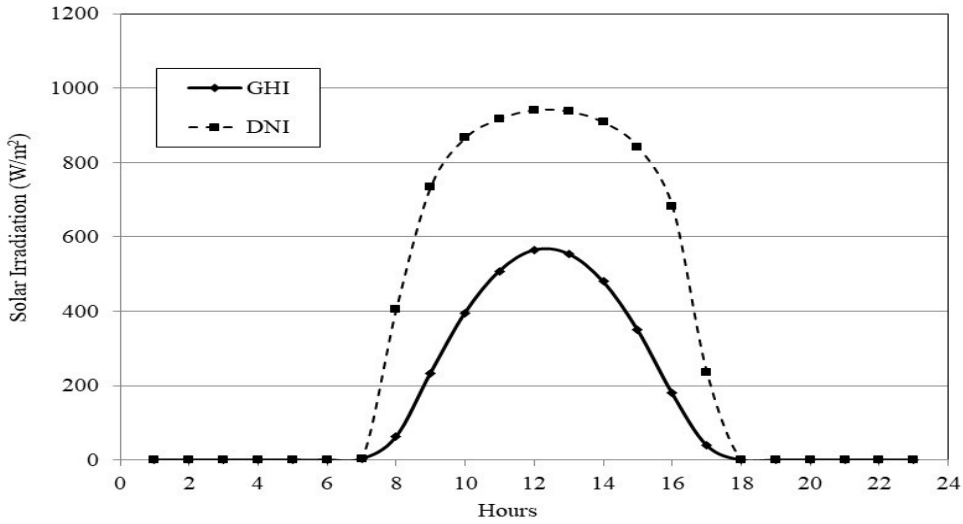
Figure 5-1: Solar irradiation during a sunny day
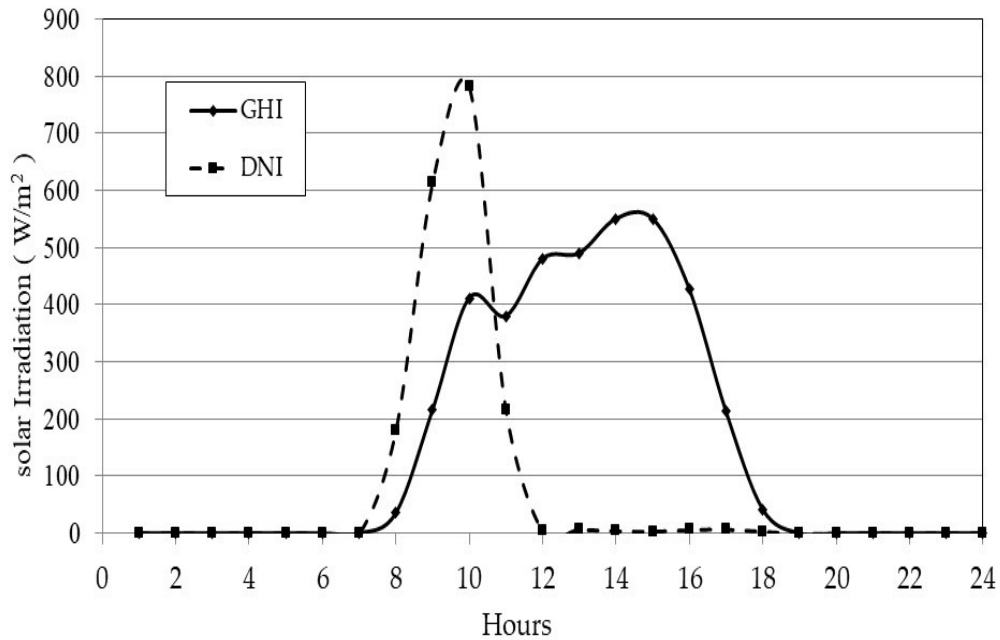
Figure 5-2: Solar Irradiation during a cloudy day

The PV and CSP power models developed for the Medina location were created

as shown in Figures 5-3 and 5-4. Subsequently, the hourly day and night system load

models were developed from historical power consumption patterns. A yearly analysis is performed to incorporate the effect of seasonality by dividing a year into four seasons: Winter (December to February), Spring (March to May), Summer (June to August), and Fall (September to November). The daytime load can be supplied by solar and conventional generation, and the nighttime load can only be supplied by conventional generation.
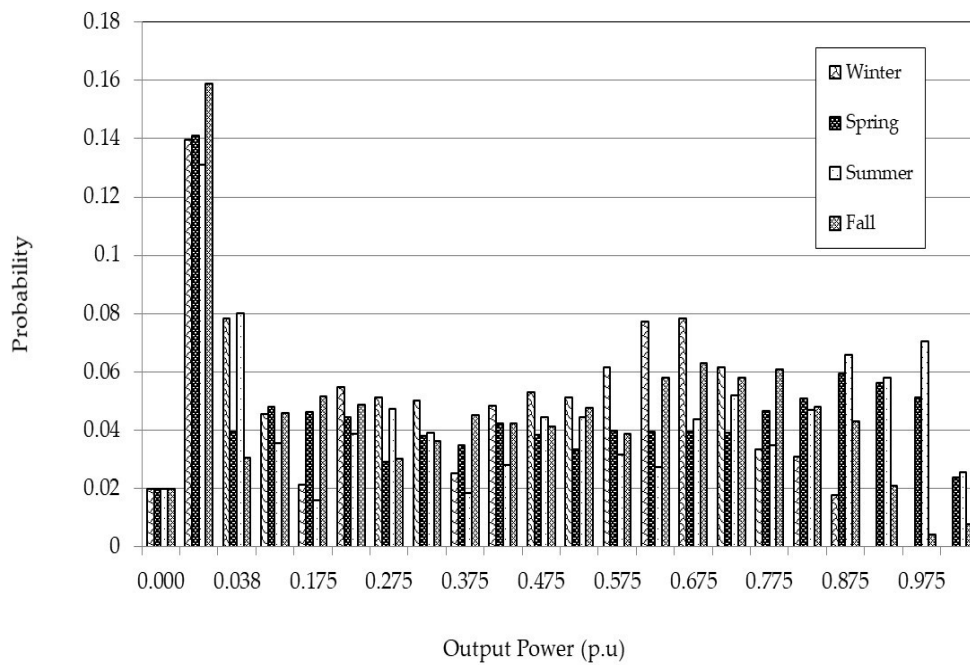
Figure 5-3: Probability Distribution of PV output Power
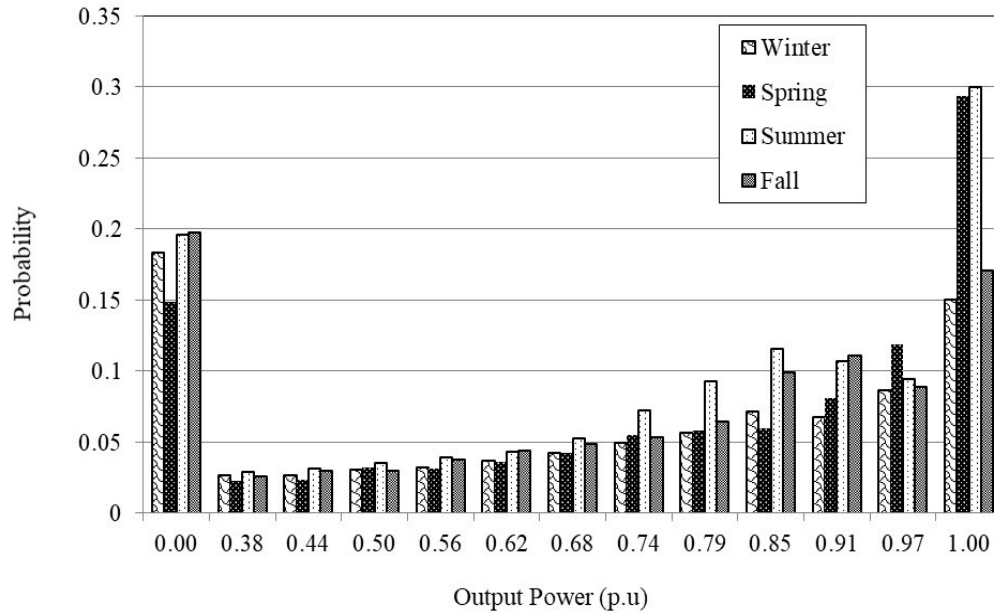
Figure 5-4: Probability Distribution of CSP output Power

5.3 A Comparison of the Reliability Contribution of CSP and PV

The RBTS integrated with CSP and PV is utilized to perform the reliability analysis to assess the reliability contribution of the CSP and PV system located at the same latitude. The capacity and load models created for each seasonal and diurnal periods are convoluted to obtain the reliability indices. The indices obtained for each season are aggregated to obtain the two annual system reliability indices, the LOLE and LOEE. The reliability contributions of CSP and PV can also be quantified through their capacity values in terms of ELCC and CC. The studies conducted in this chapter present a comparative analysis of the CSP and PV systems on the reliability contribution of these two technologies.

105

The annual incremental peak load is a key parameter in the reliability evaluation of a generation system, as generally, the system load increases with time. This parameter has been considered in this study for calculating the LOLE and LOEE with the effect of adding 10% of CSP and PV to the RBTS at the same site. Different peak load levels of 166.5, 185, 203.5 MW were also considered in this study to compare the impact of load variation on the system adequacy of CSP and PV. Figures 5-5 and 5-6 illustrate the relation between the installed PV and CSP capacity and the resulting system reliability indices of LOLE and LOEE for the different peak loads. The results demonstrate that the system LOLE and LOEE decrease significantly upon adding both the solar technologies, and the indices increase with an increase in the system peak load. It can be observed that the reliability benefit from the CSP system is significantly higher than that obtained from the PV system using the Medina data. The results showed that the CSP system is provides a higher reliability benefit than the PV system in specific areas or atmospheric conditions with high DNI.
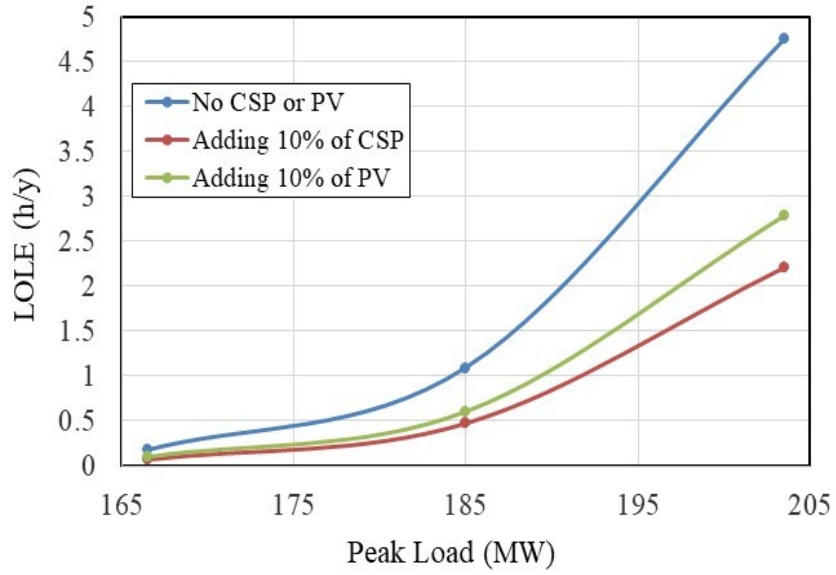
Figure 5-5: System LOLE considering 10% CSP and PV penetration
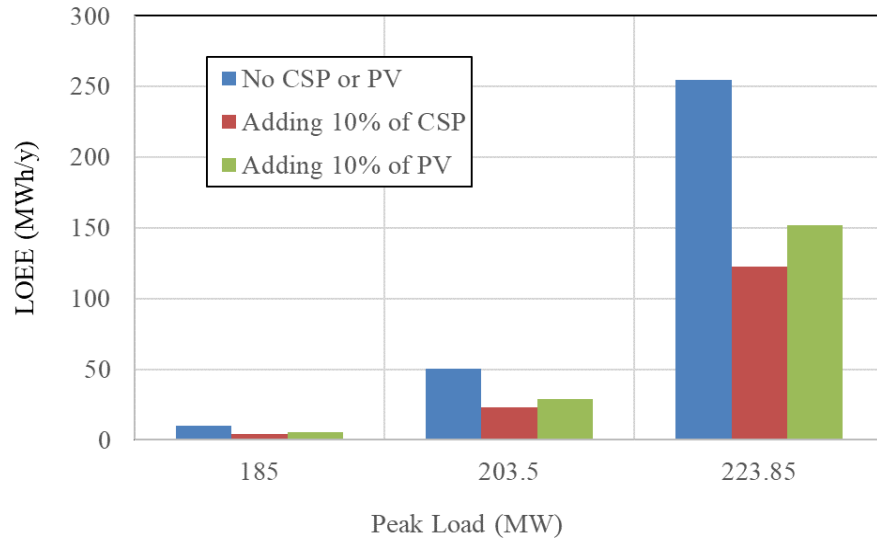
Figure 5-6: Loss of energy indices after addition of 10% CSP and PV

5.4 A Comparison of Capacity Values of CSP and PV in an Electric Power System

The capacity values of CSP and PV systems were investigated in this section by evaluating the system ELCC and CC of the respective solar technologies considering a different solar power capacity levels. A study was carried out using the RBTS modified with the addition of 24 MW, 48 MW, and 72 MW of CSP and PV, which correspond to 10%, 20%, and 30% of the RBTS capacity, respectively. The additional system peak load that can be carried by the system with the addition of CSP or PV in the system is evaluated at the acceptable LOLE criterion of 1.09 hours/year.

The system LOLE profile obtained for a range of peak loads before and after adding 24 MW of solar technologies is shown in Figure 5-7. The peak load was varied from 166 MW to 203.5 MW considering an annual load growth of 10%. It can be noticed from Figure 5-7 that there are observable load-carrying capability benefits from the CSP and PV. The ELCCs of the systems approximately increase by 4 MW to 7 MW with replacing PV by CSP. This figure indicates that the relative reliability benefits from solar energy depend on the type of added solar technologies.
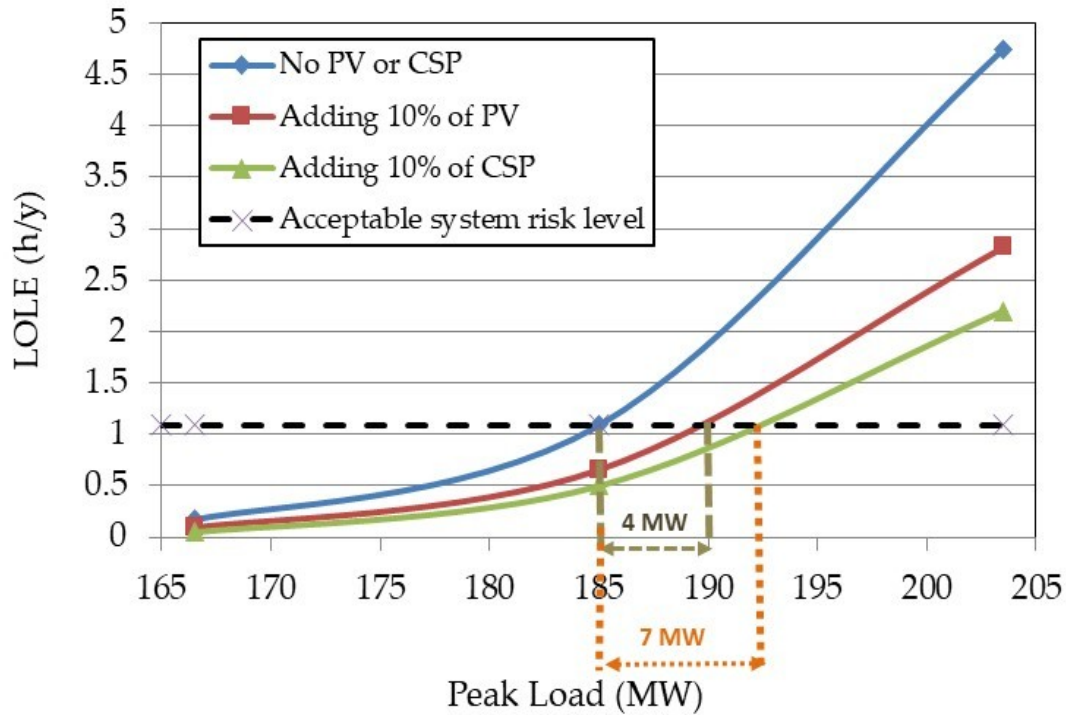
Figure 5-7: Variation in the RBTS LOLE upon the installation of 10% CSP and PV and

the annual peak load

This work was extended to assess the ELCC with an increase in solar power penetration in the RBTS. The results are shown in Figure 5-8. The comparison of the results shown in this figure illustrates that there is further ELCC benefit with growth in penetration levels for both solar technologies; however, this benefit does contribute to both to the same extent. With regard to the different ELCC contributions made by the two solar technologies, the amount that can be carried by adding 30% of CSP and PV are 10.01 MW and 7.8 MW, respectively.
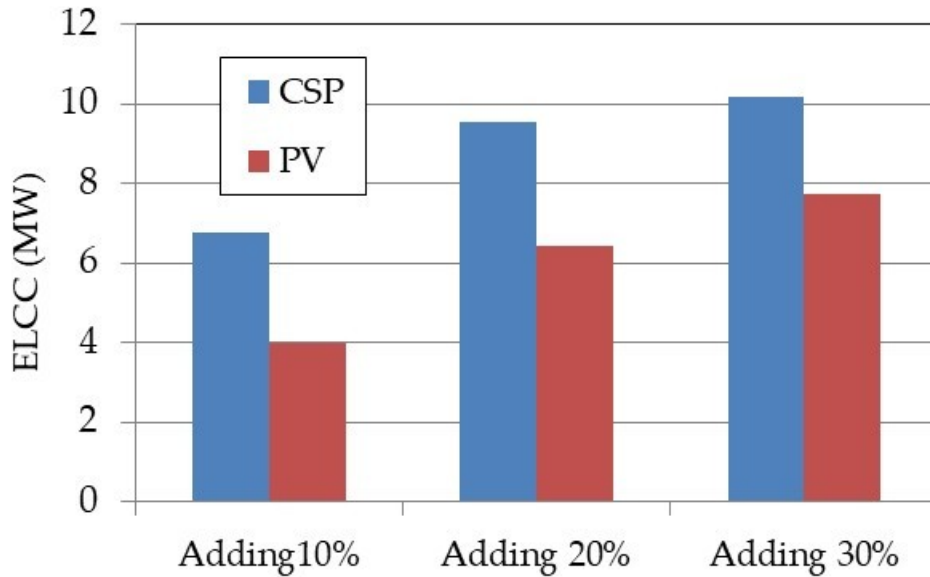
Figure 5-8: Incremental peak-load-carrying capability using CSP or PV

The obtained ELCC results, shown in Figure 5-8, are utilized as input data for Equation (2-8) to compute the CC of CSP and PV. The rated capacity is equal to 24, 48, and 72 MW. The system CC for the PV and CSP system using different penetration levels is shown in Figure 5-9. The capacity value for both technologies decreases with an increase in the penetration level of CSP and PV. The improvement of reliability tends to saturate when the capacity rating exceeds 24 MW for CSP and PV. The outcome analysis indicates that the CC of solar technology increases from 17.8% to approximately 28% upon replacing the PV system with CSP. The analysis indicates that CSP has the highest capacity value contribution when considering the Medina data.
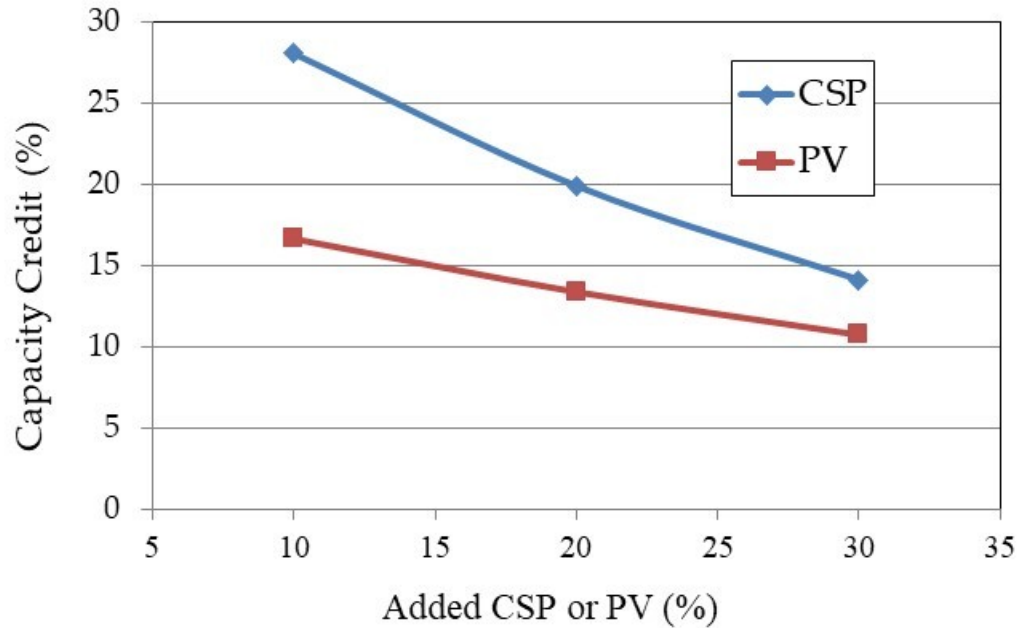
Figure 5-9: Capacity credit of CSP or PV at different penetration levels

5.5   The Impact of Seasonality on Capacity Credit of CSP and PV

The solar irradiation differs for different seasons owing to variations in the sunrise and sunset times and the strength of the solar irradiance at that particular time. An initial study of the mean seasonal variation in DNI and GHI (W/m^2) in Medina is shown in Figure 5-10. It is evident that seasons have a significant impact on the amount of DNI and GHI. The maximum amount of GHI and DNI is observed in the summer, followed by spring, fall, and winter.
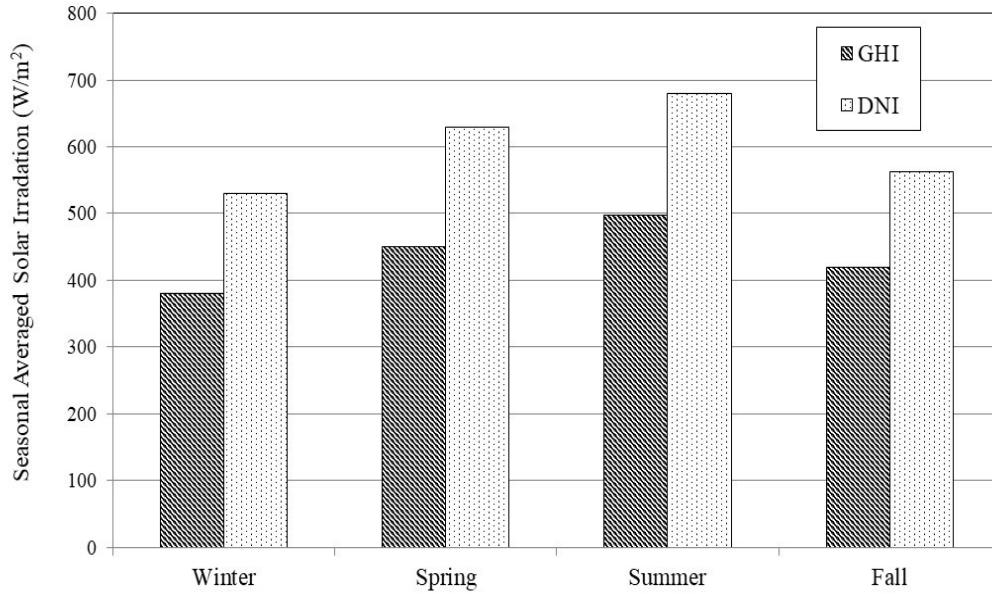
Figure 5-10: Seasonal average solar irradiation

The solar data of DNI and GHI for Medina were used to study the seasonal impact on the system CC of CSP and PV. Four models pertaining to the four different seasons were first developed to conduct this study. The PV and CSP capacity models developed for the four seasons were convolved with the RBTS capacity model and then combined with the corresponding seasonal load models to obtain the seasonal adequacy indices of the system. Different CSP and PV capacity rating of 24, 48, and 72 MW were added to the RBTS to compare the CC associated with the solar technologies for the different seasons.

Figures 5-11, 5-12, 5-13, and 5-14 represent the CC of the CSP and PV systems for the winter, spring, summer, and spring, respectively. The obtained results show that

the CC of CSP and PV systems change over time owing to weather, e.g., during winter and summer. The analysis indicated that summer provided the most reliable contribution, followed by fall, spring, and winter, in both technologies. Upon comparing the CC of PV and CSP, all figures presented in this study clearly indicated that, throughout the seasons, the CC value of the CSP system remains significantly higher than that of the PV system. For example, the CC for solar technology increases to almost twice its value, from 16.36% to 31% upon replacing 24 MW of PV with 24 MW of CSP during spring. The output results of this study cannot be generalized for all regions of KSA, especially those in the south, which have low DNI and high GHI. The reliability benefit of the CSP system is not always higher than that of the PV system, as the results depend on the irradiation data specific to the geographical locations.
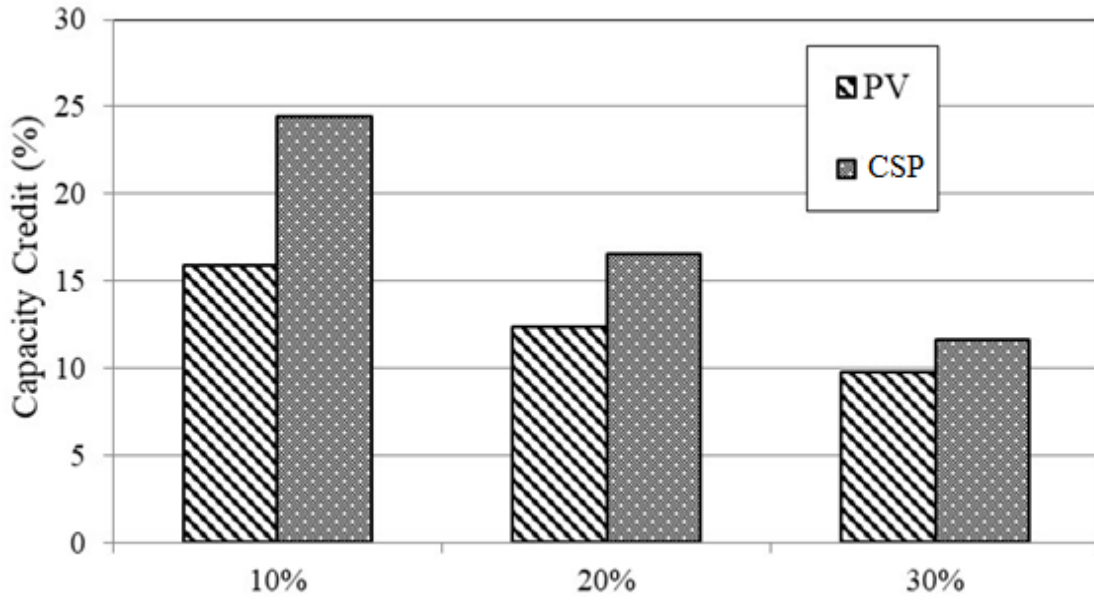
Figure 5-11: Capacity credit value after installing CSP or PV during winter
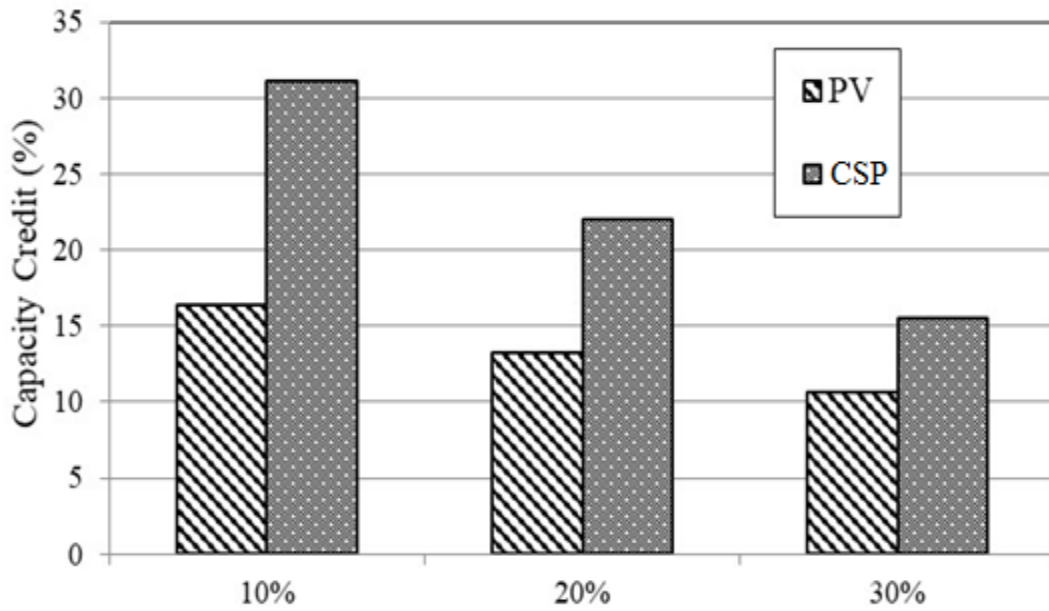
Figure 5-12: Capacity credit value after installing CSP or PV during spring
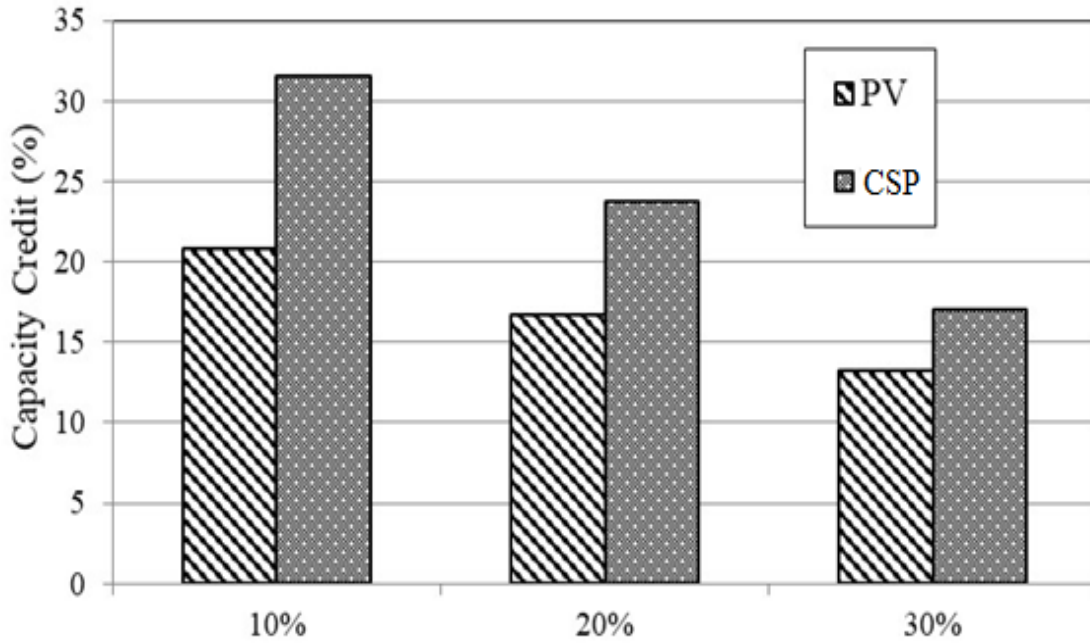
Figure 5-13: Capacity credit value after installing CSP or PV during summer
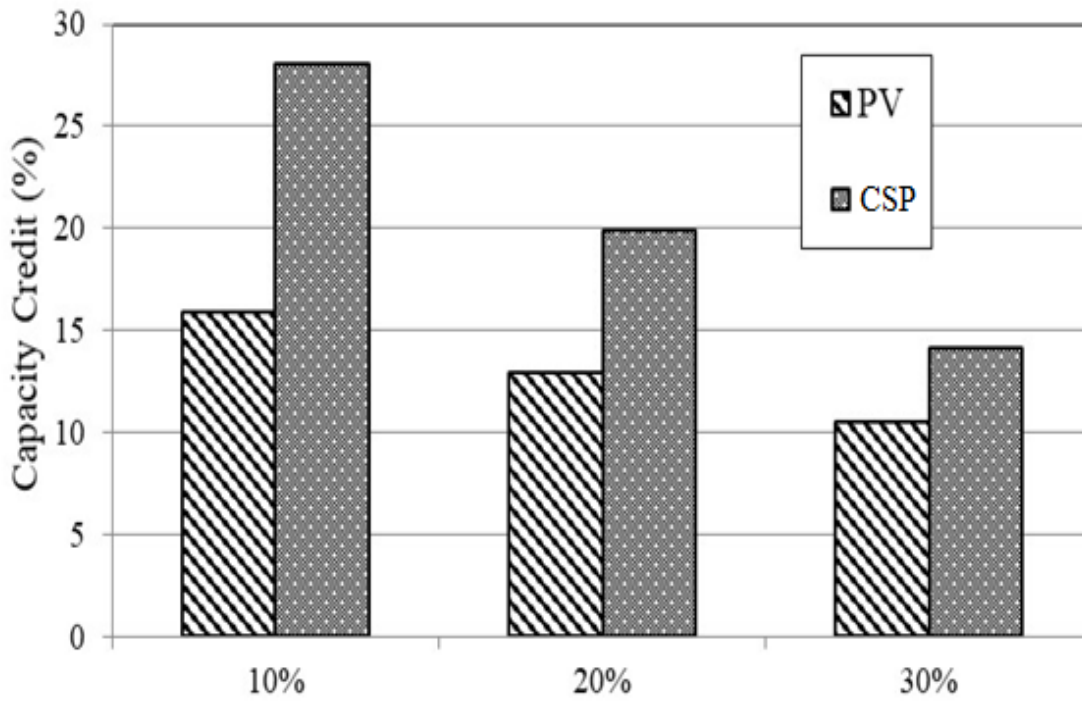
Figure 5-14: Capacity credit value after installing CSP or PV during fall

5.6   Summary

The integration of the CSP and PV power systems with electric power systems is expected to increase in the coming years. The study in this chapter presented a comparative analysis of the reliability contribution of large-scale integration of CSP and PV. The study utilized a test system model using the solar data from Medina, located in Saudi Arabia. This work considered the impact of load growth, added capacities of CSP and PV, and seasons on system reliability.

The utilization of the LOLE, LOEE, ELCC, and CC metrics led to a better understanding of the overall system adequacy contribution. The results obtined showed that the atmospheric conditions had a significant impact on the overall system reliability. The study demonstrated that the reliability contribution of solar power relied significantly on the form of solar technology being used. when the PV capacity was replaced with CSP, the reliability contribution and CC increased notably. This work provides an insight regarding the reliability of both technologies, which provides useful inputs for future plans of installing PV and CSP.

6   Reliability Model for Photovoltaic Power System Incorporating Cumulative Dust

6.1   Introduction

The output power of the PV system is mainly dependent on solar irradiation, availability of PV system components, and solar cell efficiency. Other factors related to weather conditions can also have a great impact on the output power of PV systems. Among these, dust deposition is a major concern since cumulative dust on solar panels reduces net solar energy yields. This can also have a significant impact on the reliability contribution of a PV system. It is, therefore, important to consider cumulative dust in the reliability modeling of a PV system.

A probabilistic model that describes the relationship between cumulative dust and power reduction was developed and combined with the reliability model of the PV system to incorporate the impact of the dust on overall system adequacy. The impact of implementing a dust-removal schedule in PV system maintenance planning on the reliability contribution of PV systems was also studied. This chapter illustrates the application of the proposed PV reliability model incorporating cumulative dust on the adequacy evaluation of the RBTS by conducting selected case studies. The analyses discussed in this study quantifies the impact of cumulative dust on the system reliability indices during spring and summer seasons.

6.2 Probability Distribution of Power Reduction due to Cumulative Dust on PV Panels

Deposition of dust particles on the solar panel highly affects the operation of the PV system, especially in desert regions where dust is prevalent. In other words, the efficiency of solar collectors drops gradually as dust piles up on the solar panel surface. Therefore, the rate of decreasing output power depends mainly on the rate of dust accumulation. Reference [42] performed an experimental test located in Saudi Arabia for accounting the daily dust deposition, as expressed in g/m^2 on the PV module surface. The accumulation of dust during a period is measured as shown in Figure 6-1 [42]. The regression model has been developed from this figure, which describes the amount of cumulative dust at different times of the year. A regression model involving the dates and cumulative dust was created and found to be a polynomial regression model using Equation (6-1). The polynomial Equation (6-1) is used in this work to assess the accumulation of dust in the different seasons.

Equation (6-1) was used to predict the dust accumulation during the winter, spring, summer, and fall periods in Riyadh and Medina, where the number of dust events is shown in Table 6-1 [44]. The obtained data was then used to create a discrete probability distribution of PV power reduction. The probability of each state can be

obtained using (6-2), where Y_i is the total occurrences in the interval of CD_i and CD_{i+1}.

The power reductions of each interval $\frac{(CD_{i+1}-CD_i)}{2}$ were calculated using Equation (6-3).
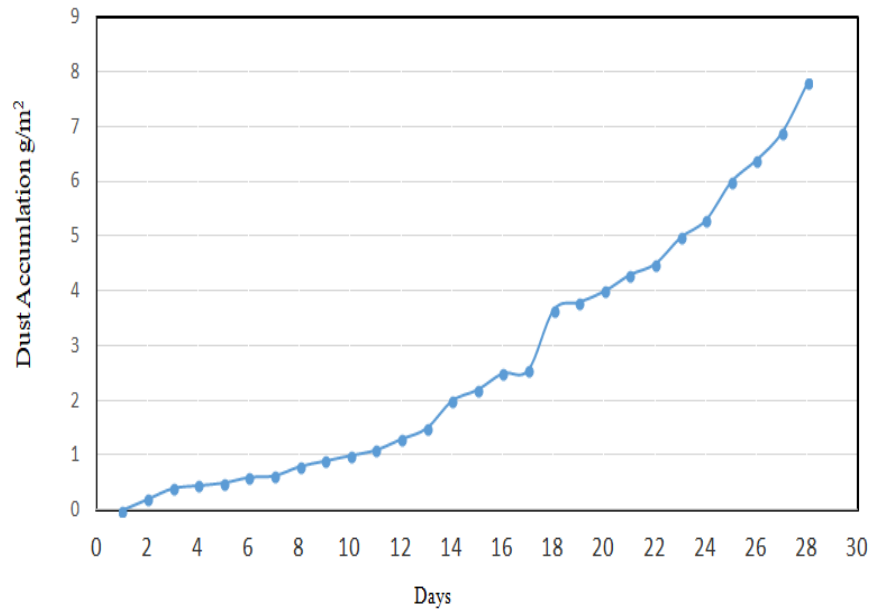
Figure 6-1: Cumulative dust deposition on the module surface [42].

$$CD = 0.0098 * (Dy)^2 - 0.0141 * (Dy) + 0.2248, \tag{6-1}$$

$$P_{CD(i)} = \frac{Y_i}{TNDE}, \tag{6-2}$$

$$T\,(\%) = 99.66 * \exp(-0.038 * CD), \tag{6-3}$$

where:

CD: Cumulative Dust g/m²

Dy: The number of dust event

P_{CDi}:   The probability of each state for cumulative dust

Y_i: Total occurrences in the interval i

$TNDE_i$:   The total number of dust event for each season

T: Reduction of the transmission coefficient

Table 6-1 was used as the input data for Equation (6-1) to estimate the accumulation of dust in the different seasons. Figure 6-2 shows the amount of dust accumulation in the Spring season based on the data recorded for Riyadh. Thereafter, the probability distribution of power reduction caused by dust for the season was created using Equations (6-2) and (6-3), and the output power distribution is shown in Figure 6-3. This figure is combined with Figure 3-5, as discussed in Chapter 3, to obtain the overall discrete probability distribution of the output power of the PV system. The process is repeated for the other seasons to obtain the PV capacity model for winter, summer, and fall seasons as well.

The developed framework was applied to a reliability test system containing the conventional generation unit and PV system to investigate the impact of cumulative dust on the reliability contribution of the PV system. The conventional generation reliability data from the RBTS are used in this work with a total installed capacity of 240 MW [46]. The generation reliability model is convolved with the hourly load model.

Several sensitivity analyses were performed to test the effectiveness of this methodology.

Table 6-1: Mean Dust Events [44]

Riyadh			
Winter	Spring	Summer	Fall
36 days	77 days	53 days	23 days
Medina			
Winter	Spring	Summer	Fall
33 days	57 days	30 days	7 days
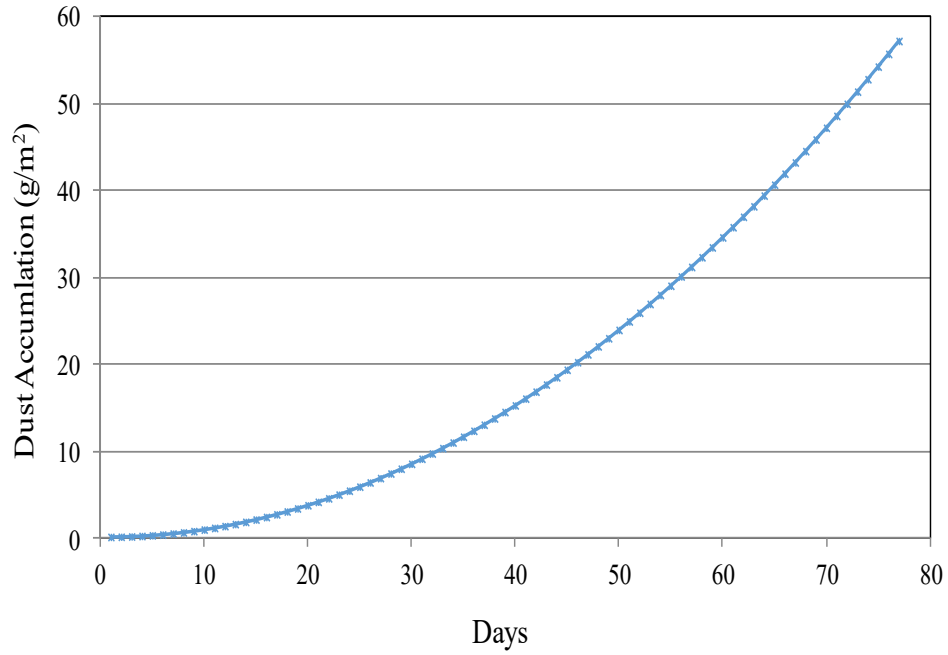
Figure 6-2: Cumulative dust deposition during spring
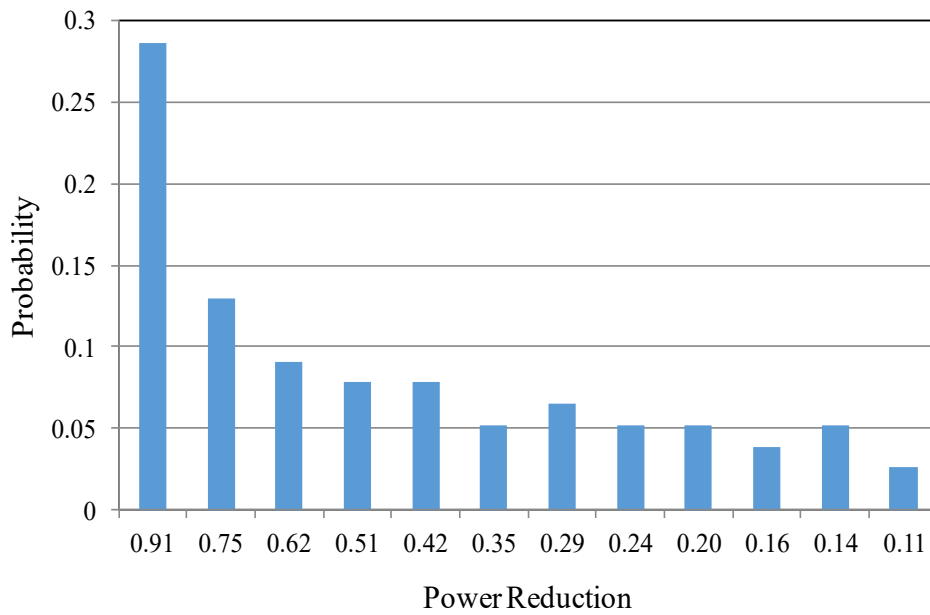
Figure 6-3: Probability distribution of power reduction, Riyadh (spring)

6.3 The Impact of Dust Accumulation on Reliability Contribution of the PV System

The system LOLE and LOEE indices were evaluated taking into consideration the two cases: (1) PV panel free from dust, and (2) PV panel surface with accumulated dust. In Case 2, the accumulated dust was removed from the PV panel surface at the end of each season, as shown in Figure 6-4. The probability distributions of power reduction were created for all the seasonal periods of the year. The obtained probabilistic model of power reduction is shown in Figures 6-5 and 6-6.
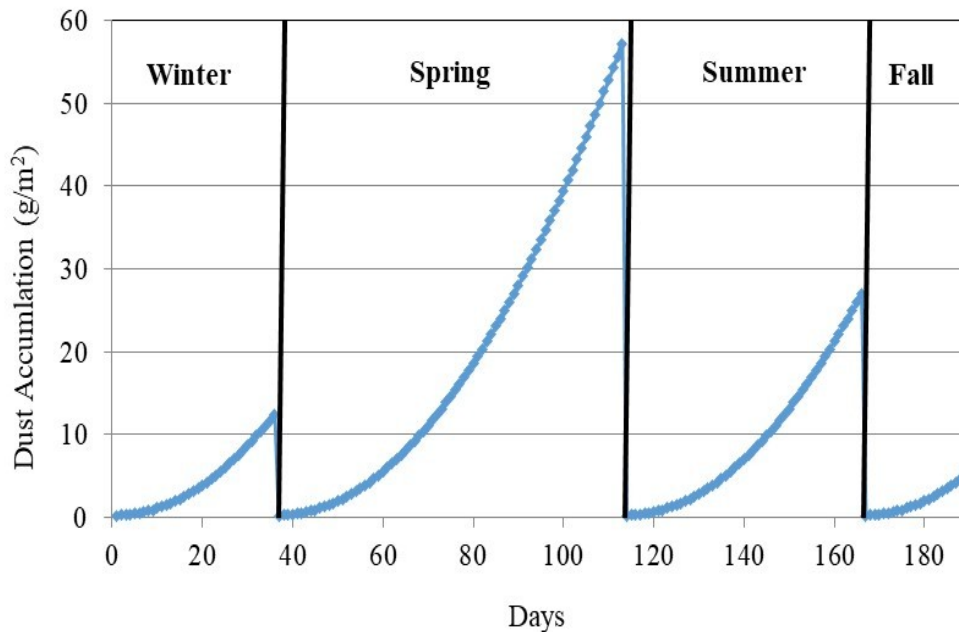
Figure 6-4: Cumulative dust
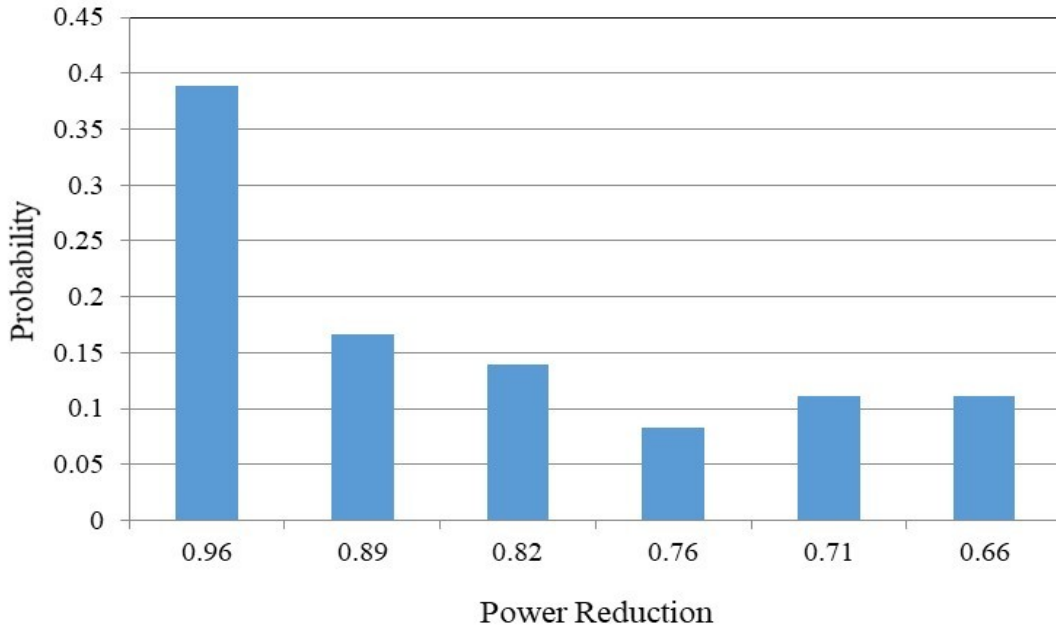
Figure 6-5: Probability distribution of power reduction, Riyadh (winter)
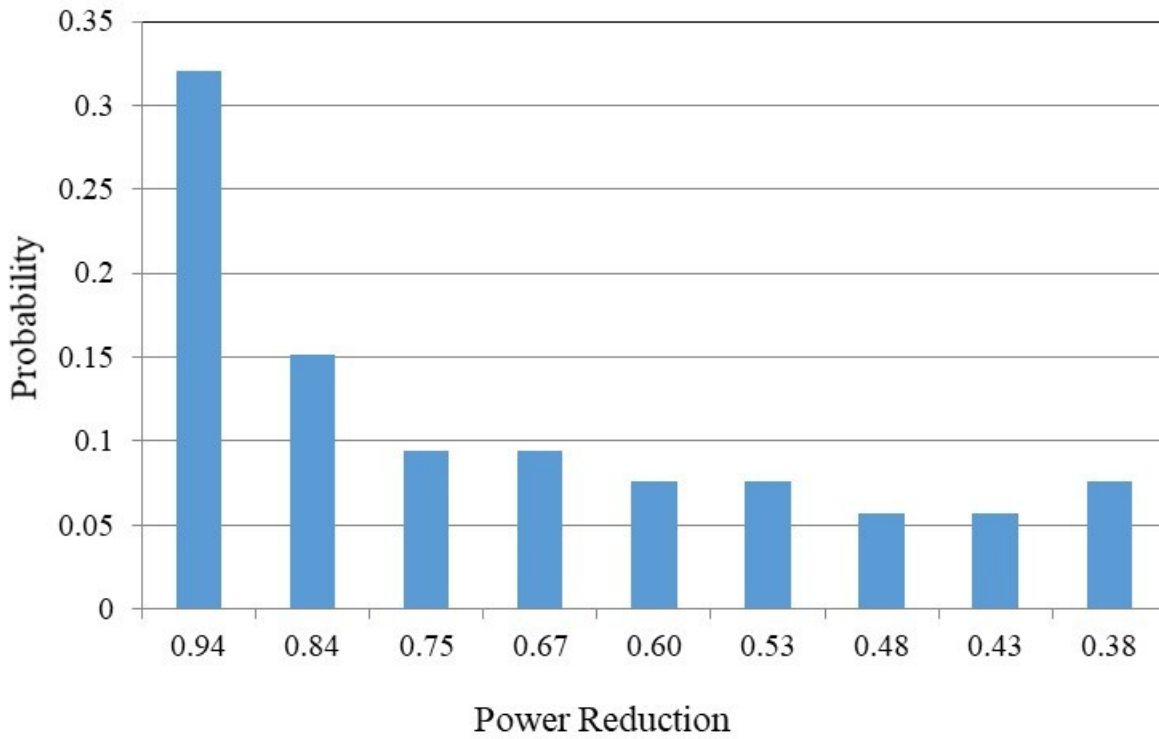
Figure 6-6: Probability distribution of power reduction, Riyadh (summer)

The seasonal hourly system load was used to create the load model for the respective period. The LOLE and LOEE were evaluate for each season, and the annual system indices can be evaluated by summing up the respective seasonal LOLE and LOLE indices using Equations (4-6) and (4-7). The peak load varied from 166.5 MW to 203.85 MW to investigate the impacts of load variation and dust accumulation on the system adequacy. The winter, spring, summer, and fall reliability system indices were calculated by first considering the addition of 24 MW of the PV system. Figures 6-7 and 6-8 show annual reliability indices of LOLE and LOEE respectively, with and without dust accumulation on the PV panels for the various peak loads.   The figures demonstrate that the PV system reliability is very sensitive to change in system peak load. The incremental reliability contribution of PV decreases significantly when the cumulative dust factor is considered. The annual system LOLE increased from 5.5 to 7.0 h/y due to the impact of accumulated dust, as shown in Figure 6-9.
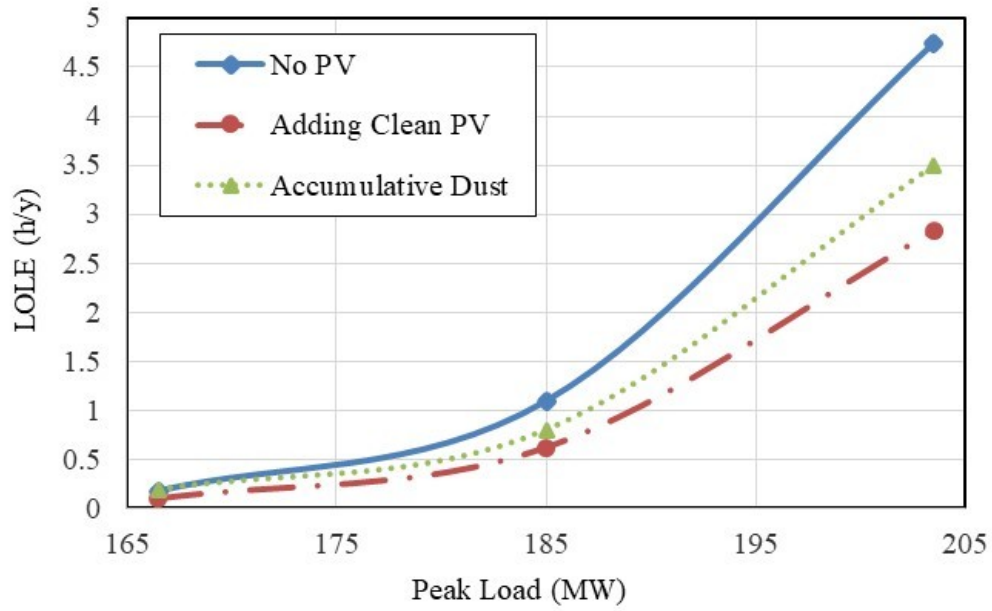
Figure 6-7: Impact of dust on the system LOLE as a function of the system peak load at

a Riyadh location
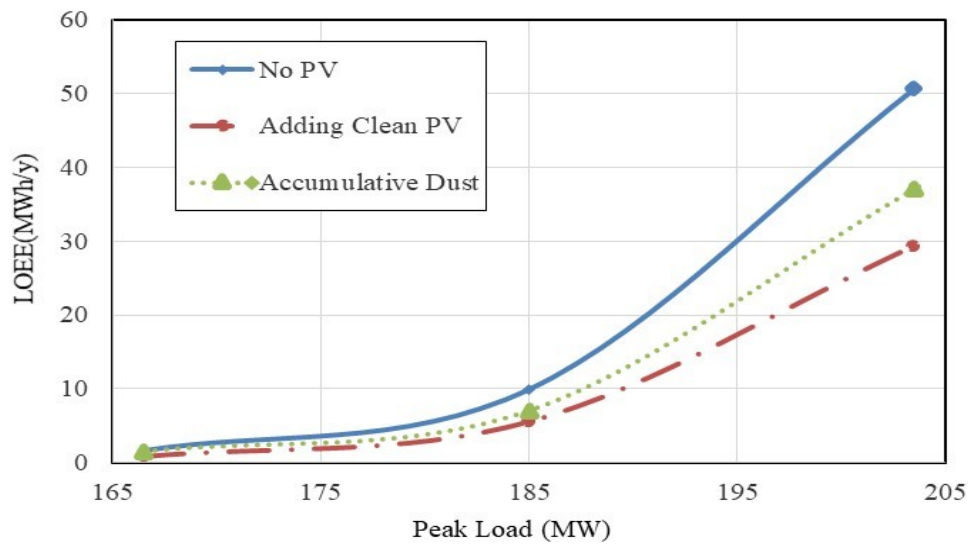
Figure 6-8: Variation in risk level of LOEE with system peak load at Riyadh
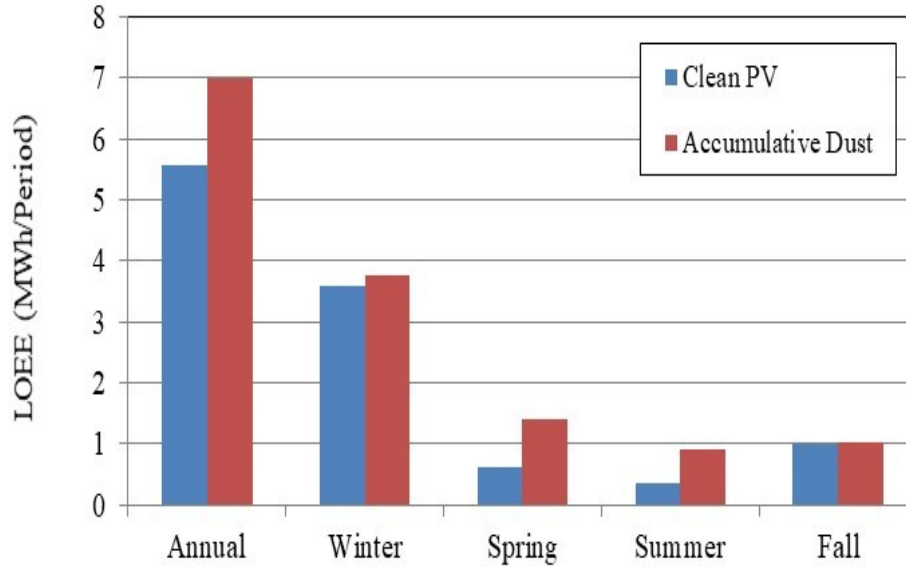
Figure 6-9: System LOEE for a peak load of 185 MW at Riyadh

6.4 The Impact of Seasonal Dust Accumulation on Effective Load-Carrying Capability and Capacity Credit of PV

The system incremental loads that can be carried with the addition of 24 MW of PV in the RBTS with a peak load of 185 MW were first evaluated with and without considering dust accumulation in this study. Equation (2-8) was utilized to evaluate the CC of PV. Table 6-2 indicates that there is a reduction in the CC of PV due to accumulated dust in the different seasons, but not to the same extent. The results also indicate that the impact of cumulative dust on the CC of PV is low during fall and high during spring.

127

Table 6-2: Capacity Credit for Different Seasons, Riyadh

Winter	
Clean PV	14.75%
Cumulative Dust	12.77%
Spring	
Clean PV	16.48%
Cumulative Dust	8.60%
Summer	
Clean PV	23.79%
Cumulative Dust	17.08%
Fall	
Clean PV	16.18%
Cumulative Dust	15.38%

A similar study was also conducted to investigate the impact of dust accumulation on the CC of PV in the Medina location. The net amount of cumulative dust using Equation (6-1) was found to be 32.37 g/m² for Medinah. It should be noted that the Riyadh has a dust accumulation of 57.24 g/m² in the same season. The discrete power reduction distribution for the Medina site is shown in Figure 6-10. This figure was convolved with the COPT of PV of Medina shown in Figure 3-5, to build the overall

probabilistic model of PV. Figure 6-11 shows that the system CC of PV for clean and dusty PV in the spring season are 16.24% and 11.3% respectively. The corresponding CC for the Riyahd location were 16.48% and 8% respectively.
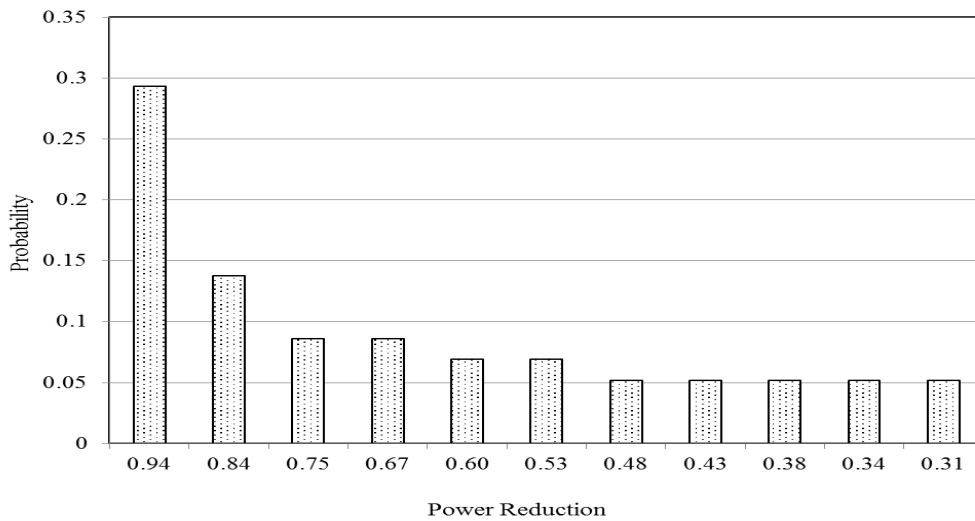
Figure 6-10: Probability distribution of power reduction in Medina (spring)
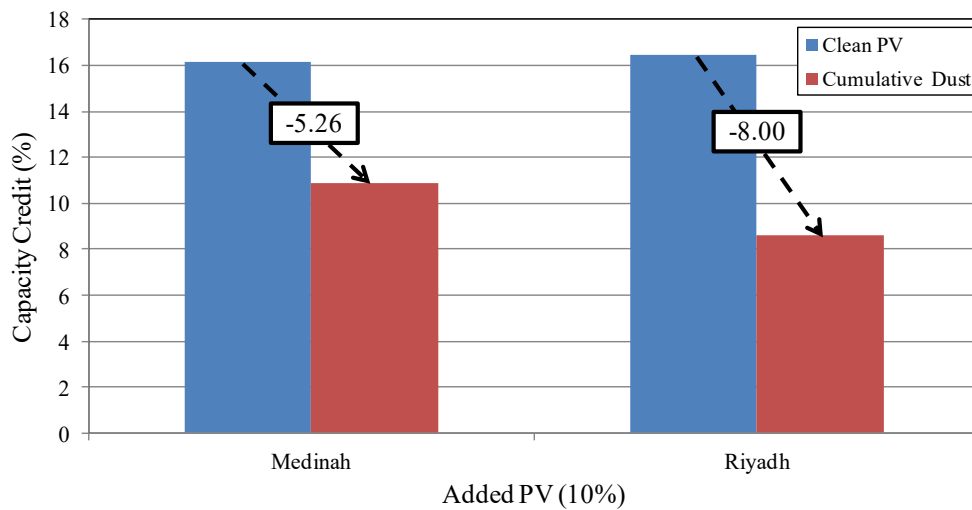
Figure 6-11: Capacity credit (%) for the spring period

6.5 Impact of Dust-Removal Schedule on the Reliability Contribution of the PV System

The accumulation of dust substantially decreases the PV system availability and therefore, reduces the reliability contribution of PV. Incorporating a proper dust removal schedule in maintenance planning of PV systems can increase the energy production and improve the reliability contribution from these energy sources. It is evident that the reliability contribution of PV in Riyadh during spring and summer is higher than that during winter and fall, as shown Figure 6-9. It can also be seen from this figure that the cumulative dust has a significant impact on the reliability contribution of PV during spring and summer, compared with winter and fall. Therefore, it is important to take these facts into consideration while planning an effective dust removal schedule. In this section, the following two cases are considered for removing the accumulated dust.

Case A

The dust is removed twice during spring and summer and once during winter and fall. Figure 6-12 shows the cumulative dust deposition in different seasons while taking the cleaning schedules into consideration. The probability distribution of power reduction for Case A was created, and is shown in Figures 6-13 and 6-14. After cleaning the dust, the output power of PV system greatly increased, which resulted in the

reduction of LOLE and LOEE as shown in Figures 6-15, 6-16, and 6-17. Table 6-3 shows that there is significant increase in overall PV CC when the dust-removal schedule is implemented. The annual CC increases from 12.29% to 15.79% with the dust-removal using the Case A schedule.
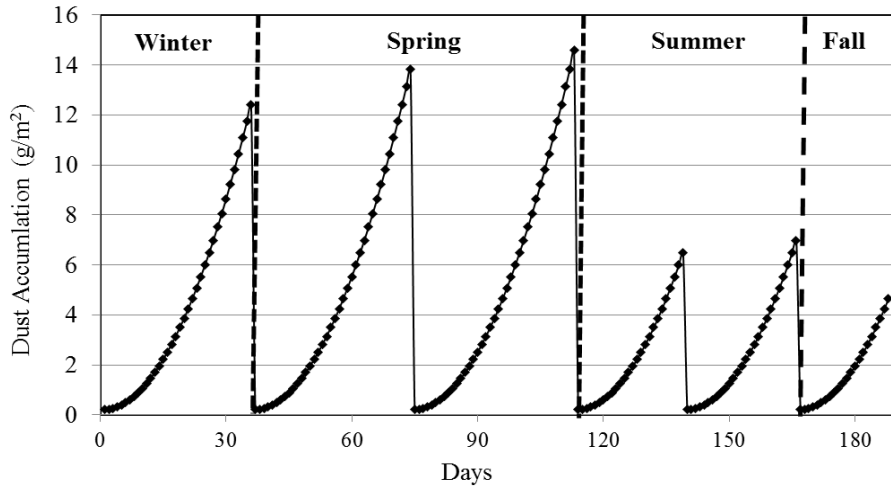
Figure 6-12: Cumulative dust in Case
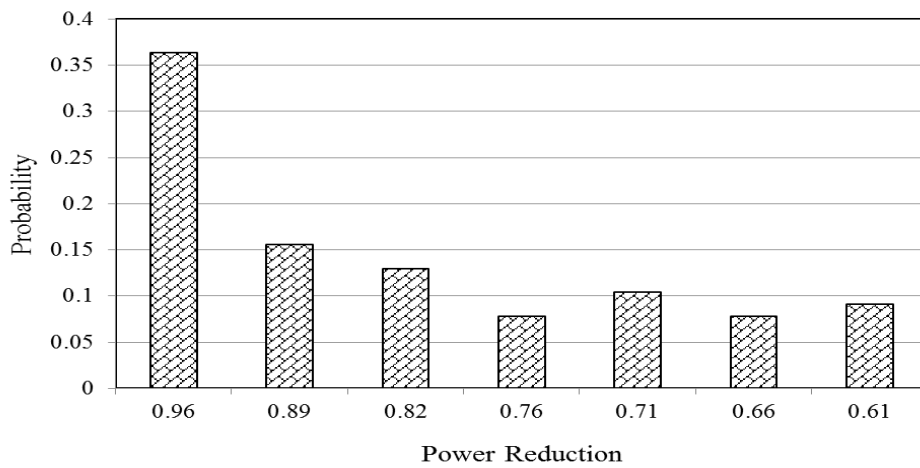
B

Figure 6-13: Probability distribution of power reduction considering Case A dust-

removal schedule (spring)
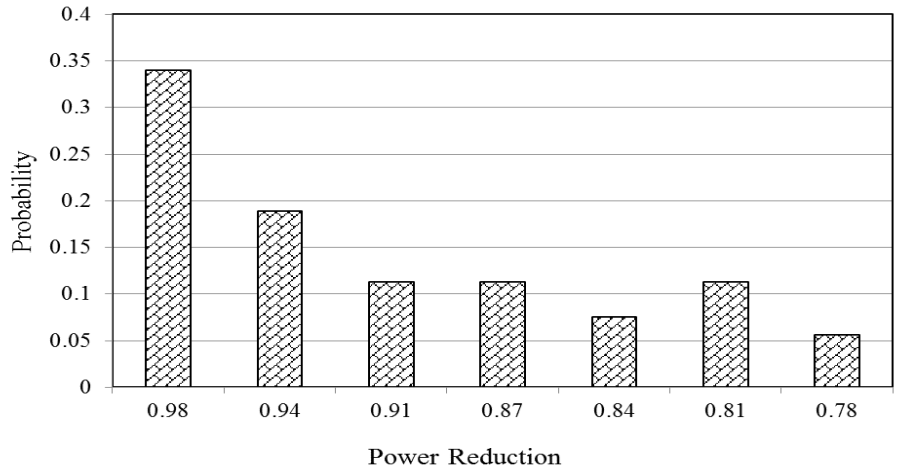
Figure 6-14: Probability distribution of power reduction considering Case A dust-

removal schedule (summer)
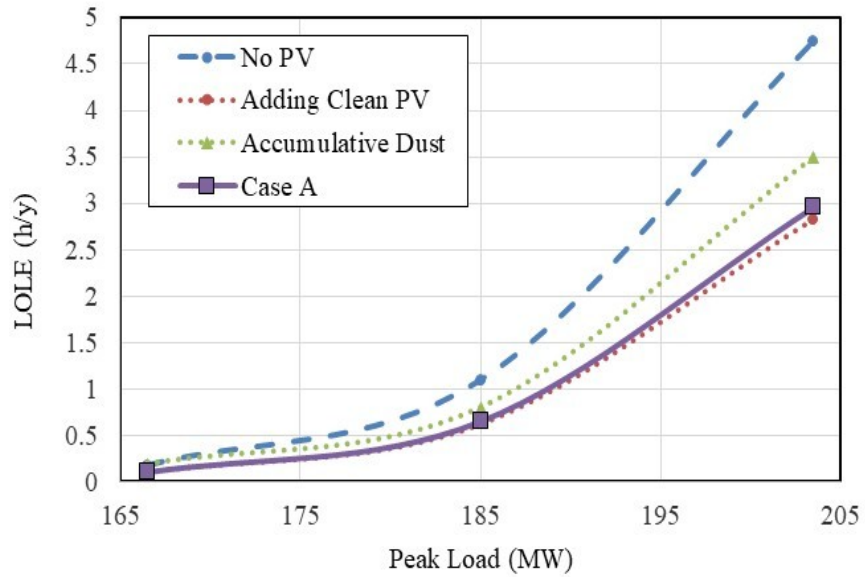
Figure 6-15: Impact of Case A dust-removal schedule on system LOLE
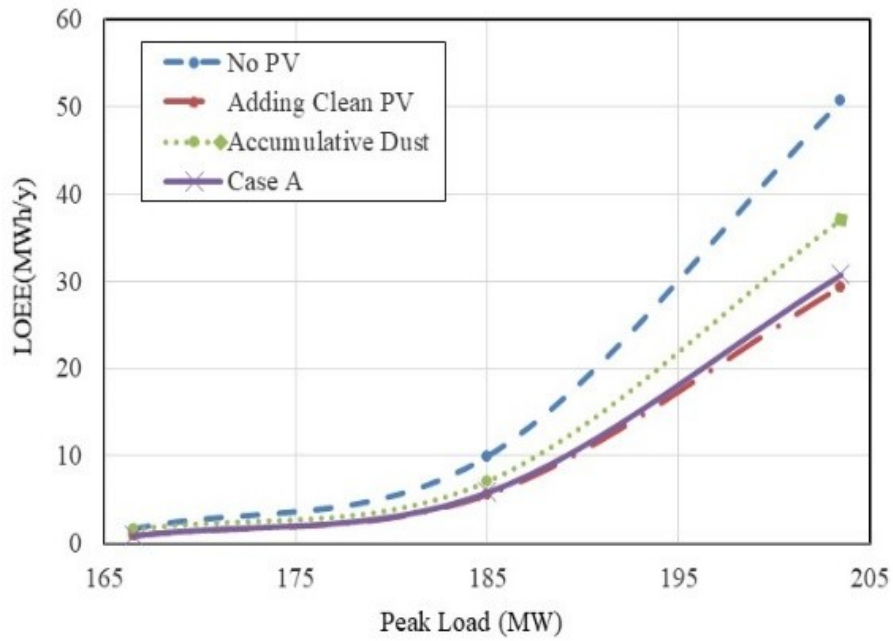
Figure 6-16: Impact of Case A dust-removal schedule on system LOEE
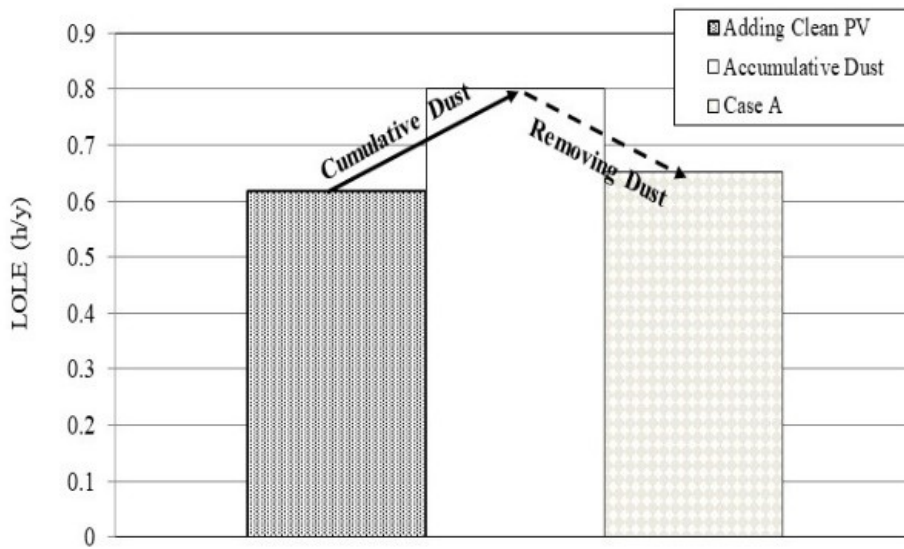
Figure 6-17: Impact of cumulative dust and removing dust on system LOLE at a peak

load of 185 MW

Table 6-3: Capacity Credit for Different Periods, Riyadh

Annual	
Clean PV	16.9%
Cumulative Dust	12.29%
Case A	15.79%
Spring	
Clean PV	16.48%
Cumulative Dust	8.60%
Case A	14.9%
Summer	
Clean PV	23.79%
Cumulative Dust	17.08%
Case A	21.81%

Case B

In this case, the dust is removed three time during spring and summer and twice during winter and fall. Figure 6-18 shows the cumulative dust deposition during winter, spring, summer, and fall with the implementation of this dust-removal schedule. The probability distribution of power reduction for Case B was created. The

reliability contribution of PV improved significantly, as shown in Figures 6-19 and 6-20. It can however be seen that there is not much difference in the results between the two dust-removal schedules that were illustrated. Case B schedule provides slightly better results than Case A at the cost of more dust removal tasks which adds to the maintenance costs. The method illustrated in this work can be used to obtain the most cost-effective dust-removal schedule by comparing the costs with the resulting benefits.
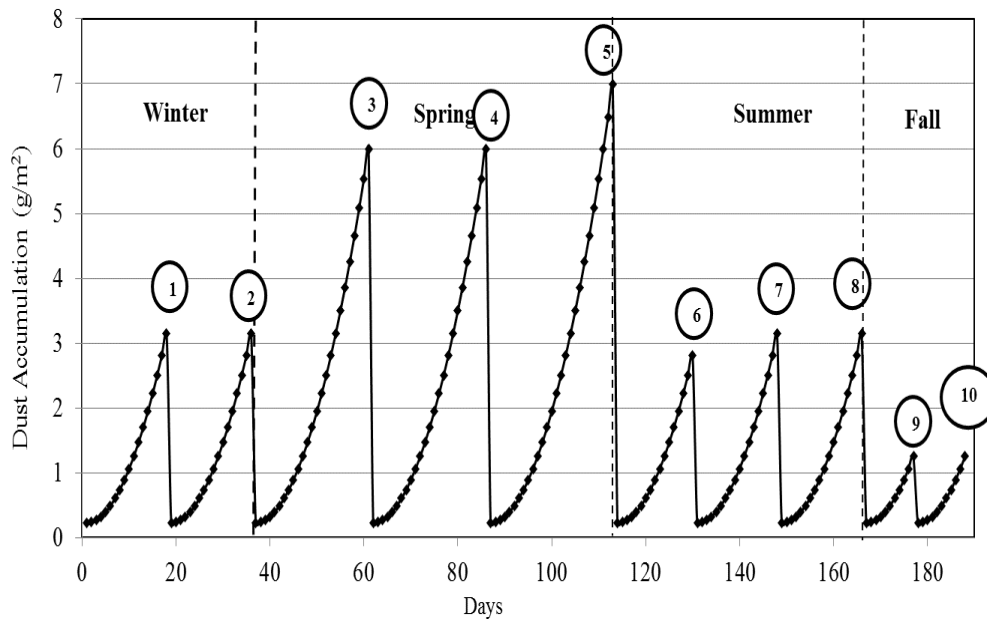
Figure 6-18: Cumulative dust in Case B
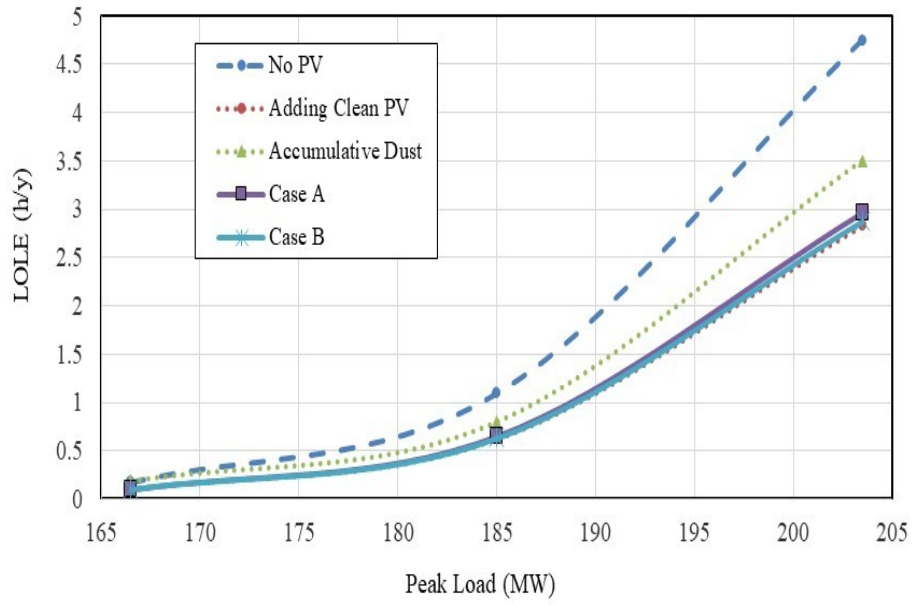
Figure 6-19: Annual indices of LOEE
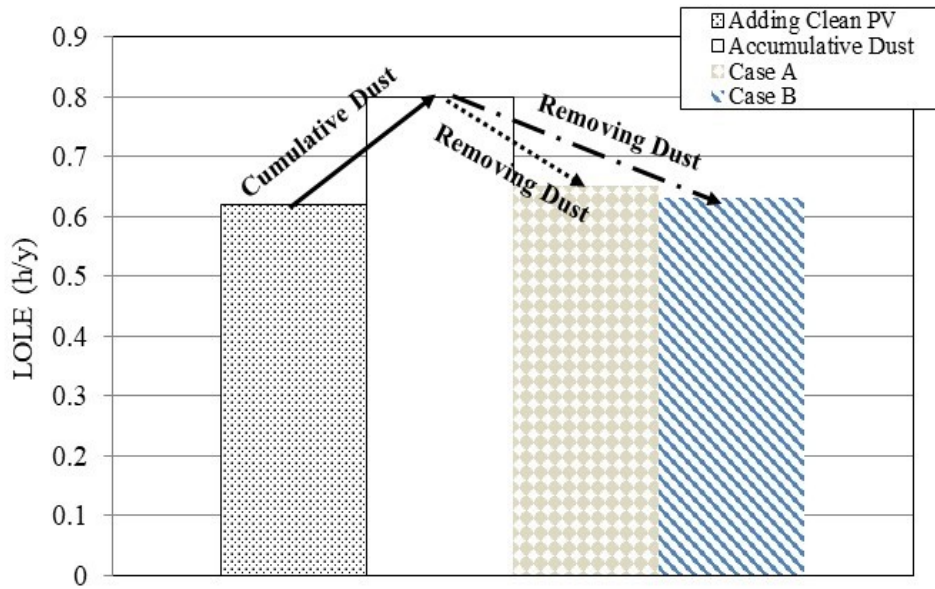
Figure 6-20: The system LOLE with using two scenarios of dust removal

6.6   Summary

Many potential PV sites, such as the KSA, may be subject to dusty environment where the wind blows dust into the air and onto the surface of the PV modules. As accumulated dust has a significant effect on the reliability contribution of PV, the effect of cumulative dust has been incorporated into this study. This chapter presents a simplified model of PV that incorporates cumulative dust on the solar panel. Combining the PV system components model, the PV power-out model, and the probabilistic model of PV power reduction caused by the cumulative dust power reduction model yields the overall PV multi-state model. The proposed method provides useful information regarding the quantitative impact of cumulative dust on the contribution of PV in terms of generation system adequacy.

The results indicate that the accumulation of dust has a significant influence on the reliability contribution of the PV system and depends on the time of the year. Moreover, the analysis and results provide a better understanding of the effect of a dust-removal schedule on the overall PV system reliability. The results indicate that the spring and summer periods require more dust removal than for winter and fall. An appropriate dust-removal schedule can be developed using the methodology illustrated in this chapter to perform a cost-benefit analysis of potential dust cleaning schedules.

7   Summary, Conclusions and Future Work

7.1   Summary and Conclusion

Solar energy has been recognized as a clean power source, and has received different forms of financial subsidies from governments and organizations. Recently, solar power technology has been receiving great attention from researchers and the power industry as an important source of renewable energy. Solar power generation technologies can be broadly classified into two types: PV power technology and CSP technology. PV and CSP systems include a combination of electric and thermal devices and relevant switchgear components which have different characteristics. The output power of PV and CSP cannot be controlled easily as conventional generation due to the intermittent nature of solar irradiation and climactic conditions at different locations. PV systems can have different topologies which have direct impacts on the reliability contribution of the solar PV systems. In this thesis, probabilistic techniques using analytical methods were employed to develop detailed reliability models of PV and CSP systems. These models were then integrated into the overall system reliability model for the evaluation of system adequacy. This work has been extended to incorporate the impact of cumulative dust on the reliability modeling of PV system.

Chapter 1 presented the basic concepts of power system reliability. This chapter discussed the research motivation and literature review. The main contributions of this work are briefly presented in this chapter.

Chapter 2 introduced an overview of generation system reliability concepts, including different methods for adequacy evaluation. The generation system adequacy assessment approaches can be classified as deterministic and probabilistic techniques, and both methods are discussed in this chapter. The deterministic approach cannot recognize the random system behavior and quantify the system risk in a given generation system. Therefore, the probabilistic method is a more appropriate method for adequacy assessment of a generation system including variable power generation systems such as the PV and CSP. An analytical probabilistic technique that uses relatively simple numerical calculations was developed and applied in the detailed studies in this thesis.

The probabilistic model developed in this thesis utilizes mathematical approaches for adequacy evaluation. A discrete probability distribution of available solar power is developed as the capacity model of the PV and CSP. The overall system generation model is then developed by integrating the PV/CSP capacity models into electric generation system. The hourly load variation profile was utilized in this work. The system risk indices can be evaluated by combining the system generation model and the load model.

The detailed reliability modeling of a PV system for generation system adequacy assessment is presented in Chapter 3. The output power of PV systems differs from the power generated by conventional sources due to the high uncertainty revolving around PV power output and the availability associated with PV system components and their relative configurations. The PV system topology comprises major components such as DC-link capacitor, inverter, circuit breaker, and transformer. The failure of these components can lead to the failure of a PV system. The functional reliability block diagrams of the central, string, and micro PV system components were built to obtain the two-state operation model. The PV power output curve is employed to derive the available PV power output from solar irradiation. This analytical model depends on hourly solar irradiation and solar panel efficiency. Significant hourly solar irradiation data are required in this section to create the multi-state capacity model of the PV. The obtained multi-state model in this step is convolved with the two-state model of the PV system components to build the overall COPT of the PV system.

The developed models and methodologies have been applied to perform a wide range of reliability sensitivity studies on a test generation system including PV system. Different key factors, such as peak-load variation, different installed PV are taken into consideration in these studies. This work was conducted using five years' solar irradiation data for Medina located at 24.52° N latitude. The results obtained in this study noted an improvement in the system reliability when PV is added to the

140

generation system; however, this incremental benefit declines with installing more PV capacity. The analysis indicates that the capacity value benefit of using the micro-inverter PV system is highest in relation to the central and string PV system. This can be noticed when the CC of PV increases from 19% to 35.5% after replacing the central PV system with the micro-inverter PV system.

The equivalent share between removing a conventional generation unit and replacing this with equivalent PV while maintaining the system reliability at the same level is studied in Chapter 3. The results demonstrated that the system LOLE can be maintained by replacing 40 kW of conventional generation with 270, 180, and 98 kW of string, central, and micro PV system, respectively. The results showed that the risk-based equivalent capacity ratios by replacing one unit of conventional generation are 7, 5, and 3 units of central, string, and micro-inverter PV capacity, respectively.

Chapter 4 involved the development of a concentrated solar power model in a probabilistic framework to compute the adequacy of a generation system including CSP. The two-states of the CSP reliability component model were created first. Next, the discrete probability distribution associated with the output power of CSP and their possible probabilities were obtained. The overall COPT of the CSP system was constructed by convolving the multi-state model of the output power of CSP with two-state models of the CSP components. The developed model in Chapter 4 is applied to the RBTS to calculate the impact of load variation, CSP penetration level, and

geographical location on the reliability benefit of CSP. The application of this study was assumed at three different latitudes of 34.86° N, 24.42° N, and 37.38° N corresponding to Daggett City located in the USA, Medina located in the KSA, and Seville located in Spain, respectively. The results indicated that the reliability degraded significantly with an increase in peak load. Moreover, the LOLE and LOEE indices decreased with increasing capacity levels of CSP to RBTS at all three locations. The analysis indicated that the adequacy benefit of using CSP depends largely on the site resources where the CSP system is installed.

The developed reliability models of PV and CSP systems are utilized in Chapter 5 to perform a comparative reliability study of the generation system integrated with a large-scale central PV and CSP systems. A wide range of indices, such as the LOLE, LOEE, ELCC, and CC were used for such comparison purpose. The application of this study was illustrated utilizing RBTS and was assumed located in Medina. A number of factors were included in the comparative study, such as system load variation, increasing PV and CSP capacity level, and seasonality. The obtained results indicated that when both CSP and PV systems are applied to the same geographical location, the adequacy contribution of using CSP is significantly higher than that of PV. The results confirmed that the summer period provides the largest CC contribution followed by spring, fall, and winter in both the technologies.

The amount of accumulated dust covering the PV surface greatly reduces the overall energy production. Chapter 6 presented the impact of cumulative dust on the reliability modeling of the PV system. This work utilized a polynomial regression model of cumulative dust obtained from an experiemental test carried out by researchers at KSU [42]. The regression model was used to predict the cumulative dust on the PV surface for each season at Riyadh and Medina. Subsequently, the probabilistic model of the power drop caused by accumulated dust was created, and this was convolved with the overall system reliability model of PV system obtained in Chapter 6. The developed analytical model in Chapter 6 was applied to the RBTS to analyze the impact of cumulative dust on the reliability contribution of PV and to investigate the impact of the dust-removal planning. The results showed that the incremental reliability benefit of adding PV to electric generation system is reduced significantly due to the accumulation of dust on the PV module. The output analysis indicated that the reliability contribution of PV system can be improved with incorporating a proper dust-removal strategy. The method demonstrated in dust removal strategy can be utilized to estimate the cost-effective dust removal while maintaining the reliability indices at an acceptable risk level.

In summary, the thesis presents some procedures that can be utilized to integrate different solar power technologies in existing generation systems to evaluate the reliability of solar power contribution. The obtained results from different case studies

conducted in this thesis demonstrated the sensitivity of the assessed reliability indices to a few important factors that were incorporated in the reliability analysis of CSP- and PV-integrated electric power generation systems.

7.2   Future Work

CSP plants can be operated as integrated solar combined cycles (ISCCs) that utilize different configurations [76], [81], [82] to reduce the average LCOE and to place the CSP system at a higher commercial position. ISCCs are modern combined cycle power plants that involve conventional/nonconventional generation and thermal input of solar energy. The main concept behind this technology is that solar plants can be operated partially using fuels [83], [84] that can be fossil or non-fossil derived, such as biomass [84], [85]. By taking advantage of the existing infrastructure associated with the development of a conventional thermal power plant, the economics of the concentrating solar thermal component can potentially be significantly enhanced.

The ISCC, with a CSP solar field, essentially contains two main parts—a CSP component and a conventional generator. These two main parts are connected in parallel. The solar field includes CSP collectors and solar boilers. The power block basically comprises of the following components: (1) Gas turbine, generator, compressor, and combustion chamber and (2) steam turbine, generator, condenser, and feed-water system. [86] Studied the fuel saving of a coal-fired plant by installing a CSP

to form an ISCC. The study found that there was 24.5% saving in fuel. Another study [87] proposed integrating solar thermal power with an existing conventional generation to evaluate the CO_2 reduction and fuel saving. This work presented an economic model for investigating the methods and mechanisms of integrating a CSP Collector with coal-fired power plants. The results showed that the new integrated system had lower generation costs than conventional coal-fired power plants. Reference [88] presented methods to integrate CSP with conventional power plants. An economic assessment showed that the ISCC has lower generation costs than fossil-fuel-generation plants. Another study [89] estimated the optimum value of installing conventional generation and CSP to provide a stable power output using an integrated solar system.

CSP–biomass hybrid plants are developing at a faster pace as a low-cost source of dispatchable renewable energy—a configuration that has a low environmental impact [90]. Reference [91] evaluated the combination of solar power and biomass, indicating that the levelized energy costs for hybrid solar–biomass power plants are competitive with other renewable energy systems in India. Hybrid plant studies in the literature review have primarily focused on the LCOE. There is a noticeable lack of research addressing the reliability impacts of ISCCs, which considers conventional or nonconventional generation, such as biomass. Therefore, a quantitative reliability assessment of the different ISCC technologies is essential for determining the reliability contribution of CSP in electric power systems.

Integration of thermal energy storage (TES) with CSP systems is a potential solution to the limitation in the availability of solar energy. TES can balance and compensate for variation in both load and generation systems. In this manner, energy storage can play a vital role in the CSP system applications and create opportunities to integrate high penetration of CSP units in system grids. The first commercial CSP/TES plant, including both CSP and power towers, was built and became operational in Spain in 2008 [91]. Developments like this, and others that have since been established, have made it necessary to conduct assessments for all the major components being used at these plants. This is because the LCOE production through CSP, with or without storage, has fallen behind that of wind power and PV.

TES, an additional component of the CSP system, has a significant influence on the plant operation. A simulation model has been presented in [59] to facilitate the prediction of the power output of CSP–TES using a System Advisor Model. The results indicated that the simulation model can be generalized to reproduce the performance of any trough plant. References [92], [93] evaluated the performance of CSP solar plants in a system grid using a validation of the FLAGSOL performance model. The validation was conducted by simulating an operating CSP solar thermal power plant and comparing the model's output results with the actual plant. The work published in [93] was expanded in [94], which assessed the economic benefits of adding energy storage to CSP. In general, the charging and discharging operations of TES depend on the

146

availability of thermal components in the energy storage. There is a lack of research

conducted regarding developing a proper reliability model of CSP that incorporates

TES.

References

[1] R. Billinton and R. N. Allan, "Reliability evaluation of engineering systems- Concepts and techniques," *New York: Plenum Press, 1992.*, 1992.

[2] R. Billinton and R. N. Allan, "Power-system reliability in perspective," *Electronics and Power,* vol. 30, *(3),* pp. 231-236, 1984.

[3] R. Billinton and R. N. Allan, *Reliability Evaluation of Power Systems.* (2nd ed.) *New York and London: Plenum Publishing,* 1996.

[4] W. Li and R. Billinton, "Reliability Assessment of Electrical Power Systems using Monte Carlo Methods", *New York : Plenum Press,* 1994.

[5] R. Billinton, M. Fotuhi-Firuzabad and L. Bertling, "Bibliography on the application of probability methods in power system reliability evaluation 1996-1999," *Power Systems, IEEE Transactions on,* vol. 16, *(4),* pp. 595-602, 2001.

[6] R. Allan *et al,* "Bibliography on the application of probability methods in power system reliability evaluation: 1987-1991," *Power Systems, IEEE Transactions on,* vol. 9, *(1),* pp. 41-49, 1994.

[7] R. Billinton, "Criteria used by Canadian utilities in the planning and operation of generating capacity," *Power Systems, IEEE Transactions on,* vol. 3, *(4),* pp. 1488-1493, 1988.

[8] J. F. Prada, "The value of reliability in power systems-pricing operating reserves", Energy Laboratory, 1999.

[9] Fatih. B, International Energy Agency, "CO_2 Emissions from fuel combustion," 2015.

[10] S. P. Europe, "Global market outlook for solar power 2017–2021," *Solar Power Europe: Bruxelles, Belgium,* 2017.

[11] P. Zhang *et al*, "Reliability assessment of photovoltaic power systems: Review of current status and future perspectives," *Appl. Energy,* vol. 104, pp. 822-833, 2013.

[12] V. Poghosyan and M. I. Hassan, "Techno-economic assessment of substituting natural gas based heater with thermal energy storage system in parabolic trough concentrated solar power plant," *Renewable Energy,* vol. 75, pp. 152-164, 2015.

[13] J. L. Sawin and E. Martinot, "Renewables bounced back in 2010, finds REN21 global report," *Renewable Energy World,* vol. 29, 2011.

[14] R. REN21, *Global Status Report, REN21 Secretariat, Paris, France,* 2017.

[15] U. Desideri and P. E. Campana, "Analysis and comparison between a concentrating solar and a photovoltaic power plant," *Appl. Energy,* vol. 113, pp. 422-433, 2014.

[16] S. Vergura and V. D. J. Lameira, "Technical-financial comparison between a PV plant and a CSP plant," *Revista Eletrônica Sistemas & Gestão,* vol. 6, *(2),* pp. 210-220, 2011.

[17] R. P. Mukund, *Wind and Solar Power Systems, Taylor and Francis Group,* 1999.

[18] N. Jenkins *et al,* "Embedded Generation (Power & Energy Ser. 31), INSPEC," 2000.

[19] J. Eyer and G. Corey, "Energy storage for the electricity grid: Benefits and market potential assessment guide," *Sandia National Laboratories,* 2010.

[20] G. Masson *et al, Global Market Outlook for Photovoltaics 2013–2017.European Photovoltaic Industry Association (EPIA), European Commision may 2013,* 2013.

[21] C. Philibert, International Energy, Agency, Technology Roadmap: Concentrating Solar Power. 2010.

[22] P. Lall, "Tutorial: temperature as an input to microelectronics-reliability models," *Reliability, IEEE Transactions on,* vol. 45, *(1),* pp. 3-9, 1996.

[23] A. Roy, S. B. Kedare and S. Bandyopadhyay, "Optimum sizing of wind-battery systems incorporating resource uncertainty," *Appl. Energy,* vol. 87, *(8),* pp. 2712-2727, 2010.

[24] R. Karki and R. Billinton, "Reliability/cost implications of PV and wind energy utilization in small isolated power systems," *Energy Conversion, IEEE Transactions on,* vol. 16, *(4),* pp. 368-373, 2001.

[25] R. Billinton and R. Karki, "Maintaining supply reliability of small isolated power systems using renewable energy," in *Generation, Transmission and Distribution, IEE Proceedings-*, 2001.

[26] R. Karki, A. Alferidi and R. Billinton, "Reliability modeling for evaluating the contribution of photovoltaics in electric power systems," in *Photovoltaic Specialists Conference (PVSC), 2011 37th IEEE*, 2011.

[27] W. Durisch *et al*, "Characterisation of photovoltaic generators," *Appl. Energy*, vol. 65, *(1)*, pp. 273-284, 2000.

[28] W. Ho *et al*, "Design of distributed energy system through Electric System Cascade Analysis (ESCA)," *Appl. Energy*, 2012.

[29] S. H. Madaeni, R. Sioshansi and P. Denholm, "Estimating the capacity value of concentrating solar power plants: A case study of the southwestern United States," *Power Systems, IEEE Transactions on Power System*, vol. 27, *(2)*, pp. 1116-1124, 2012.

[30] P. Denholm and M. Mehos, "Enabling greater penetration of solar power via the use of CSP with thermal energy storage," *Solar Energy: Application, Economics, and Public Perception*, pp. 99, 2014.

[31] J. Usaola, "Capacity credit of concentrating solar power," *Renewable Power Generation, IET,* vol. 7, *(6),* pp. 680-688, 2013. . DOI: 10.1049/iet-rpg.2012.0295.

[32] H. Price, "Assessment of parabolic trough and power tower solar technology cost and performance forecasts," *National Renewable Energy Laboratory, Golden, CO,* 2003.

[33] J. Hernández-Moro and J. Martínez-Duart, "Analytical model for solar PV and CSP electricity costs: Present LCOE values and their future evolution," *Renewable and Sustainable Energy Reviews,* vol. 20, pp. 119-132, 2013.

[34] (M. Stancati and M. Amon). *Saudi, SoftBank Announce Massive Solar Power Project,2018.* Available: https://www.wsj.com/articles/saudis-softbank-group-announce-worlds-largest-solar-power-project-1522214824.

[35] A. Sayigh, "Effect of dust on flat plate collectors," in *Sun: Mankind's Future Source of Energy*Anonymous 1978, .

[36] M. S. El-Shobokshy and F. M. Hussein, "Degradation of photovoltaic cell performance due to dust deposition on to its surface," *Renewable Energy,* vol. 3, *(6-7),* pp. 585-590, 1993.

[37] S. Mekhilef, R. Saidur and M. Kamalisarvestani, "Effect of dust, humidity and air velocity on efficiency of photovoltaic cells," *Renewable and Sustainable Energy Reviews*, vol. 16, *(5)*, pp. 2920-2925, 2012.

[38] M. M. Rahman *et al*, "Effects of natural dust on the performance of PV panels in Bangladesh," *International Journal of Modern Education and Computer Science*, vol. 4, *(10)*, pp. 26, 2012.

[39] N. S. Beattie *et al*, "Understanding the effects of sand and dust accumulation on photovoltaic modules," *Renewable Energy*, vol. 48, pp. 448-452, 2012.

[40] Z. Moradi-Shahrbabak, A. Tabesh and G. R. Yousefi, "Economical Design of Utility-Scale Photovoltaic Power Plants With Optimum Availability," *Industrial Electronics, IEEE Transactions on*, vol. 61, *(7)*, pp. 3399-3406, 2014. . DOI: 10.1109/TIE.2013.2278525.

[41] A. Alferidi and R. Karki, "Development of Probabilistic Reliability Models of Photovoltaic System Topologies for System Adequacy Evaluation," *Applied Sciences*, vol. 7, *(2)*, pp. 176, 2017.

[42] M. El-Shobokshy, A. Mujahid and A. Zakzouk, "Effects of dust on the performance of concentrator photovoltaic cells," *IEE Proceedings I (Solid-State and Electron Devices)*, vol. 132, *(1)*, pp. 5-8, 1985.

[43] H. K. Elminir *et al*, "Effect of dust on the transparent cover of solar collectors," *Energy Conversion and Management*, vol. 47, *(18-19)*, pp. 3192-3203, 2006.

[44] A. Labban, "Dust storms over Saudi Arabia: temporal and spatial characteristics, climatology and synoptic case studies," PhD Thesis at RMIT University, 2015.

[45] N. Alabbadi and A. Alshehiween, "Saudi arabian solar radiation network operation data collection and quality assessment," King Abdulaziz City for Science and Technology, 2005.

[46] R. Billinton *et al*, "A reliability test system for educational purposes-basic data," *Power Systems, IEEE Transactions on*, vol. 4, *(3)*, pp. 1238-1244, 1989.

[47] R. Allan and R. Billinton, "Power system reliability and its assessment. 2. Composite generation and transmission systems," *Power Eng J*, vol. 6, *(6)*, pp. 291-297, 1992.

[48] R. Allan and R. Billinton, "Tutorial. Power system reliability and its assessment. Part 1: Background and generating capacity," *Power Eng J*, vol. 6, *(4)*, pp. 191-196, 1992.

[49] D. Koval and A. Chowdhury, "Outage data concepts for generation and transmission equipment," in *IEEE Power Engineering Society General Meeting, 2006.*

[50] R. Allan *et al*, "Bibliography on the application of probability methods in power system reliability evaluation: 1987-1991," *Power Systems, IEEE Transactions on,* vol. 9, *(1),* pp. 41-49, 1994.

[51] R. Allan *et al*, "Bibliography on the application of probability methods in power system reliability evaluation," *Power Systems, IEEE Transactions on,* vol. 14, *(1),* pp. 51-57, 1999.

[52] R. Bansal, T. Bhatti and D. Kothari, "Discussion and closure of" Bibliography on the application of probability methods in power system reliability evaluation"," *IEEE Trans. Power Syst.,* vol. 17, *(3),* pp. 924, 2002.

[53] Newfoundland and Labrador Hydro, ""Isolated Systems generating planning practices", A survey of canadian utilites," November. 1995.

[54] P. Subcommittee, "IEEE reliability test system," *Power Apparatus and Systems, IEEE Transactions on, (6),* pp. 2047-2054, 1979.

[55] L. Garver, "Effective load carrying capability of generating units," *Power Apparatus and Systems, IEEE Transactions on, (8),* pp. 910-919, 1966.

[56] R. Duignan *et al*, "Capacity value of solar power," in *Power and Energy Society General Meeting, 2012 IEEE,* 2012.

[57] Jaeseok Choi *et al*, "Assessment of CO2 reduction by renewable energy generators," in *Innovative Smart Grid Technologies (ISGT), 2010,* 2010, . DOI: 10.1109/ISGT.2010.5434742.

[58] D. Hirschmann *et al*, "Reliability prediction for inverters in hybrid electrical vehicles," *Power Electronics, IEEE Transactions on,* vol. 22, *(6),* pp. 2511-2517, 2007.

[59] P. Wikstrom, L. A. Terens and H. Kobi, "Reliability, availability, and maintainability of high-power variable-speed drive systems," *Industry Applications, IEEE Transactions on,* vol. 36, *(1),* pp. 231-241, 2000.

[60] Yantao Song and Bingsen Wang, "Survey on Reliability of Power Electronic Systems," *Power Electronics, IEEE Transactions on,* vol. 28, *(1),* pp. 591-604, 2013. . DOI: 10.1109/TPEL.2012.2192503.

[61] M. Handbook, *217 F Notice 2," Reliability Prediction of Electronic Equipment", 1995*.

[62] S. Anand, S. K. Gundlapalli and B. G. Fernandes, "Transformer-Less Grid Feeding Current Source Inverter for Solar Photovoltaic System," *Industrial Electronics, IEEE Transactions on,* vol. 61, *(10),* pp. 5334-5344, 2014. . DOI: 10.1109/TIE.2014.2300038.

[63] A. Ristow *et al*, "Development of a methodology for improving photovoltaic inverter reliability," *Industrial Electronics, IEEE Transactions,* vol. 55, *(7),* pp. 2581-2592, 2008.

[64] J. Liu and N. Henze, "Reliability consideration of low-power grid-tied inverter for photovoltaic application," in *24th European Photovoltaic Solar Energy Conference and Exhibition*, 2009.

[65] A. Ghaedi *et al*, "Reliability evaluation of a composite power system containing wind and solar generation," in *Power Engineering and Optimization Conference (PEOCO), 2013 IEEE 7th International*, 2013.

[66] F. Chan and H. Calleja, "Reliability estimation of three single-phase topologies in grid-connected PV systems," *Industrial Electronics, IEEE Transactions*, vol. 58, *(7)*, pp. 2683-2689, 2011.

[67] S. Harb and R. S. Balog, "Reliability of candidate photovoltaic module-integrated-inverter topologies," in *Applied Power Electronics Conference and Exposition (APEC), 2012 Twenty-Seventh Annual IEEE*, 2012.

[68] B. Abdi *et al*, "Reliability considerations for parallel performance of semiconductor switches in high-power switching power supplies," *Industrial Electronics, IEEE Transactions*, vol. 56, *(6)*, pp. 2133-2139, 2009.

[69] W. Kuo and M. J. Zuo, *Optimal Reliability Modeling: Principles and Applications.* 2003.

[70] A. Lisnianski, "Extended block diagram method for a multi-state system reliability assessment," *Reliab. Eng. Syst. Saf.,* vol. 92, *(12),* pp. 1601-1607, 2007.

[71] M. Bollen, *Literature Search for Reliability Data of Components in Electric Distribution Networks.* Dept. Elect. Eng., Eindhoven Univ. Technol., Eindhoven,The Netherlands, Tech. Rep. 93-E-276, Aug .1993.

[72] B. Gen, "Reliability and cost/worth evaluation of generating systems utilizing wind and solar energy," 2005.

[73] R. Perez, R. Seals and R. Stewart, "Assessing the load matching capability of photovoltaics for US utilities based upon satellite-derived insolation data," in *Photovoltaic Specialists Conference, 1993., Conference Record of the Twenty Third IEEE,* 1993.

[74] R. Perez *et al*, "Update: Effective load carrying capability of photovoltaics in the united states," in *Proc. ASES Annual Conference, Denver, CO,* 2006.

[75] C. K. Ho, "Software and codes for analysis of concentrating solar power technologies," *SAND2008-8053.Albuquerque, NM: Sandia National Laboratories,* 2008.

[76] Y. Zhang *et al*, "Modeling the potential for thermal concentrating solar power technologies," *Energy Policy,* vol. 38, *(12),* pp. 7884-7897, 2010.

[77] S. Izquierdo *et al*, "Analysis of CSP plants for the definition of energy policies: the influence on electricity cost of solar multiples, capacity factors and energy storage," *Energy Policy,* vol. 38, *(10),* pp. 6215-6221, 2010.

[78] M. Montes, A. Abánades and J. Martínez-Val, "Performance of a direct steam generation solar thermal power plant for electricity production as a function of the solar multiple," *Solar Energy,* vol. 83, *(5),* pp. 679-689, 2009.

[79] Z. Yao *et al*, "Modeling and simulation of the pioneer 1MW solar thermal central receiver system in China," *Renewable Energy,* vol. 34, *(11),* pp. 2437-2446, 2009.

[80] A. Kassem, K. Al-Haddad and D. Komljenovic, "Concentrated solar thermal power in Saudi Arabia: Definition and simulation of alternative scenarios," *Renewable and Sustainable Energy Reviews,* vol. 80, pp. 75-91, 2017.

[81] Agence internationale de l'énergie, *Energy Technology Perspectives 2012: Pathways to a Clean Energy System.* 2012.

[82] M. Montes *et al*, "Performance analysis of an integrated solar combined cycle using direct steam generation in parabolic trough collectors," *Appl. Energy,* vol. 88, *(9),* pp. 3228-3238, 2011.

[83] S. Anders *et al*, "Potential for renewable energy in the San Diego region," *Published by the San Diego Regional Renewable Energy Group*, 2005.

[84] R. Soria *et al*, "Hybrid concentrated solar power (CSP)–biomass plants in a semiarid region: A strategy for CSP deployment in Brazil," *Energy Policy*, vol. 86, pp. 57-72, 2015.

[85] D. Arvizu *et al*, "Direct solar energy in IPCC special report on renewable energy sources and climate change mitigation," *United Kingdom and New York, NY, USA*, 2011.

[86] B. Pai, "Augmentation of thermal power stations with solar energy," *Sadhana*, vol. 16, *(1)*, pp. 59-74, 1991.

[87] E. Hu *et al*, "Solar power boosting of fossil fuelled power plants," in *Proceedings of the International Solar Energy Congress*, 2003.

[88] Y. Yang *et al*, "Research on solar aided coal-fired power generation system and performance analysis," *Science in China Series E: Technological Sciences*, vol. 51, *(8)*, pp. 1211-1221, 2008.

[89] E. A. Tora and M. M. El-Halwagi, "Optimal design and integration of solar systems and fossil fuels for sustainable and stable power outlet," *Clean Technologies and Environmental Policy*, vol. 11, *(4)*, pp. 401-407, 2009.

[90] Á. Pérez and N. Torres, "Solar parabolic trough–biomass hybrid plants: A cost–efficient concept suitable for places in low irradiation conditions," in *SolarPACES Conference*, 2010.

[91] J. Nixon, P. Dey and P. Davies, "The feasibility of hybrid solar-biomass power plants in India," *Energy*, vol. 46, *(1)*, pp. 541-554, 2012.

[92] A. M. Patnode, *Simulation and Performance Evaluation of Parabolic Trough Solar Power Plants*, University of Wisconsin-Madison. 2006.

[93] H. Price, P. Svoboda and D. Kearney, "Validation of the FLAGSOL parabolic trough solar power plant performance model," *Solar Engineering*, pp. 527-527, 1995.

[94] H. Price, "A parabolic trough solar power plant simulation model," in *ASME 2003 International Solar Energy Conference*, 2003.